The effect of water storages on temporal gravity measurements and the benefits for hydrology

Benjamin Creutzfeldt

Institute of Earth and Environmental Sciences

The effect of water storages on temporal gravity measurements and the benefits for hydrology

Cumulative dissertation

for the degree of
Doctor of Natural Sciences (Dr. rer. nat.)
in Geoecology

submitted to the
Faculty of Mathematics and Natural Sciences
at the University of Potsdam, Germany

by
Noah Angelo Benjamin
Creutzfeldt

Referees:
Bruno Merz, University of Potsdam, Germany
Michel Van Camp, Royal Observatory of Belgium, Belgium
Markus Weiler, Albert-Ludwigs-University of Freiburg, Germany

Submitted: April 2010
Defended: October 2010
Published: Novemver 20010

Published online at the
Institutional Repository of the University of Potsdam:
URL http://opus.kobv.de/ubp/volltexte/2010/4857/
URN urn:nbn:de:kobv:517-opus-48575
http://nbn-resolving.org/urn:nbn:de:kobv:517-opus-48575

Contents

List of figures

List of tables

Abstract

Temporal gravimeter observations, used in geodesy and geophysics to study variation of the Earth's gravity field, are influenced by local water storage changes (WSC) and – from this perspective – add noise to the gravimeter signal records. At the same time, the part of the gravity signal caused by WSC may provide substantial information for hydrologists. Water storages are the fundamental state variable of hydrological systems, but comprehensive data on total WSC are practically inaccessible and their quantification is associated with a high level of uncertainty at the field scale.

This study investigates the relationship between temporal gravity measurements and WSC in order to reduce the hydrological interfering signal from temporal gravity measurements and to explore the value of temporal gravity measurements for hydrology for the superconducting gravimeter (SG) of the Geodetic Observatory Wettzell, Germany.

A 4D forward model with a spatially nested discretization domain was developed to simulate and calculate the local hydrological effect on the temporal gravity observations. An intensive measurement system was installed at the Geodetic Observatory Wettzell and WSC were measured in all relevant storage components, namely groundwater, saprolite, soil, top soil and snow storage. The monitoring system also contained a suction-controlled, weighable, monolith-filled lysimeter, allowing an all time first comparison of a lysimeter and a gravimeter. Lysimeter data were used to estimate WSC at the field scale in combination with complementary observations and a hydrological 1D model. Total local WSC were derived, uncertainties were assessed and the hydrological gravity response was calculated from the WSC. A simple conceptual hydrological model was calibrated and evaluated against records of a superconducting gravimeter, soil moisture and groundwater time series. The model was evaluated by a split sample test and validated against independently estimated WSC from the lysimeter-based approach.

A simulation of the hydrological gravity effect showed that WSC of one meter height along the topography caused a gravity response of 52 µGal, whereas, generally in geodesy, on flat terrain, the same water mass variation causes a gravity change of only 42 µGal (Bouguer plate approximation). The radius of influence of local water storage variations can be limited to 1000 m, and 50 % to 80 % of the local hydro¬logical gravity signal is generated within a radius of 50 m around the gravimeter.

At the Geodetic Observatory Wettzell, WSC in the snow pack, top soil, unsaturated saprolite and fractured aquifer are all important terms of the local water budget. With the exception of snow, all storage components have gravity responses of the same order of magnitude and are therefore relevant for gravity observations. The comparison of the total hydrological gravity response to the gravity residuals obtained from the SG, showed similarities in both short-term and seasonal dynamics. However, the results demonstrated the limitations of estimating total local WSC using hydrological point measurements.

The results of the lysimeter-based approach showed that gravity residuals are caused to a larger extent by local WSC than previously estimated. A comparison of the results with other methods used in the past to correct temporal gravity observations for the local hydrological influence showed that the lysimeter measurements improved the independent estimation of WSC significantly and thus provided a better way of estimating the local hydrological gravity effect. In the context of hydrological noise reduction, at sites where temporal gravity observations are used for geophysical studies beyond local hydrology, the installation of a lysimeter in combination with complementary hydrological measurements is recommended.

From the hydrological view point, using gravimeter data as a calibration constraint improved the model results in comparison to hydrological point measurements. Thanks to their capacity to integrate over different storage components and a larger area, gravimeters provide generalized information on total WSC at the field scale. Due to their integrative nature, gravity data must be interpreted with great care in hydrological studies. However, gravimeters can serve as a novel measurement instrument for hydrology and the application of gravimeters especially designed to study open research questions in hydrology is recommended.

Zusammenfassung

Zeitabhängige Gravimetermessungen, die in der Geodäsie und der Geophysik zur Messung der Variationen des Erdschwerefelds eingesetzt werden, werden durch lokale Wasserspeicheränderungen beeinflusst, die – aus dieser Perspektive – ein hydrologisches Störsignal verursachen. Gleichzeitig hat der durch Wasserspeicheränderungen hervorgerufene Teil des Gravimetersignals das Potential, wichtige Informationen über hydrologische Speicher zu enthalten, da diese zwar eine grundlegende Zustandsgröße hydrologischer Systeme darstellen, ihre Quantifizierung jedoch mit einem hohen Maß an Unsicherheiten auf der Feldskala einhergeht.

Diese Studie untersucht die Beziehung zwischen zeitabhängigen Gravimetermessungen und Wasserspeicheränderungen, um die Messungen von hydrologischen Störsignalen zu bereinigen und den Nutzen der Gravimetermessungen für die Hydrologie zu erkunden. Dies geschieht am Beispiel des Supraleitgravimeters (SG) des Geodätischen Observatoriums Wettzell in Deutschland.

Ein von uns entwickeltes 4D Vorwärtsmodel mit einer räumlich genesteten Diskretisierungsdomäne dient der Simulation lokaler hydrologischer Masseneffekte auf Gravimetermessungen. Zusätzlich wurde ein intensives Messsystem am Geodätischen Observatorium Wettzell installiert, um die Wasserspeicheränderungen in allen relevanten Speicherkomponenten, d. h., im Grundwasser, in der ungesättigten Zone und im Schneespeicher zu erfassen. Das Monitoringsystem beinhaltete auch einen wägbaren, monolithischen Lysimeter mit Matrixpotentialübertragung, wodurch zum ersten Mal ein Direktvergleich eines Gravimeters mit einem Lysimeter vorgenommen werden konnte. Zur Bestimmung der Wasserspeicheränderungen auf der Feldskala wurden die Lysimetermessungen mit komplementären hydrologischen Beobachtungen und einem 1D-Modell kombiniert. Die Gesamtwasserspeicheränderungen konnten somit bestimmt, Unsicherheiten abgeschätzt und der hydrologische Masseneffekt auf Gravimetermessungen berechnet werden. Abschließend wurde ein einfaches, konzeptionelles, hydrologisches Modell mittels der SG-Zeitreihen, Bodenfeuchte- und Grundwassermessungen kalibriert und evaluiert. Dieses wurde dann durch einen "Split-Sample-Test" evaluiert und auf Grundlage von Wasserspeicheränderungen abgeleitet basierend auf den Lysimetermessungen validiert.

Die Simulation des hydrologischen Masseneffekts auf Gravimetermessungen zeigte, dass Wasserspeicheränderungen von einem Meter Höhe entlang der Topographie einen Erdschwereeffekt von 52 µGal hervorriefen, während in der Geodäsie im Allgemeinen die gleiche Wassermassenvariation in flachem Terrain einen Erdschwereeffekt von nur 42 µGal (Bouguer-Platte) hervorruft. Der Einflussradius der lokalen Wasserspeicheränderungen kann auf 1000 m begrenzt werden, und 50 % bis 80 % des lokalen hydrologischen Erdschweresignals wird in einem Radius von 50 m um den Gravimeter generiert.

Wasserspeichervariationen in Schneedecke, Oberboden, ungesättigtem Saprolith und geklüfteten Aquifer, sind allesamt wichtige Größen der lokalen Wasserbilanz. Abgesehen von Schnee beeinflussen alle Speicheränderungen die Gravimetermessungen in derselben Größenordnung und sind daher für diese von Bedeutung. Ein Vergleich des lokalen hydrologischen Gravitationseffekts mit den SG Residuen zeigte sowohl ereignisbezogene als auch saisonale Übereinstimmungen. Die Ergebnisse wiesen jedoch auch die Grenzen bei der Bestimmung der gesamten lokalen Wasserspeichervariationen mithilfe hydrologischer Punktmessungen auf.

Die Ergebnisse des Lysimeter-basierten Ansatzes zeigten, dass SG Residuen mehr noch, als bisher dargestellt, durch lokale Wasserspeicheränderungen hervorgerufen werden. Ein Vergleich der Resultate mit anderen Methoden, die in der Vergangenheit zur Korrektur zeitabhängiger Erdschwerebeobachtungen durch Bestimmung des lokalen hydrologischen Masseneffekte verwendet wurden, zeigte eine erhebliche Verbesserung der unabhängigen Berechnung von Wasserspeicheränderungen durch Lysimetermessungen. Wir sprechen somit von einer verbesserten Methode zur Bestimmung des lokalen hydrologischen Erdschwereeffekts. Daher ist die Installation eines Lysimeters im Zusammenhang mit der Reduzierung des hydrologischen Störsignals an Standorten, wo zeitabhängige Erdschwerebeobachtungen für über die lokale Hydrologie hinausgehende geophysikalische Studien stattfinden, zu empfehlen.

Aus hydrologischer Sicht konnte diese Studie zeigen, dass die Verwendung von zeitabhängigen Gravimetermessungen als Kalibrierungsdaten die Modellergebnisse im Vergleich zu hydrologischen Punktmessungen verbesserte. Auf Grund ihrer Fähigkeit, über verschiedene Speicherkomponenten und ein größeres Gebiet zu integrieren, bieten Gravimeter verallgemeinerte Informationen über die Gesamtwasserspeicherveränderungen auf der Feldskala. Diese integrative Eigenschaft ruft bei der Interpretation von Erdschweredaten in hydrologischen Studien zu Vorsicht auf. Dennoch können Gravimeter der Hydrologie als neuartiges Messinstrument dienen, und die Nutzung von speziell für die Beantwortung noch offener Forschungsfragen der Hydrologie entwickelter Gravimeter wird hier empfohlen.

Acknowledgement

What appears between those covers is the results of several years of research at the Deutsches GeoForschungsZentrum GFZ. Although the work was written by me, the research was not conducted in vacuum, but is an aggregation of many different inputs I received. Therefore, I owe my gratitude to all those people who have made this thesis possible:

My deepest gratitude is to my advisor, Andreas Güntner, for having motivated me to write a doctoral thesis. His door was always open to me. He lent me an ear whenever I had questions or concerns and was always prepared to discuss and consider new ideas.

Bruno Merz provided me with the possibility to take my doctor's degree at the "Hydrology" section. I am very grateful to him for helping me to put new ideas into practise and for enabling me to carry out my measurements, which did not always come at a bargain price.

I am indebted to Axel Bronstert for familiarising me with the depths and abysses of hydrology and for having agreed to review my work.

I also owe my gratitude to Michel Van Camp for his comprehensive reviews that significantly improved two papers of mine and for accepting to be a reviewer of my thesis.

I am heartily thankful to Heiko Thoss for helping me with the installation of the measuring systems and for initiating me in the mysteries of geophysics and the technical finesse of measuring instruments. As my roommate, he often had to endure my temper and was always prepared to engage in a heated debate.

I also would like to make a special reference to the HYGRA group: Angela Heim, Enrico Grams, Philip Müller, Matthias Munz and Jörg Wummel who assisted me with many studies, time-consuming laboratory work and accompanied me to many of my field campaigns. In this context, I would also like to acknowledge the section members Jürgen Neumayer, Corinna Kroner, Christoph Förste and Maiko Abe.

My special thanks go to the members of the Division of Geodesy of the Federal Agency for Cartography and Geodesy (BKG) and especially the National Reference Systems for Gravity section. Herbert Wilmes can be taken as representative of all of them. I am also indebted to Hartmut Wziontek for showing me the geodesist's perspective and for always being available to answer geodetic questions. I would also like to extend my gratitude to Mr. Schlüter and Ulrich Schreiber, to name but two of the members of the Geodetic Observatory Wettzell who provided me with insights on Satellite Laser Ranging and Very Long Baseline Interferometry. I am also thankful to Thomas Klügel for allowing me to access the great number of data he collected in his many years of work.

I owe my deepest gratitude to the many people of Wettzell who with their different forms of assistance made a great contribution to the success of my field campaigns. They familiarised me with the Bavarian way of life. Here, special mention should be made of Müller Sepp who always provided me with the missing part, farmer Josef Vogel for allowing me to use his land and Fischer Sepp for helping me to dig all these holes.

The installation and operation of the measuring system in Sutherland, South Africa would not have been possible without the help of Pieter Fourie, and I would also like to thank the members of the South African Astronomical Observatory.

Of course, I am also deeply grateful to all the reviewers and editors who substantially contributed to improve the quality of the different publications.

My heartfelt thanks go to my colleagues Susanna Werth, Thomas Gräff, Steffi Uhlemann, Florian Elmer, Björn Guse, Heiko Apel and Sören Haubrock. All of them helped me to make this work a reality.

Most importantly, none of this would have been possible without the love and patience of my family and my LOVELY girlfriend.

Chapter 1:

Introduction, motivation and objective

Introduction

1.1 Geophysical importance

At first glance, earthquakes, global variations of water masses, atmospheric circulation, volcanism, post-glacial rebound, depletion of local water storages or convection flows in the Earth's core have little in common, except that they represent objects of fundamental research, and understanding them is of paramount importance to mankind. These phenomena occur over a wide range of spatial and temporal scales in the atmosphere, the Earth's crust, the Earth's mantle and Earth's core. But what unites these different phenomena is that these processes can cause variations of the Earth's gravity field and their gravity effect can cover different orders of magnitude (see Figure 1.1).

Observing variations of the Earth's gravity field allows for the investigation of these geodynamic, hydrological and geophysical processes, but temporal gravity observations are an integral signal, integrating over gravity variations of different origins. For an unambiguous interpretation, this integral gravity signal has to be separated into the different components. This task can only be accomplished with an interdisciplinary approach where different disciplines are co-operating closely and may benefit from each other at the same time.

When we focus on the different components of temporal gravity variations, we learn that the hydrological signal is the least understood signal component in relation to its importance. The hydrological component has to be estimated in the temporal gravity signal to tap the full potential of temporal gravity observations for studying geophysical phenomena beyond local hydrology. Therefore, the question arises: How can we estimate the hydrological gravity effect and how can we reduce the hydrological component from the gravity signal?

1.2 Hydrological importance

Life on this planet is not possible without water. But freshwater is a finite and vulnerable resource. The growing gap between water supply and demand poses a threat to the development of mankind. As formulated by the United Nations in their *Agenda 21* [1992], for a sustainable development we need an integrated management of water resources "based on the perception of water as an integral part of the ecosystem, a natural resource and a social and economic good, whose quantity and quality determine the nature of its utilization". The basis for an effective water use and management is the quantification of the hydrological cycle and the amount of water stored in different reserves such as groundwater, soil moisture, surface water and water in snow and glaciers.

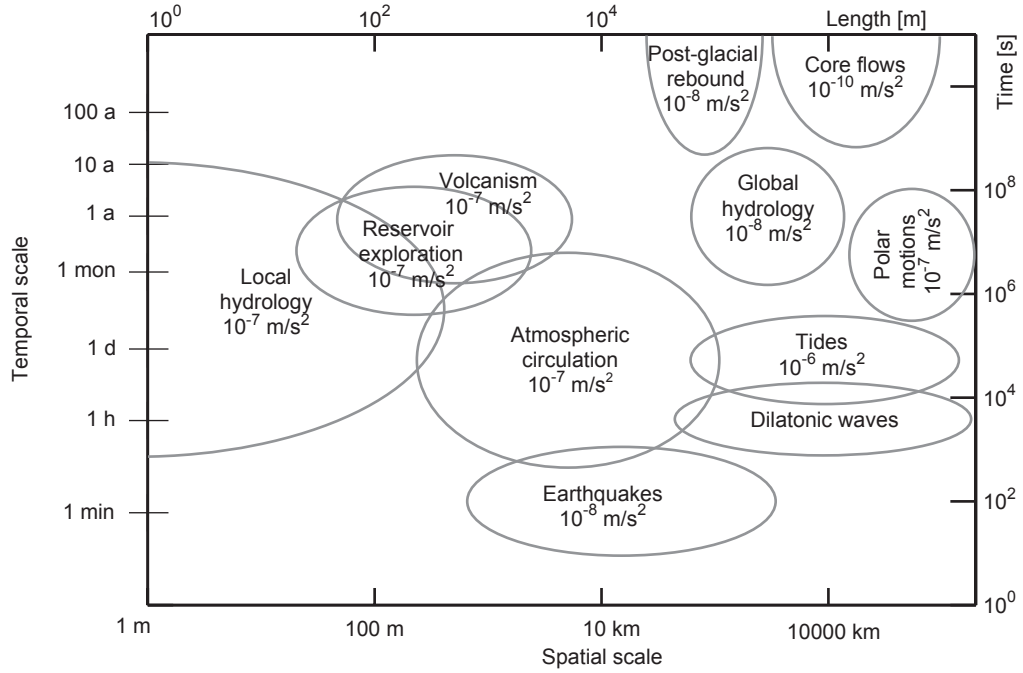

Figure 1.1: Geophysical phenomena and the related processes, which cause variations of the Earth's gravity field at a range of characteristic space-time scales.

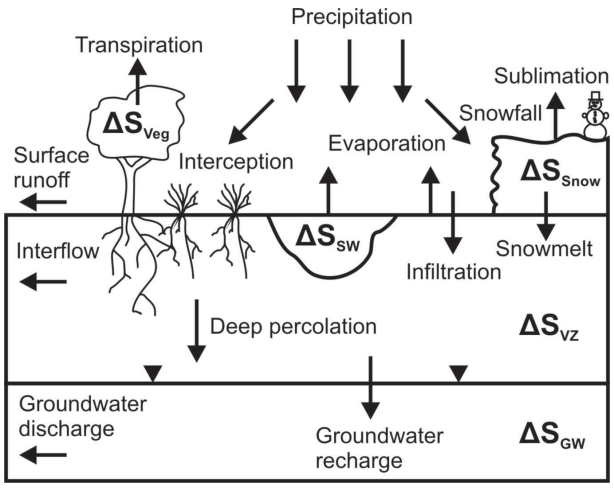

Figure 1.2: Terrestrial water cycle with main water storages and hydrological processes.

The hydrological cycle is based on the principle of mass conservation, which determines the water balance. In general terms, the terrestrial water balance relates water storage changes (ΔS) to the precipitation (P), the evapotranspiration (ET) and the runoff (R)

$$\Delta S = P - ET - R \quad (1.1)$$

Focusing on the storage term in the water balance equation, we can distinguish different storage components, namely water stored in the snow storage (ΔS_{snow}), in the vegetation (ΔS_{Veg}), in the vadose zone storage (ΔS_{VZ}), in the groundwater storage (ΔS_{GW}) and in the surface water storage (ΔS_{SW}):

$$\Delta S = \Delta S_{snow} + \Delta S_{Veg} + \Delta S_{VZ} + \Delta S_{GW} + \Delta S_{SW} \quad (1.2)$$

In this study, vadose zone is the unsaturated zone. For water movement, the driving forces in this zone are differences in the total water potential. Groundwater refers to the saturated subsurface zone where water is free to move under the influence of gravity. The different storages are closely related through different hydrological processes (Figure 1.2).

Despite the important role of water storages and their variations in hydrology, the estimation of water storages at an appropriate scale is still a challenging task. This applies especially to sub-surface storages, which are considered as only measurable on the point scale but are highly variable in space and time.

Temporal gravity data are influenced by water storage changes. Therefore, the question arises: Can temporal gravity measurements be used to measure water storage changes and, hence, allow for a better characterization of the hydrological system?

1.3 Gravity and the relation to hydrology

Gravitation, the weakest of the four fundamental interaction forces, is the force that acts between all objects because of their mass. In the *philosophiae naturalis principia mathematica* [1687], Isaac Newton expressed the interaction force between two masses by the Universal Law of Gravitation

$$F = G\frac{M \times m}{R^2} \quad (1.3)$$

The gravitational force F [N] is directly proportional to the product of the two masses M and m [kg] and inversely proportional to the square of the distance between the masses R [m]. The gravitational constant G, one of the natural constants, is approximately equal to 6.673×10^{-11} Nm²/kg². The second law of Newton's Law of Motion states that a force (F) is equal to the change in momentum per change in time

$$F = m \times g \quad (1.4)$$

For an object with a constant mass, the force (F) equals mass (m) times the acceleration, whereas the acceleration g refers to the acceleration that the Earth imparts on all objects, the Earth's gravity. When we combine both equations to

$$g = \frac{G \times M}{R^2} \quad (1.5)$$

we see that the Earth's gravity depends on the Earth radius ($R \approx 6.38\times10^{-6}$ m) and the Earth's mass ($M \approx 5.98\times10^{-24}$ kg). The *standard gravity* is, by definition, 9.81 m/s².

Gravimeters are instruments used to observe the Earth's gravity field, whereas 'gravimetry' refers to the method of measuring the Earth's gravity. In gravimetry, the strength of the Earth's gravity field is expressed frequently in the unit gal (symbol Gal) in the honor of Galileo Galilei, whereas 1 Gal is defined as 1 centimeter per square second.

The Earth's gravity varies with space and time. Latitude, altitude and the geological settings can cause spatial gravity variations. The gravity effect of latitude is due to differences in the centrifugal acceleration and the Earth's radius (R) (The polar radius is 21 km less than the equatorial radius). As a result, the gravity measured at the poles is 5.19 Gal larger than at the equator, implying that objects will weight 0.5 % more at the poles. The change in altitude equals a change in the distance to the Earth's centre and, hence, a change in gravity. Topography has also an effect on gravity measurements since in addition to a change in altitude it also determines the total rock mass below the gravimeter, something that also influences the gravitational pull. The effect of latitude, altitude

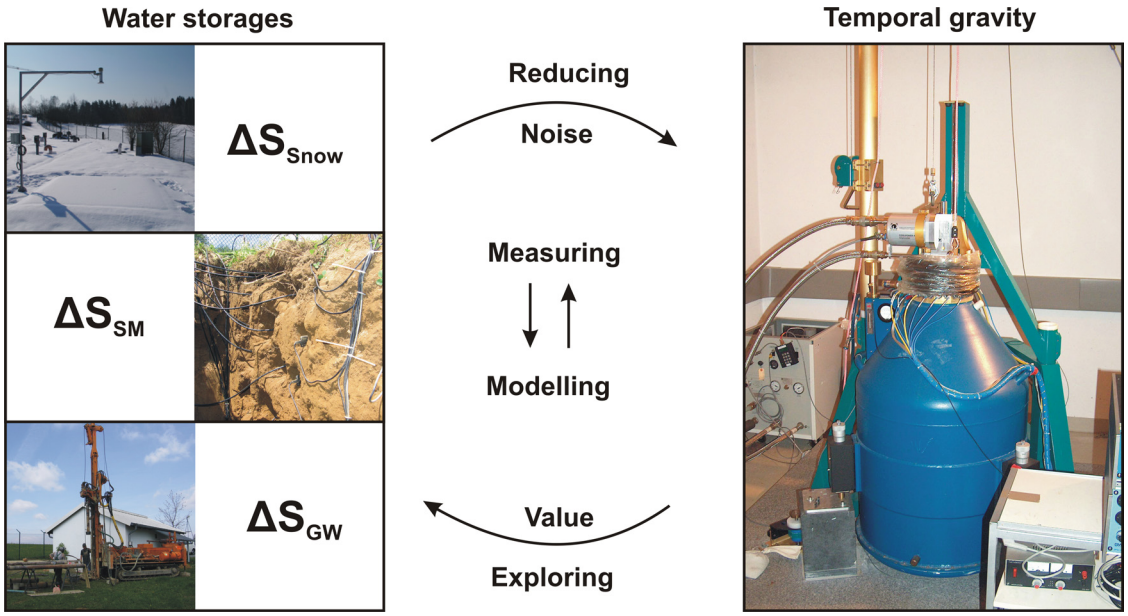

Figure 1.3: Objective and structure of the study

and topography are accounted for by the latitude, free-air and Bouguer correction, respectively. Finally, the different densities of the geological material, frequently the target value in gravity surveys, have an effect on gravity measurements [*Reynolds*, 1997].

When we look at temporal gravity variations, we find that ocean and Earth's tides due to sun and moon cause a motion of the Earth in the sub-meter range and gravity variations of approximately 0.2 Gal. The gravity effect of polar motion – the movement of the Earth's rotation axis – and mass variations in the atmosphere are one order of magnitude smaller. The gravity effect of tides, polar motion and the atmosphere is well-known and these influences can therefore be reduced from the gravimeter signal. The remaining signal is considered to be largely influenced by hydrological mass variations. Therefore, the temporal gravimeter signal (Δg_{Total}) is influenced by different sources of gravity variations

$$\Delta g_{Total} = \Delta g_{Tides} + \Delta g_{Pol} + \Delta g_{Atmos} + \Delta g_{Hydro} + \Delta g_{Others} \quad (1.6)$$

such as tide effects (Δg_{Tides}), effects from the polar motion (Δg_{Pol}), atmospheric effects (Δg_{Atmos}), the effect of water mass variations (Δg_{Hydro}) and other effects (Δg_{Others}) discussed above (Figure 1.1).

The total hydrological gravity effect can be split up into a local and a large-scale hydrological component. The variations of local water masses have an impact on gravimeter measurements due to the Newtonian attraction of water masses, while only the vertical component is registered by gravimeters. At one particular point *p(x,y,z)*, the gravity change (Δg) due to the change of water masses at a certain location *p'(x',y',z')* can be calculated

$$\Delta g(p) = G\Delta\rho(p')\int_{x_1}^{x_2}\int_{y_1}^{y_2}\int_{z_1}^{z_2}\frac{(z'-z)}{|p'-p|^3}dxdydz \quad (1.7)$$

where the continuous landscape is decomposed into rectangular elementary bodies with the volume element *dxdydz* and the triple integral, which integrates over the body volume defined by the $x_1y_1z_1$ and $x_2y_2z_2$ coordinates in a Cartesian coordinate system. Here, the change of water masses is expressed by the density change $\Delta\rho$ in each elementary body, whereas the total gravity effect is derived by summation of all gravity changes in each elementary body [*Forsberg*, 1984; *Nagy*, 1966].

Large-scale water mass variations can influence gravimeter measurements because of the Newtonian attraction on the one hand and the deformation of the Earth caused by a change of load on the Earth on the other. The loading effect can be estimated based on the well-known Green's functions [*Farrel*, 1972; *Llubes et al.*, 2004; *Neumeyer et al.*, 2008].

The relation of hydrological masses and temporal gravity signals makes co-operation between the two different disciplines, hydrology and geodesy, imperative. Only in a cross-disciplinary approach will it be possible to interpret all the different components of the gravimeter signal. Geodesists, geophysicists and hydrologists have to work together closely to tap the full potential of gravimeter measurements and to create a win-win situation, so that the gravimeter can be used as a novel hydrological measurement tool and the hydrological component can be reduced from the gravimeter signal.

1.4 Objective

The objective of this study is to **investigate the relationship** between hydrological mass variations and temporal gravity measurements in order to **reduce the interfering hydrological signal**, the noise, from temporal gravity measurements and to **explore the value of temporal gravity measurements** for hydrology. In line with the objective, we developed the following detailed questions, each building on the previous one:

1. In principle, the Newtonian attraction between two masses, here water masses and the gravimeter test mass, is well known. The question, however, is: How is the gravitational signal influenced by water mass as a spatiotemporal variable continuum in the landscape?
2. For an unambiguous interpretation of the gravity signal the influence of local WSC on gravimeter observations needs to be defined. The problem is that water storages and their changes are considered to be only measurable on the point scale. Hence, the question arises: How can we estimate the local hydrological gravity effect and reduce the hydrological interfering signal from the gravity signal?
3. Temporal gravimeter measurements are influenced by WSC, but it is difficult to unambiguously identify the source of the gravimeter signal. Therefore, the question is: Can gravimeters serve as a novel measurement instrument for hydrology and, hence, allow for a better characterization of the hydrological system?

1.5 Tasks and structure

Following the objectives and detailed research questions, this work aims at understanding an open and complex system and estimating its influence on gravimeter measurements. The objective will be evaluated for the using the Geodetic Observatory Wettzell as an example. This study will focus on the Newtonian attraction of local hydrological masses. The large-scale hydrological effect was recently evaluated by *Wziontek et al.* [2009c] and, hence, is not the focus of this study. For the sake of simplicity and due to the cross-disciplinary character of this study, this work was carried out in four different parts:

Firstly, it is necessary to understand the principle interaction of the hydrological system and gravimeter measurements, to define the study area and to investigate the relevance of the different water storages. A method is to be developed to calculate the hydrological gravity response, i.e. the gravimeter response due to variations of water masses. The hydrological gravity response is to be simulated based on this approach and e.g. the radius of influence or relevant water storages are to be defined. The following parts of the study will also use this approach to calculate the gravimeter response from spatiotemporal WSC.

Secondly, it is necessary to understand the hydrological system in order to estimate the hydrological gravity effect on gravimeter observations. In order to avoid integrating information that may not originate from local WSC, it is essential to exclude any calibration against the gravimeter signal when estimating the local WSC. The relevant hydrological processes and storages should be identified and quantified using observations only, to avoid making assumptions about the hydrological system. Both require the installation of an intensive monitoring system to measure WSC in all possible relevant storages, which where identified in the previous task.

Thirdly, if the relevant storages and hydrological processes are identified, the approach to estimate the hydrological gravity effect should be modified to improve the independent quantification of the influence of water storage changes on gravity measurements. The results of the developed approach are to be evaluated in the context of existing approaches to correct for the local hydrological influence and of the large-scale hydrological gravity effect.

Finally, the value of gravimeters for local hydrological applications is to be evaluated. Gravimeter measurements are influenced by local WSC, so the question is: Can we use this part of the gravimeter signal as information about the hydrological system? Hence, the benefits of gravimeter for local hydrology should be assessed also in comparison to classical hydrological point measurements. This task can only be accomplished in case that the local hydrological gravity effect is defined in the previous part.

Although each task can be seen separately, all four of them are strongly interrelated and build up on each other (Figure 1.3). The structure of this study follows the tasks developed, meaning that the study is divided into four main parts:

1. Part: Simulating the influence of water storage changes on the superconducting gravimeter of the Geodetic Observatory Wettzell, Germany.
2. Part: Measuring the effect of local water storage changes on in-situ gravity observations: Case study of the Geodetic Observatory Wettzell, Germany
3. Part: Reducing local hydrology from high precision gravity measurements: A lysimeter-based approach.
4. Part: The benefits of gravimeter observations for modelling water storage changes at the field scale.

Chapter 2:

Simulating the influence of water storage changes on the superconducting gravimeter of the Geodetic Observatory Wettzell, Germany.

Simulating the influence of water storage changes on the superconducting gravimeter of the Geodetic Observatory Wettzell, Germany.

Abstract

Superconducting gravimeters (SG) measure temporal changes of the Earth's gravity field with high accuracy and long term stability. Variations in local water storage components (snow, soil moisture, groundwater, surface water and water stored by vegetation) can have a significant influence on SG measurements and – from a geodetic perspective – add noise to the SG records. At the same time, this hydrological gravity signal can provide substantial information about the quantification of water balances.

A 4D forward model with a spatially nested discretization domain was developed to investigate the local hydrological gravity effect on the SG records of the Geodetic Observatory Wettzell, Germany. The possible maximum gravity effect was investigated using hypothetical water storage changes based on physical boundary conditions. Generally, on flat terrain, a water mass change of one meter in the model domain causes a gravity change of 42 μGal. Simulation results show that topography increases this value to 52 μGal. Errors in the Digital Elevation Model can influence the results significantly. The radius of influence of local water storage variations is limited to 1000 m. Detailed hydrological measurements should be carried out in a radius of 50 to 100 m around the SG station. Groundwater, soil moisture and snow storage changes dominate the hydrological gravity effect at the SG Wettzell. Using observed time series for these variables in the 4D model and comparing the results to the measured gravity residuals shows similarities in both seasonal and shorter-term dynamics. However, differences exist, e.g. the range comparison of the mean modeled (10 μGal) gravity signal and the measured (19 μGal) gravity signal, making additional hydrological measurements necessary in order to describe the full spatio-temporal variability of local water masses.

Published as:

Creutzfeldt, B., A. Güntner, T. Klügel, and H. Wziontek (2008), Simulating the influence of water storage changes on the superconducting gravimeter of the Geodetic Observatory Wettzell, Germany, Geophysics, 73(6), WA95, http://dx.doi.org/10.1190/1.2992508.

2.1 Introduction

The interrelation of hydrology and gravity is attracting increasing attention in hydrological and geodetic sciences. From a hydrological perspective, the estimation of water storage and its spatio-temporal variation is important in order to quantify water balances and for effective water use and management. Direct measurements of water storage changes (WSC) are, however, still a challenging task. Gravity observations provide a promising tool. From a geodetic perspective, the local hydrological gravity effect is an interfering signal which adds noise to gravimetric measurements and must therefore be eliminated from the gravity records.

Generally, the hydrological gravity effect is caused by the gravitational attraction of water masses and their variation. The interrelation of WSC and gravity variation is expressed by Newton's law of gravitation and is the basis for ground-based observations with gravimeters as well as for remote sensing carried out by the GRACE satellite mission. In addition to Newton's attraction term, variations of the Earth's gravity field due to the elastic deformation of the Earth's crust caused by the water load have to be taken into account at the global and regional scale [*Farrel*, 1972].

Bonatz [1967] was the first to study the relationship between hydrology and gravity by simulating the effect of soil moisture on gravity measurements. He concluded that it is not useful, for geodetic applications, to develop gravimeters with higher accuracy because soil moisture can contribute to the gravimetric signal up to 10 μGal and more. Nonetheless, more accurate gravimeters were developed – superconducting gravimeters (SG), for example. These are relative gravimeters with a measurement resolution of 0.01 μGal but, due to noise of atmospheric or seismic origin, their measurement accuracy decreases and ranges between 0.1 to 1 μGal [*Goodkind*, 1999; *Hinderer et al.*, 2006]. *Damiata and Lee* [2006] investigated the relationship between groundwater properties and the gravitational response. They concluded that it is necessary, from the hydrological perspective, to develop inexpensive gravimeters with sub-μGal accuracy. SGs are cost intensive in acquisition and operation, but are state of the art in terms of temporal resolution, stability and accuracy. Hence, they are suitable for studying the interrelationship of hydrology and gravity. For geodetic and hydrological applications, the problem remains that gravimetric records are an integral signal of accelerations of different origins (Earth and ocean tides, mass redistribution in the atmosphere, oceans, polar motion, continental hydrology, etc.). It is therefore still a challenging task to separate the influence of WSC from the rest of the signal.

Generally, gravity variations caused by water storage changes can be represented either by empirical relationships or by a physically-based approach. The empirical relationship is either established using a simple regression between hydrological and gravity data [*Harnisch et al.*, 2006; *Imanishi et al.*, 2006], or by translating the WSC to gravity changes on the basis of the Bouguer approximation. Within the Bouguer approximation, the water mass change is treated as the change in thickness of an infinitely extended plate (e.g. one meter change in water height causes a change in gravity of 42 μGal). Here, the information on WSC is often derived from precipitation and/or groundwater level measurements [*Bower and Courtier*, 1998; *Crossley et al.*, 1998; *Peter et al.*, 1995]. The advantage here is that detailed hydrological properties and processes do not have to be considered and the gravity signal can be corrected for the hydrological influence without knowledge of the complex hydrological system.

A more physically based approach is the analytical solution of a circular disc to calculate gravity change from WSC in the geometric body [*Bonatz*, 1967]. Although the spatial distribution of masses can be considered to a certain extent by dividing the cylinder into many disks and nesting different cylinders [*Abe et al.*, 2006], complex situations cannot be modeled with that method.

Because water masses are highly variable in space and time, emphasis was placed on the development of physically-based 4D models to investigate the hydrological gravity effect [*de Jong and Ros*, 2004; *Hasan et al.*, 2006; *Hokkanen et al.*, 2006; *Meurers et al.*, 2006; *Naujoks et al.*, 2007; *Prutkin and Klees*, 2007; *Van Camp et al.*, 2006; *Virtanen*, 2001]. The actual model implementation varies depending on the subject of the study. Often, rectangular prisms are used for the abstraction of the topography and the subsurface [*Hasan et al.*, 2006; *Kroner et al.*, 2007], but spherical segments [*Neumeyer et al.*, 2004] or 3D polygons (TINs) [*Hokkanen et al.*, 2006] can also be used. These models allow for the exact calculation of the gravity signal caused by WSC and for the consideration of the topography and spatial distribution of masses.

The beginnings of these different methods, initially developed in geodesy and applied geophysics, date back to the 1960s. They are mainly used to eliminate the effect of topographic masses on gravity anomalies (terrain correction), to fulfill the boundary condition in determining the Earth's gravitational potential, or for exploring the composition of the upper crust. Nonetheless, computation of hydrologically-induced gravitational effects differs from standard application in terrain correction in terms of variability of density in space and time, in the magnitude of the effect and intended accuracy in the sub μGal range.

Decomposition of masses into rectangular homogeneous prisms is common both in geophysics and in geodesy. This is reflected by the extensive literature on the sub-

ject, including *Mader* [1951], *Nagy* [1966], *Kolbenheyer* [1967], *Ehrismann* [1973] and *Forsberg* [1984]. An alternative and more general approach is the use of homogeneous polyhedra (see e.g. *Rausenberger* [1888], *Götze* [1976], *Pohanka* [1988] and *Petrović* [1996]), which tends to be a more efficient method in terms of the relationship between processing time and accuracy [*Petrović and Skiba*, 2001]. Neglecting the dimensions of the volume elements and assuming the concentration of the mass at a single point is a simple approach, allowing direct application of Newton's law. An intermediate solution is given by *MacMillan* [1958], where a series expansion for rectangular homogeneous prisms leads to a modified point mass representation. Especially in the near field, accuracy depends on the distance between the element center and the point of observation and on the element size. *Mufti* [1973] shows that the MacMillan approach is applicable for terrain corrections at all points with a distance not less than three times the side-length of the corresponding element.

To overcome accuracy limitations in the near field, *Klügel and Wziontek* [2007] combined an analytical solution with the point-mass equation in a correction model for atmospheric effects on gravimetric time series. In their approach, the mass attraction in the immediate area around the gravimeter is calculated using an analytical expression for cylindrical disks, while the point-mass model is used for more distant areas. The approach of using different models for different areas of influence around a gravimeter was also pursued by *Leirião* [2007] and *He* [2007]. For the closest area around the gravimeter, they use a prism equation which integrates fully over each volume element. To reduce computing time for large distances, the point-mass equation is used, while for intermediate distances the MacMillan equation is used. Finally, this model switches between these equations depending on a criterion that relates distance to cell size.

Some open questions remain regarding 4D modeling of WSC. Firstly, topographic information needed for 4D modeling is generally provided by a Digital Elevation Model (DEM). Its accuracy depends on the data source (topographic map, laser scan, survey) and the resolution. Consequently, the question is: How do topography and the DEM accuracy influence the gravity calculation? The second question is related to the scale. *Llubes et al*. [2004] concluded that for hydrological effects on gravimeters, it is only necessary to distinguish between the local and global scale. In their study, the influence of the local scale was set roughly to a few kilometers. For local 4D modeling, however, appropriate hydrological data on WSC are vital and therefore more exact knowledge of the radius of influence is needed for proper instrumentation with hydrological measurement devices. As total WSC is usually composed of several water storage components (snow, soil moisture, groundwater, surface water, water stored by vegetation), the question is how the gravitational signal is influenced by each of these storage components and how the radius of influence varies for each component. A final question is whether a planar approximation of the Earth's gravity field is sufficient in the model domain if the local scale is set to a few kilometers.

In this study, an appropriate 4D model is set up to investigate these open questions using the SG at the Geodetic Observatory Wettzell in Germany as an example. The possible maximum influence of all hydrological WSC components is assessed and the influence of real hydrological data on SG measurements is analyzed.

2.2 Study area

The study area is the area around the SG, which is located in a small building at the Geodetic Observatory Wettzell, operated by the Federal Agency for Cartography and Geodesy (BKG). The dual sphere SG CD029 is positioned near ground level and is based on a concrete foundation (Figure 2.1). Accuracy estimates for the SG gravity change recordings are better than 1 μGal and may even reach 0.1 μGal because the station is located in an area with little noise interference. Earlier studies showed that the SG records are influenced by WSC. Based on a simple regression model, *Harnisch and Harnisch* [2006; 2002] estimated the effect of precipitation and groundwater level on the SG Wettzell to be up to 14 μGal and 20 μGal, respectively.

The station is located on a mountain ridge of the Upper Palatinate Forest. The mean annual precipitation amounts to 863 mm, the potential evapotranspiration according to the Haude equation is 403 mm, and the mean annual temperature is 7 °C. Land use is characterized mainly by grassland and forestry.

The geology of the station can be classified into 4 different zones: (1) the soil zone with mainly loamy-sandy brown soils (Cambisols) and with an underlying solifluction layer, (2) the weathered zone mainly out of grus (physically-weathered gneiss), (3) the fractured zone and (4) the basement zone. This classification is based on data from 11 boreholes with a mean depth of 22 m (see Table 2.1 for a detailed description of the different zones).

The hydrogeological situation is characterized by a highly variable, complex and unconfined groundwater table with a mean groundwater level of 8 m and a seasonal fluctuation of 3-4 m. The two surface water bodies, the Höllenstein (storage volume 1.4 km³) and the Blaibacher (storage volume 1.5 km³) reservoir, are located at a distance of 1500 m to 3000 m from the station (Figure 2.2).

2.3 Method

The model for simulating the homogeneous elementary body attraction of spatially-distributed WSC is imple-

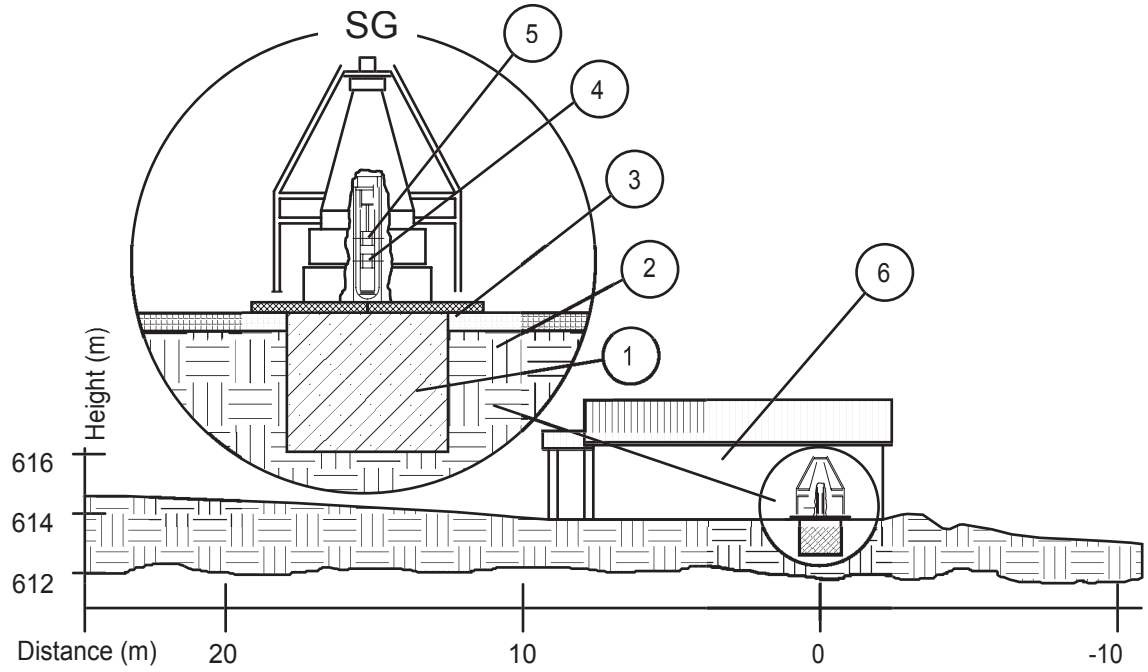

Figure 2.1: The superconducting gravimeter of the Geodetic Observatory Wettzell (coordinates in Gauss Krüger, zone 4, Bessel Ellipsoid: x = 4564212 m, y = 5445520 m). (1) Concrete foundation with the size of 1.4 × 1.4 × 1.2 m (width × depth × height), (2) Soil, (3) Baseplate (height = 613.80 m), (4) Sensor 1 (height = 614.2 m), (5) Sensor 2 (height = 614.4 m) and (6) SG building.

mented in MATLAB and is based on the MacMillan equation [*MacMillan*, 1958] presented by *Leirião* [2007]:

$$\Delta g = G\Delta\rho\Delta x\Delta y\Delta z \left[-\frac{z}{d^3} - \frac{5}{24}\frac{\left(\alpha x^2 + \beta y^2 + \omega z^2\right)z}{d^7} + \frac{1}{12}\frac{\omega z}{d^5} \right] \quad (2.1)$$

with $\alpha = 2\Delta x^2 - \Delta y^2 - \Delta z^2$, $\beta = -\Delta x^2 + 2\Delta y^2 - \Delta z^2$, $\omega = -\Delta x^2 - \Delta y^2 + 2\Delta z^2$ and $d = \sqrt{x^2 + y^2 + z^2}$. x, y and z are the centre coordinates of an elementary body relative to the sensor (m). Δx, Δy and Δz are the side lengths of a rectangular body ($\Delta xy = \Delta x = \Delta y$) (m), G is the universal gravitational constant (Nm^2/kg^2) and $\Delta\rho$ is the density change in an elementary body (kg/m^3). The z component of gravity variation is calculated for each body and the total gravity effect is derived by summation of all gravity changes in each elementary body. The MacMillan equation has the advantage over the point-mass approximation, in that the shape of cuboids is considered [*Leirião*, 2007]. In contrast to the prism approach [*Heck and Seitz*, 2007], which solves the volume integral of each body, it is possible to calculate WSC using the MacMillan approach on the basis of matrices, which significantly reduces the calculation time. This is vital for 4D gravity modeling. A nested discretization of the model domain was used to reduce the approximation error of the MacMillan equation in the near field (Figure 2.2). This error was assessed by comparing the results of the MacMillan approach to the gravity change, which was calculated using an analytical solution of a cylinder with the same mass variation, distance to the sensor, height and volume as in the MacMillan approach. Nested discretization also makes it possible to use high resolution DEMs in the near field and therefore allows for the consideration of detailed topographic and subsurface structures. Using a higher resolution reduces the step effect resulting from the abstraction of a continuous landscape by raster DEMs. Finally, the nested approach takes into account the fact that data availability for SG studies concerning hydrology is generally better in the immediate vicinity of the SG than at larger distances.

Two DEMs were available for the study area: A DEM 25 (cell size 25 m, extent 20 km and mean height accuracy 1-3 m) [*BKG*, 2004], and a DEM 10 (cell size 10 m, extent 5 km and mean height accuracy 1 m) [*LVG*, 2007]. Data on river lines, lakes [*BKG*, 2005] and the base plate of the houses of the Geodetic Observatory Wettzell were also available. During a differential GPS (DGPS) survey, around 14,000 height points were collected in a region spanning 300 m around the SG (height error < 0.1 m). From these different data sources a final DEM with varying resolution depending on the distance to the SG was

Table 2.1: Characterization of the different underground zones by thickness (m), depth (m), porosity (%) and specific yield (%). Count refers to the number of probes. The values are mean values with the corresponding standard deviation (*Specific yield for the fractured zone was derived from one pump test. The value of the standard deviation was estimated from literature (see text)).

		Soil zone	Weathered zone	Fractured zone	Basement zone
Count		10	10	9	9
Mean thickness		2.0 ± 0.8	5.5 ± 3.9	8.8 ± 5.0	-
Mean depth	From	0 ± 0	2.0 ± 0.8	7.3 ± 4.3	16.1 ± 4.9
	To	2.0 ± 0.8	7.5 ± 4.1	16.1 ± 4.9	-
Porosity	Count	60	16	-	-
	Mean	43 ± 5	37 ± 4	-	-
Specific yield	Count		4	1	-
	Mean		7 ± 4	3 ± 2*	-

created by excluding the most inaccurate data (DEM DGPS) (Figure 2.2). Two additional DEMs were processed to assess the influence of DEM accuracy on gravity modeling: The DEM 10, where only the DGPS points had been excluded and the DEM 25 with the exclusion of the DGPS points and the DEM 10. Finally, the quality of each DEM was assessed by an independent validation set derived during the DGPS survey (Table 2.2). The positional reference for all data used is the projected coordinate system – Gauss Krüger, Zone 4, Bessel Ellipsoid. The normal heights are given using the DHHN 92 height system. Because all subsequent computations refer to a planar approximation of the Earth's gravity field, the influence of the curvature of the equipotential surfaces was estimated by comparing the heights with a spherical approximation using the equation of Petrahn [2000]:

$$h_{corr} = h_{DEM} - \frac{1}{2R} d^2 \qquad (2.2)$$

where h_{DEM} is the height of the DEM (m) referring to the plane, R the Earth's radius of around 6370 km and d is the distance of a raster cell to the reference point (m). For example, at a distance of 10 km, the height decreases by about 7.8 m.

In the simulation model, the effect of WSC is calculated by assuming a homogeneous density change in an elementary body. However, WSC in ground, surface and snow water is equivalent to water level changes, meaning that the density change is heterogeneously distributed within each body. This simplification error can be minimized by reducing the layer thickness of the model.

The possible maximum influence of hydrological masses on the SG sensor was estimated assuming hypothetical maximum changes of different water storages based on real boundary conditions. Therefore, the effect of the SG house was considered in this step, assuming no WSC in the soil and weathered zone and only snow storage change on the roof of the SG house. Mass changes in the subsurface were estimated on the basis of water level change, soil porosity and specific yield (see Table 2.1). The mean depth of the groundwater table was calculated to be 8 ± 3 m based on three groundwater wells 200 m to 300 m away from the SG. The soil porosity was calculated from the measured bulk density and an assumed particle density of 2650 kg/m³. In the soil zone, porosity was used to estimate the maximum water mass change as soil moisture can range between saturation and a water content close to 0 Vol%. In deeper zones, it is unlikely that the moisture content would decrease to values lower than field capacity. For deeper zones, therefore, the specific yield – the drainable porosity – was used to derive the possible change of water masses. For the weathered zone, the specific yield was determined from undisturbed soil probes which were taken at depths between 1.5 m and 6.3 m, and was deduced on the basis of water retention curves (pF curves). For the fractured zone, the specific yield was roughly estimated to be around 3 %. This value was derived from a pump test using the Cooper-Jacob straight line method. According to *Rubbert* [2008], the specific yield varies from less than 0.1 % to up to 5 % for the fractured zone (see Table 2.1). The maximum measured snow height in the study area is 0.9 m, and snow density can vary between 50 kg/m³ (freshly fallen snow) and 500 kg/m³ (old snow), so the mean snow density was set at 275 kg/m³. The effect of surface water change in both reservoirs on gravity was assessed by draining them completely, using a stage-storage relationship and starting at their maximum possible water level. Finally, the effect of water stored in the vegetation and intercepted on the vegetation surface was investigated. The interception storage capacity depends on the climate conditions and on the morphology of the vegetation cover and can be about 5 mm (1 mm water corresponds to 1 kg/m²) [*Baumgartner and Liebscher*, 1996]. During the vegetation period, the water variations in the vegetation were set to 5 mm [*Schulz*, 2002]. Maximum water storage change due to vegetation then amounts to up to 10 mm.

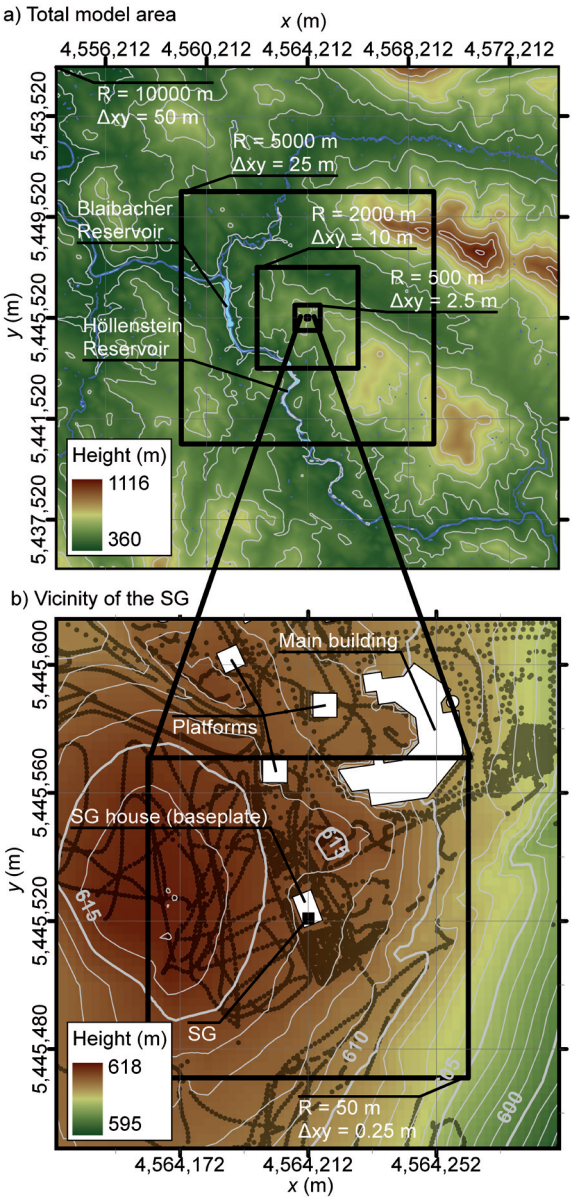

Figure 2.2: Spatial extent of the nested model domains (black squares) and the topography (DEM DGPS) for (a) the total model area and for (b) the vicinity of the SG. The model elementary cell size (Δxy) varies with the domain radius R (half the side length of the domain square). Dark grey dots are the measured DGPS points, and light grey lines are height contours (a) 100 m interval; (b) 1 m interval.

Finally, real data (daily values taken from 29 Nov 2000 to 31 Dec 2006) for groundwater, soil moisture and snow were used to model the effect of WSC on the gravitational signal. Groundwater level data were available from a monitoring well located at a distance of 200 m from the SG, where the groundwater data were adjusted to match the mean groundwater depth of 8 m. The specific yield of 5 % for the groundwater was derived by using the average specific yield of the weathered and fractured rock zone (see Table 2.1). Soil moisture was measured close to the station at a depth of 0.5 m with a TRIME sensor (measurement accuracy of ± 4 %). These data were applied to the topsoil layer (0-1 m depth) only. Variations in snow water storage were derived from precipitation, temperature and snow height data. Gaps in the climate time series have been filled using data from the nearby Höllenstein reservoir climate station. Precipitation and temperature are measured at the Wettzell Observatory climate station. Snow height was derived by interpolating snow heights measured at two different stations around the observatory. The snow water equivalent was determined by considering as snow all precipitation that fell when the temperature was below 0.7 °C, where snowfall takes place only when the snow height measured is greater than zero (input into snow storage). The melted snow water equivalent was calculated using the degree-day method, which is based on the positive daily temperatures (snow storage reduction) [*Dyck and Peschke*, 1983]. For each day, the total snow storage was derived from the snow storage input and reduction. The snow density was calculated using the storage and height data. The temperature threshold of 0.7 °C and the degree-day factor of 1.1 were calibrated by detecting snow fall and thawing on webcam pictures from 2005. Visual validation using pictures from 2006 proved their suitability. The hydrological gravity effect of these real data was calculated for a quadratic area with a side length of 100 m x 100 m and the SG in the centre, assuming that water variations measured by the different sensors are constant for the whole area. 1 January 2000 was used as the reference date for gravity variations induced by WSC.

Table 2.2: Validation results for the different DEMs. Count refers to the number of validation points. Max., Min., and Mean are the minimum, maximum, and mean of the residuals in meters, RMSE is the root mean square error (m), and ME is the mean error (m).

	Count	Min.	Max.	Mean	RMSE	ME
DEM DGPS	147	−0.60	0.48	−0.01	0.13	0.08
DEM 10	147	−2.27	6.88	0.37	1.08	0.72
DEM 25	147	−5.24	5.02	−2.01	2.46	2.12

2.4 Results and discussion

A comparison of the nested simulation model and the analytical cylinder solution shows that the difference in the results of both models is below the 0.01 µGal range for the whole area. This confirms the suitability of the nested simulation model for this study. Using the height correction according to Equation 2.2 results in a difference of 0.03 µGal in the simulated gravity response for the SG.

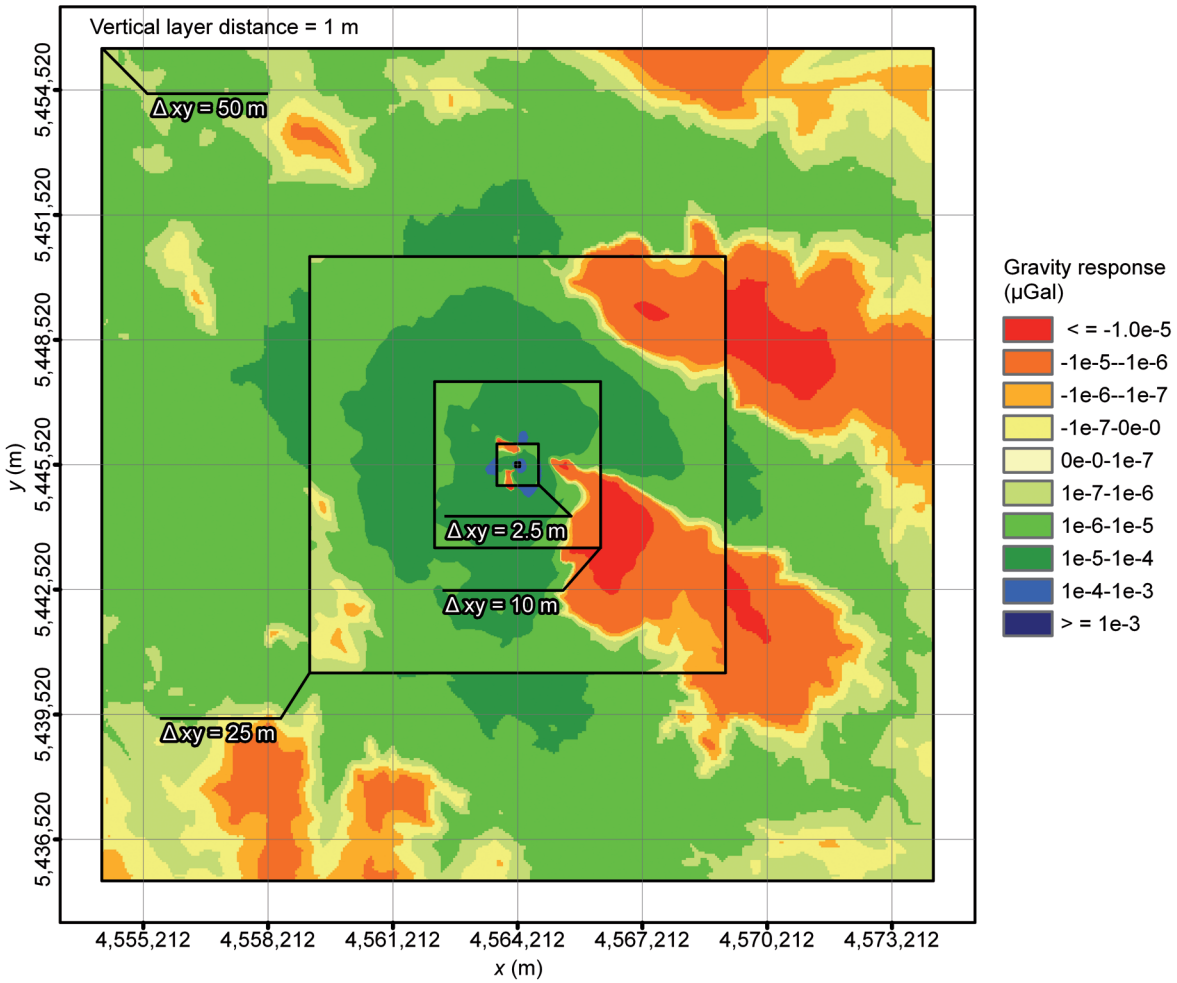

Figure 2.3: Spatial distribution of the gravity response resulting from a water mass change of 1 m (density change 1000 kg/m³) at the terrain surface (vertical layer distance to the sensor = 1 m), calculated for each element (with varying element size Δxy) for the whole nested model.

This implies that the curvature of equipotential surfaces of the gravity field can be neglected in local studies.

Taking the topography into account, a water mass change of one meter (density 1000 kg/m³) causes a gravity change of 52.49 µGal in a quadratic layer with a side length of 20 km, with a vertical distance of the WSC layer of 1 m below the gravimeter (i.e. in the top meter of the soil) and the gravimeter located in the centre of this area. The corresponding spatial distribution of the gravity response is shown in Figure 2.3. Gravity response refers to the total gravity signal of the SG that is caused by the assumed water mass change in the model domain. In this context, the spatial distribution of the gravity response refers to the contribution of each elementary body in the model domain to the total SG signal. Figure 2.3 illustrates that some areas have a negative contribution because they are located at higher elevations than the SG. Note that the spatial distribution in Figure 2.3 shows some discontinuities because the size of the elementary bodies changes depending on the distance to the SG in the nested modeling approach. When increasing the vertical distance of the layer where WSC occurs to 10 m and 20 m below the SG, the signal decreases to 51.33 µGal and 50.60 µGal, respectively (Figure 2.4). While some areas with a higher topographical position to the west of the SG show a negative gravity effect for a vertical distance of 1 m (Figure 2.4a), the spatial distribution becomes more symmetrical and includes only positive values for deeper WSC (Figures 2.4b, 2.4c). Comparing these results of the model for real topography with a flat terrain model, the same water mass changes in three different vertical distances amount to 41.90 µGal, 41.71 µGal and 41.53 µGal, respectively. These values are almost identical to the values derived by the Bouguer approximation, which also indicates that for surficial mass changes the main part of the signal is generated in the model domain. The effect of water mass changes on the SG sensor in Wettzell is thus intensified by 20 %, 19 % and 18 % as a consequence of the topography. For other SG stations too, *Meurers et al.* [2006] demonstrate that the topographical setting around the SG

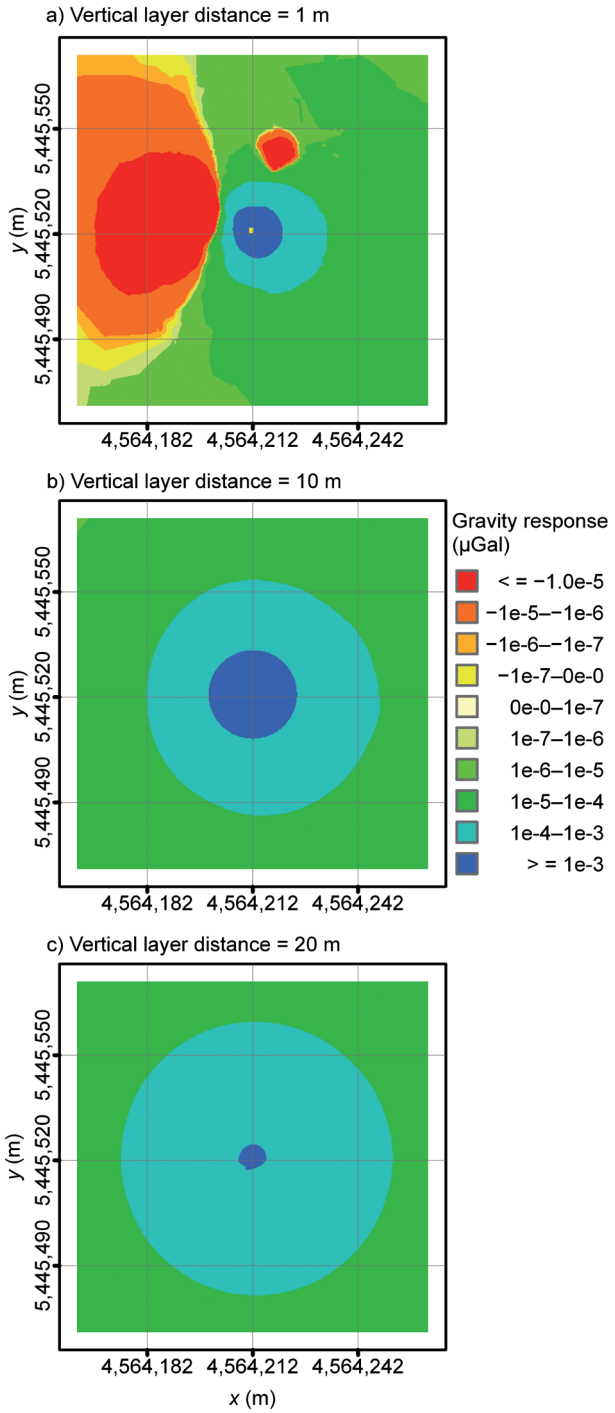

Figure 2.4: Spatial distribution of the gravity response resulting from a water mass change of 1 m (density change 1000 kg/m³) in a layer with a vertical distance of (a) 1 m, (b) 10 m, and (c) 20 m to the sensor, for an area of 100 × 100 m around the SG.

may have very different but significant effects on the SG signal.

As topography has a significant effect on the gravitational signal, the influence of DEM errors must be assessed. The results obtained with the different DEMs are displayed in Table 2.3. Assuming the same WSC as above, the difference between the results for DEM DGPS and DEM 10 falls within the range of a few µGal, whereas the difference between the results for DEM DGPS and DEM 25 is one magnitude higher and may amount to as much as 20 %. In the near field of the SG, in particular, DEM accuracy has a significant effect. At larger distances, the difference is smaller because the terrain effect weakens (Table 2.3) and also the topography data basis converges. DEMs with an RMSE of 1 m may still be suitable for gravity modeling when the acceptable error margin is set to 1 µGal and additional local topographic information is available. Similarly, *Virtanen* [1999] stresses that elevation should be mapped in detail up to a distance of about 200 m from the SG. However, DEMs with higher RMSE such as the DEM 25 are unsuitable for gravity modeling when the focus is on hydrological processes.

In the same context, information on the subsurface structures in the immediate vicinity of the SG has to be considered in the model. As presented in Figure 2.1, the SG is placed on a concrete foundation. In the above example, however, we assumed a water mass change of one meter in the topsoil for the entire model domain. When we take the concrete foundation of the SG into account and assume no water mass change in this particular area, the total SG signal decreases markedly by 8.47 µGal to 44.02 µGal. Similarly, the effect of the base plate of the SG building and its umbrella effect – which inhibits infiltration of rainfall into the soil – should be taken into account in the model.

Figure 2.5 summarizes the gravity response of the model – for real topography and taking into account the foundation – as a function of the radius of influence and a function of the depth of the mass changes. Here, radius of influence (R) refers to a square with the SG located in its centre and the square side length being twice the radius R. Both parameters – radius and depth – describe the area which gives rise to the SG gravity response. For the flat terrain model with a vertical layer distance of 1 m (and 20 m), 98 % (66 %) of the signal is generated in an area of R=50 m, 100 % (95 %) in an area of R=500 m and 100 % (98 %) in an area of R=2000 m. Signal generation for the model with real topography is as follows: 80 % (52 %) with R=50 m, 91 % (84 %) with R=500 m and 97 % (93 %) with R=2000 m. This shows that the gravity response does not simply depend on the radius of influence, but is also a function of the mass change distribution over depth and a function of topography. It follows from this that it is important to distinguish between the different water storage components because near-surface mass variations like soil moisture have a smaller sphere of influence than deeper mass changes like groundwater (see Figure 2.4).

In the following, we analyze separately the possible

Table 2.3: Gravity response caused by a water mass change of 1 m (density 1000 kg/m³) calculated for the different DEMs as a function of vertical layer distance and radius of influence R.

DEM	Vertical layer distance (m)	Response (µGal) R: 50 m	Response (µGal) R: 500 m	Response (µGal) R: 2000 m	Response (µGal) R: 10000 m
DEM DGPS	1	42.04	47.79	51.08	52.46
	20	27.91	44.59	48.91	50.60
DEM 10	1	42.72	48.65	51.94	53.35
	20	27.87	44.68	49.00	50.69
DEM 25	1	33.96	38.26	41.45	42.86
	20	28.46	44.04	48.27	49.96

maximum effect of WSC on gravimetric observations for the different water storage components. Figure 2.6 shows the relationship between the gravity response and the WSC in the snow cover, soil moisture and groundwater. A groundwater table rise of 4 m from 10 to 6 m below the terrain surface over the entire model domain in an aquifer with an average specific yield of 5 %, results in a gravity change of around 10 µGal (lower section of Figure 2.6), whereas this value amounts to 22 µGal for a maximum specific yield of 11 %. The distinct gravity response in this theoretical experiment indicates that in addition to detailed groundwater level monitoring, precise estimation of the specific yield and of the interface between weathered and fractured zone are also vital for accurate modeling of the effect of groundwater variations. Also, *van Camp* [2006] pointed out the need for a detailed mapping of subsurface characteristics in combination with the recording of time series.

The unsaturated zone was divided into two layers for this modeling experiment, i.e., into soil (0-2 m) and weathered zone (2-6 m) (Figure 2.6). This was done not only because of the geologic situation, but also to consider the dominant processes of precipitation, evapotranspiration and drainage in the soil and of drainage in the weathered zone. In the weathered zone, a maximum soil moisture change of 7 ± 4 Vol% causes a gravity response of 17 ± 10 µGal. Water saturation in the topsoil causes a maximum gravity change of 21 ± 2 µGal. Measurements of the topsoil water content, however, show that soil moisture varies between 15 Vol% and 40 Vol%. When translated

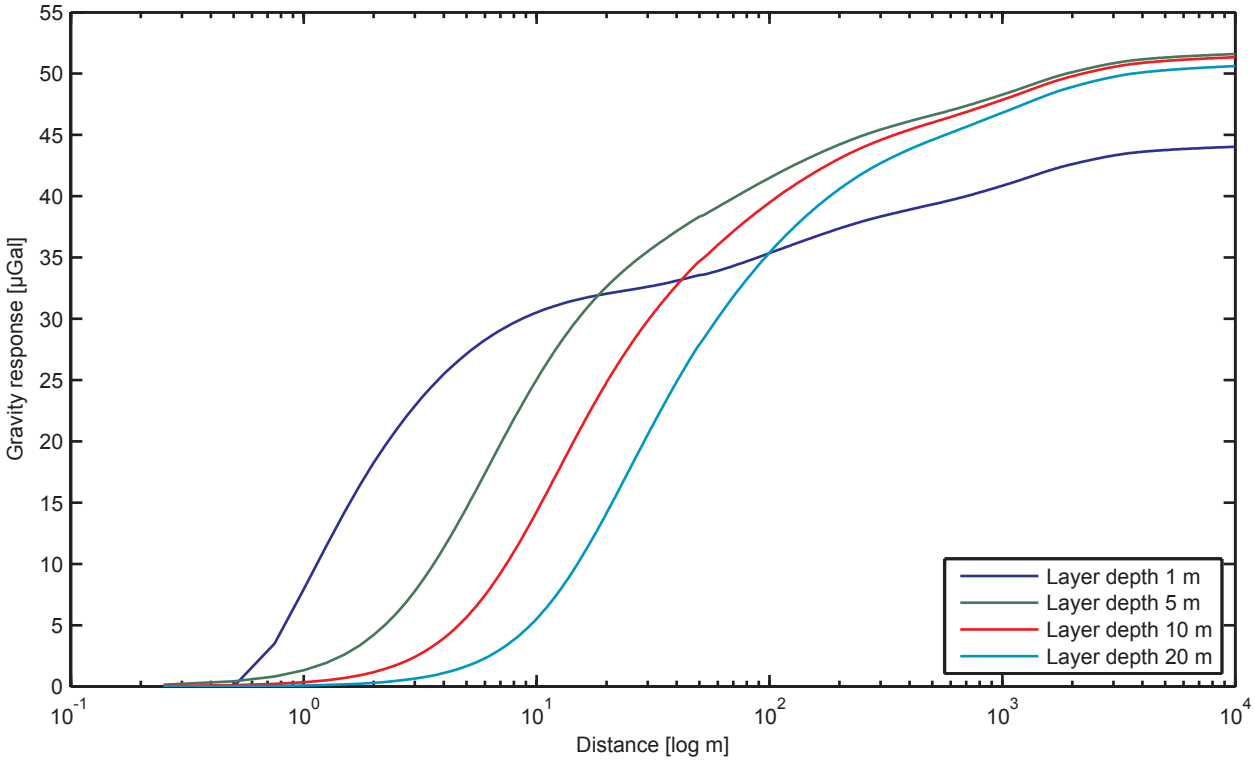

Figure 2.5: Gravity response resulting from a water mass change of 1 m (density change 1000 kg/m³) as a function of the radius of influence and the vertical layer distance of the mass change.

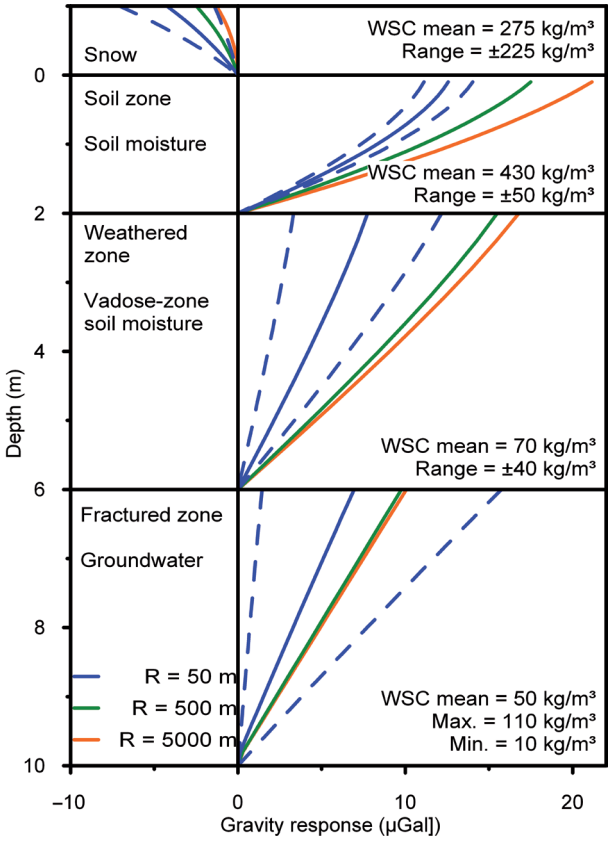

Figure 2.6: Gravity response for water storage change (WSC) in each storage compartment (snow, soil moisture, vadose zone soil moisture and groundwater). The storage compartments are progressively saturated with water from bottom-up. Dashed lines represent the maximum range of the gravity response for R=50 m taking the uncertainty of relevant parameters into account.

into gravity change, this results in a value of 12 µGal. The infiltration process can have a significant effect on the gravity signal because saturation and drainage account for mass redistribution in the soil column.

While WSC below the terrain surface generally leads to a gravity increase, snow reduces the gravity because it accumulates mainly above the SG sensor and on the roof of the SG building (top of Figure 2.6). At greater distances, the effect of snow masses is reversed because the SG is located on an elevated mountain ridge and, consequently, snow mass accumulation in the valleys adds to the gravimetric signal. Nonetheless, the highest signal change can be expected during the period of snow melt because the mass redistributes from above to below the sensor due to infiltration of snow melt water into the soil.

The gravitational effects of surface and vegetation water change are below the significance level of the SG recordings. In the unlikely event that both reservoirs are completely drained from maximum storage capacity, a gravity change of 0.19 µGal is calculated. As there are no other major water surface bodies in the study area, the effect of surface water on the SG records can be neglected in future gravity studies at the Wettzell site. However, as shown by *Bonatz and Sperling* [1995], water redistribution in surface water bodies may cause a significant gravity response for particular locations. The water storage capacity of vegetation is too small to cause marked gravity changes, which results in a maximum vegetation effect of 0.07 µGal.

When summarizing the above results for the individual water storage components, it follows that local hydrological mass variations can contribute up to 49 µGal to the SG records of the Geodetic Observatory Wettzell, where as much as 64 % of this signal is generated within a radius of 50 m, 90 % within a radius of 500 m, 97 % within a radius of 2000 m and 99 % within a radius of 5000 m. Note that these simulation results were obtained on the basis of parameters that represent the maximum plausible water mass variation in each storage component from a hydrological perspective. In real-world settings, however, it is very unlikely that all the changes will occur at the same time. For example, the annual phases of snow storage or groundwater level variations are frequently shifted in time compared to soil moisture variations [*Güntner et al.*, 2007]. Individual effects therefore compensate for each other in part. Also, maximum water storage change is not expected to occur homogeneously over the entire study area, as assumed here. In addition, other hydrological processes, such as evapotranspiration or groundwater discharge, which may reduce the variation in hydrological storages, are disregarded in the theoretical modeling experiments. As a consequence, the hydrologically-induced gravity response shown here can be considered as an extreme. It might only be observable in long-time records of the SG because of the negative correlation between frequency and intensity of extreme events in hydrology.

Figure 2.7 shows the modeled gravity response derived from the measured data for the period of November 2000 to December 2006, with the corresponding minimum and maximum possible response. The mean, maximum and minimum range of the modeled WSC effect amounts to 10.24 µGal, 19.49 µGal and 6.06 µGal. Generally, groundwater has the biggest share in the hydrological gravity signal and contributes up to 8.28 µGal by a specific yield of 5 %, 18.21 µGal by a specific yield of 11 % and 1.66 µGal by a specific yield of 1 %, followed by soil moisture with 5.46 µGal and snow with -1.25 µGal. Groundwater and soil moisture-induced gravity variations were estimated with a LaCoste & Romberg gravimeter by *Naujoks at al.* [2008] at the Geodynamic Observatory Moxa, Germany and by *Mäkinen and Tattari* [1988] at the Hyrylä Station, Finland to be up to 17 µGal and 13 µGal, respectively. The order of magnitude of snow-induced gravity variations is also similar to those

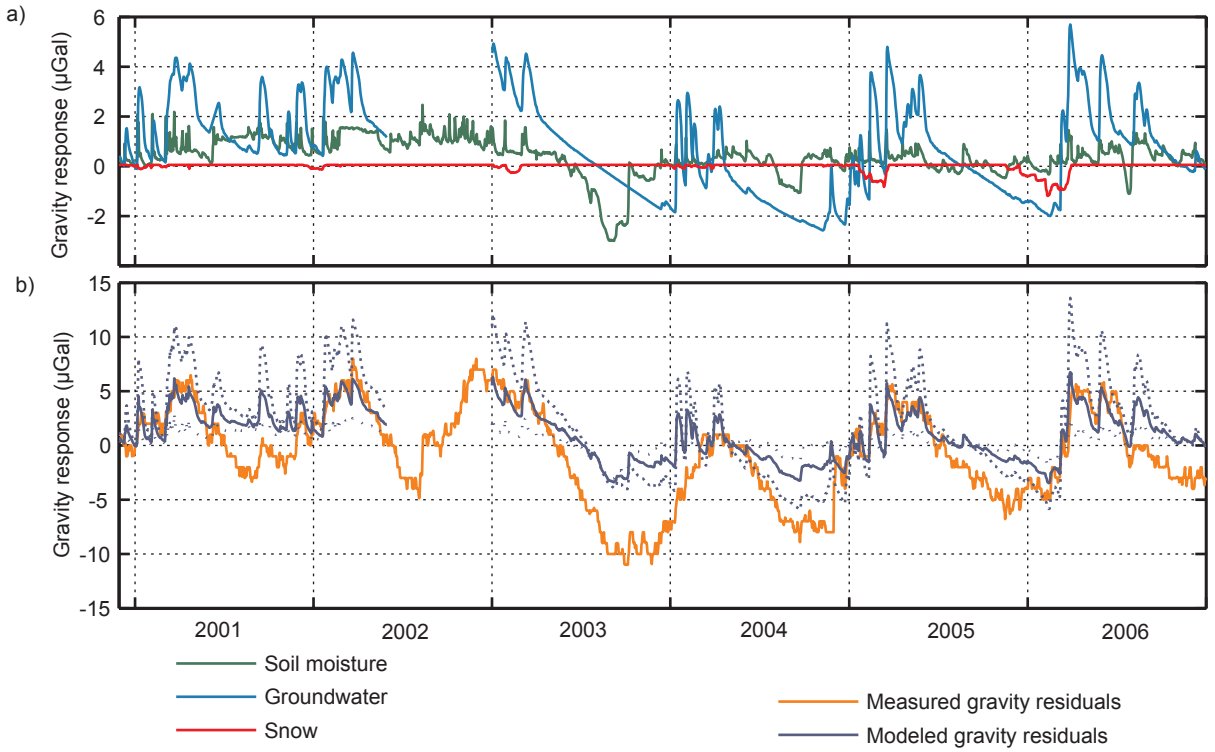

Figure 2.7: (a) The modeled gravity effect of the different water storage components from 29 November 2000 to 31 December 2006 and (b) the gravity residuals measured by the SG and the total sum of the modeled gravity signal with a mean specific storage of 5 % for groundwater. Dotted blue lines are the total sum of the modeled gravity for maximum (11 %) and minimum (1 %) specific storage.

reported by *Virtanen* [1999] for the Methsähovi Station in Finland. The time series of the groundwater effect is dominated by a seasonal pattern. On top of this, significant short-term variations during wet periods can also be observed. These events are also partly represented with smaller magnitudes in the soil moisture time series. During 2003, in which Central Europe experienced an exceptionally dry summer period, groundwater and soil moisture storage were depleted causing a minimum in the gravity signal. The modeled gravity signal shows a reasonable temporal correlation with the gravity residuals of the SG (corrected by tides, earth oscillation, instrument drift and atmospheric pressure). Especially during wet periods, the modeled and measured variations fit well, whereas for dry periods the time series diverge. Apart from the uncertainties due to the processing of the gravity residuals, these differences may have several reasons which are discussed in the following part.

The model based on the observation data is a simplification of the real conditions because WSC are highly variable in space and the sensors installed cannot capture this variability. With regard to groundwater, the area surrounding the observatory is highly complex due to the undulating topography combined with the geological conditions. Groundwater level measurements in nearby monitoring wells are only weakly correlated and so the assumption that the aquifer is a continuous layer that follows the topography is not valid. The aforementioned result that the modeled and measured series deviate especially during dry periods may be due to the fact that the groundwater well used here is located in a depression while the SG building is built on a ridge. This implies that groundwater below the gravimeter depletes faster while the decrease of the groundwater level at the gauge is delayed due to inflowing water from the surrounding area.

For the calculated soil moisture gravity effect it should be considered that, firstly, in hydrology, soil moisture is regarded as a highly variable parameter in space and time. Therefore, only one sensor cannot be considered as a representative sample to estimate the soil moisture dynamics and patterns around the SG. Secondly, no information was available on the soil moisture distribution over depth. Finally, apart from soil moisture measurements being influenced by different soil parameters, requiring site-specific calibration for accurate measurements, the results depend on the soil moisture measurement technique itself.

The accuracy of the snow model was not assessed statistically, but it was found to match closely with webcam photos when a visual comparison was made. Snow density, however, could not be validated by this method.

2.5 Conclusions

The results indicate that the hydrological effect of local water storage variations has to be considered in high-accuracy studies of gravity monitoring. A nested model discretization is especially useful for investigating the gravity response of SGs caused by WSC. Topography plays an important role in gravity signal modeling. Therefore, not only must topography be included in the model domain, but also DEM accuracy has to be taken into account and, if necessary, DEM uncertainties have to be reduced with supplementary measurements. The exact location of the SG, the surrounding and subsurface structures in the immediate vicinity are vital for the calculation of the WSC effect on gravity. With regards to the radius of influence of mass changes on the SG recordings, gravity is not only a function of the distance of mass changes but also depends on the topography and on the distribution of mass changes over depth. For local studies at sites of superconducting gravimeters with current accuracies of about 0.1 to 1 μGal, a limitation of the radius of influence to 1000 m seems to be justified for hydrological mass variations because around 90 % of the signal is generated in this area. The greatest benefits from detailed studies of WSC can be expected within a radius of 50 to 100 m around the SG station. In local studies, the curvature of equipotential surfaces can be neglected.

The results of the modeled gravity effect for theoretical WSC, as well as for real data, lead to the conclusion that groundwater has the largest contribution to the gravity signal, followed by soil moisture and snow; but they may also indicate that until now the influence of WSC in the vadose zone might be underestimated. For the Wettzell Observatory, surface water and WSC in the vegetation cover can be neglected. The two time series of the total modeled gravity signal and the measured gravity residuals show similar seasonal and shorter-term dynamics. At the same time, several differences exist due to the limited coverage and representativeness of hydrological data, as they do not fully describe the spatio-temporal variations of water storage for the individual components. Apart from temporal changes to the groundwater level, the spatial characterization of the aquifer in terms of porosity and the transition between the weathered and fractured zone are fundamental. Therefore, complementary measurements of groundwater level variations in additional boreholes and the estimation of the physical properties of the borehole cores in combination with geophysical methods are the subjects of ongoing work in the study area.

Soil moisture contributes significantly to the gravitational signal, but is highly variable in space and time. To estimate 4D soil moisture patterns for future analyses, a detailed multi-sensor soil moisture monitoring system has recently been installed around the SG Wettzell. The snow effect can account for several μGal, but generally has the reverse effect compared to groundwater or soil moisture. Up to now, the snow storage change is estimated using a simple model, but in future it will be estimated based on direct measurements of the snow water equivalent.

Chapter 3:

Measuring the effect of local water storage changes on in-situ gravity observations: Case study of the Geodetic Observatory Wettzell, Germany

Measuring the effect of local water storage changes on in-situ gravity observations: Case study of the Geodetic Observatory Wettzell, Germany

Abstract

Local water storage changes (WSC) are a key component of many hydrological issues, but their quantification is associated with a high level of uncertainty. High precision in-situ gravity measurements are influenced by these WSC. This study evaluates the influence of local WSC – estimated using hydrological techniques – on gravity observations at the Geodetic Observatory Wettzell, Germany. WSC are comprehensively measured in all relevant storage components, namely groundwater, saprolite, soil, top soil and snow storage, and their gravity response is calculated. Total local WSC are derived and uncertainties are assessed. With the exception of snow, all storage components have gravity responses of the same order of magnitude and are therefore relevant for gravity observations. The comparison of the total gravity response of local WSC to the gravity residuals obtained from a superconducting gravimeter shows similarities in both short-term and seasonal dynamics. A large proportion of the gravity residuals can be explained by local WSC. The results demonstrate the limitations of measuring total local WSC using hydrological methods and the potential use of in-situ temporal gravity measurements for this purpose. Nevertheless, due to their integrative nature, gravity data must be interpreted with great care in hydrological studies.

Published as:

Creutzfeldt, B., A. Güntner, H. Thoss, B. Merz, and H. Wziontek (2010), Measuring the effect of local water storage changes on in-situ gravity observations: Case study of the Geodetic Observatory Wettzell, Germany, Water Resources Research, 46, W08531, http://dx.doi.org/10.1029/2009WR008359.

3.1 Introduction

Until now, local water storage changes (WSC) have been considered as only measurable on the point scale (e.g. piezometer wells, soil moisture probes), but they are a key component in catchment characterization [*Kirchner*, 2009]. High precision in-situ gravity measurements are influenced by local WSC in groundwater, soil moisture, snow or surface water storage. Gravity observations may be used for hydrological modeling because many hydrological models are based on the water balance equation; they are generally run with input fluxes and the system parameters are calibrated to match the outflow fluxes. Permanent gravity observations provide information about system changes and may be used as an additional calibration parameter. For example, *Werth* [2009a] calibrated a global hydrological model against runoff and global gravity variations using a two-dimensional calibration scheme.

Many different studies have highlighted the relationship between local WSC and in-situ gravity measurements, for example, for removing the "hydrological noise" from gravity observations [e.g. *Bower and Courtier*, 1998; *Crossley et al.*, 1998; *Virtanen*, 2001], for comparing the signal with the results from the GRACE satellite gravity mission [e.g. *Crossley et al.*, 2003; *Llubes et al.*, 2004; *Neumeyer et al.*, 2008], for studying hydrological processes or for deriving hydrological parameters. In groundwater studies, time lapse gravity measurements in conjunction with pump tests or groundwater table fluctuations are used to estimate in-situ the specific storage coefficient [e.g. *Gehman et al.*, 2008; *Pool and Eychaner*, 1995]. In the study by *Hokkanen et al.* [2006], the fracture gaps and the porosity were used as a calibration parameter. *Van Camp* [2006] used soil moisture measurements to calculate the gravity effect of soil moisture, using the block content of the soil as a calibration factor. *Jacob et al.* [2009] used the gravity measurement to derive the apparent porosity in the vadose zone.

Recently, the focus has been on the combination of spatially semi-distributed hydrological models and gravity observations. *Hasan et al.* [2008] calibrated a lumped soil moisture storage model and a hillslope-storage Boussinesq model for the groundwater against runoff and in-situ gravity signals. *Naujoks et al.* [2009] used a hydrological model based on hydrological response units. The derived hydrological masses were spatially distributed according to a geophysical underground model and finally compared to the gravity data.

In spite of these promising results, the hydrological effect is still the least understood signal component in gravity measurements. After correcting the integral gravity signal for comparatively well-known effects of polar motion, ocean and Earth tides and atmospheric mass variations, the remaining signal – the gravity residuals – is considered to be caused mainly by WSC. Besides the influence of local water masses by Newtonian attraction, the deformation of the Earth's crust and the Newtonian attraction due to large-scale water storage variations also influence the gravity residuals. In the case of the Geodetic Observatory Wettzell, Germany, local WSC can contribute up to tens of μGal to the gravity residuals [*Creutzfeldt et al.*, 2008] while the influence of large-scale WSC is about one order of magnitude smaller [*Wziontek et al.*, 2009c].

The influence of local WSC (attraction), large-scale storage changes (attraction and deformation), and other non hydrology-related mass effects on in-situ gravity observations needs to be defined before (1) using superconducting gravimeters (SGs) as a measurement tool for small-scale hydrological studies, (2) comparing local gravity observations with global gravity observations such as those from the GRACE satellite mission, and (3) studying geodynamic phenomena based on gravity data such as postglacial rebound or oscillations of the Earth's core (e.g. Slichter modes). Since the influence of local WSC is considered to be the major part of the SG residuals, this study will focus on the estimation of local hydrological masses and the corresponding gravity response.

As pointed out by *Gettings et al.* [2008], *Jacob et al.* [2008] or *Naujoks et al.* [2009], it is necessary to consider all relevant hydrological water storage components in local studies. As highlighted by *Pool* [2008], focusing on only one storage component may lead to an incorrect result. We are not aware of any study that has measured all possible water storages and compared them to the gravity signal.

In this study, we monitor all different local water storage components using hydrological measurement techniques and we determine their effect on in-situ gravity observations. In order to avoid integrating information that may not originate from local WSC, it is essential to exclude any calibration against the SG signal when estimating the local WSC from the observations. We therefore apply a purely observation-based approach to the superconducting gravimeter at the Geodetic Observatory Wettzell, Germany that we selected for our study.

For this site, *Creutzfeldt et al.* [2008] showed that between 52 % and 80 % of the local hydrological gravity signal is generated within a radius of 50 m around the SG. The higher percentages apply to situations where WSC occur closer to the terrain surface, meaning that soil moisture has a smaller sphere of influence than groundwater. About 90 % of the signal is generated in an area within a radius of around 1000 m. Therefore, within the scope of this study, we focus on the direct vicinity of the SG Wettzell and on water (re-)distribution over depth. We assume that for this small radius of influence, the variability of the hydrological state variables and their gravity effect are more pronounced over depth than over

area. Following this assumption, we explicitly resolve the variability over depth in a 1D approach. The unresolved spatial variability is recognized partially in a simple uncertainty analysis based on observation data. We pursue this 1D approach by focusing separately on each storage component, namely snow (section: 3.3 Snow storage), soil moisture (section: 3.4 Top soil and soil storage (unsaturated zone)), groundwater (section: 3.5 Groundwater storage (saturated zone)) and saprolite water (section: 3.6 Saprolite storage (unsaturated zone)). Processing of the SG data, calculation of the gravity response due to the WSC and the comparison are described in the section 3.7 'Gravity and water storage change'. Finally, we discuss the different sources of uncertainty and the potential applications/limitations of the hydrological use of SG measurements.

3.2 Study area

The Geodetic Observatory Wettzell, operated by the Federal Agency for Cartography and Geodesy (BKG), is located on a mountain ridge in the southeast of Germany [*Schlüter et al.*, 2007]. Around the SG, we mapped the topography using differential GPS (DGPS) and created a Digital Elevation Model (DEM) by merging 14,000 DGPS measurements and an existing DEM with a cell size of 10 m and mean height accuracy of 1 m (see Figure 3.1).

The study area is characterized by a temperate climate with a mean annual precipitation of 863 mm, a potential evapotranspiration (according to *Haude* [1955]) of 403 mm, and a mean annual temperature of 7 °C (climate station Höllenstein-Kraftwerk, 1947-2005). The hydrologically relevant climate parameters (air temperature, relative humidity, wind, precipitation, snow, global radiation and net radiation) are measured at the Observatory Wettzell. Data gaps were filled with data of climate station Nr. 127 Allmannsdorf (Distance ~6 km) [*LfL*, 2009]. For the study period between 18 July 2007 and 31 March 2009, precipitation amounted to 1390 mm and the average air temperature was 7.75 °C. All data used in this study are processed to one hour intervals.

The area around the SG Wettzell is rural, characterized by a mosaic of grassland and forest. The immediate area around the SG Wettzell is dominated by grassland. The geology consists of acidic metamorphic rocks (Biotite-Gneiss). In general, this basement zone merges seamlessly with a fractured zone, followed by a saprolite cover consisting mainly of Grus (weathered Gneiss). The saprolite can be covered by a periglacial weathering cover [*Völkel*, 1995].

The SG Wettzell is positioned near ground level and is based on a concrete foundation with a size of 1.4 × 1.4 × 1.2 m (width × depth × height) in a building with a length of 9.7 m and a width of 5.7 m. The base plate has a thickness of 0.3 m and precipitation from the SG roof is drained away through a tank ~20 m from the SG [*Creutzfeldt et al.*, 2008].

The underground was characterized using undisturbed and disturbed soil samples from two different boreholes and three different soil pits (Figure 3.2). The soil samples were analyzed in the laboratory: (1) the grain size distribution was estimated by sieving and through the sedimentation method, (2) the organic matter by

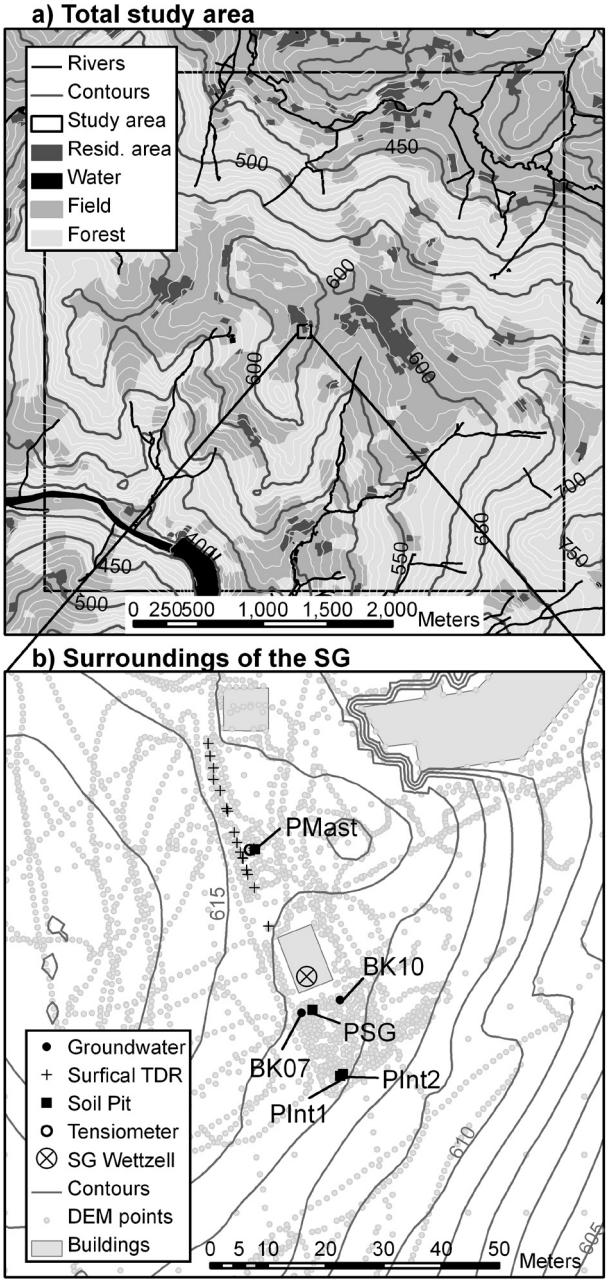

Figure 3.1: (a) Map of the total study area with land-use classification [*BKG*, 2005], rivers and contour lines (contour distance 50 m (dark grey) and 10 m (light grey)). (b) Map of the surroundings of the SG with hydrological sensors, DGPS measurement points and contour lines (contour distance 1 m).

Table 3.1: Physical characteristics of the different hydrolog. storage components. Numbers of samples in brackets.

Parameter	Unit	Top soil storage	Soil storage	Saprolite storage	Groundwater storage
Description	-	Ap horizon	IIBv/IIIfBt/IVCv horizon	Saprolite	Fractured zone
Depth	m	0.00-0.30	0.30-1.25	1.25-11.00	11.00-19.00
Organic matter	%	5.30 ± 0.69 (3)	4.29 ± 1.75 (3)	-	-
Gravel (>2000 µm)	%	6.97 ± 1.59 (3)	3.08 ± 1.65 (3)	14.40 ± 7.74 (22)	-
Sand (>63 µm)	%	53.50 ± 7.70 (3)	57.15 ± 11.45 (3)	80.49 ± 2.92 (22)	-
Silt (>2 µm)	%	26.61 ± 5.91 (3)	24.80 ± 7.60 (3)	17.29 ± 2.63 (22)	-
Clay (<2 µm)	%	14.59 ± 2.66 (3)	13.76 ± 2.51 (3)	1.96 ± 0.95 (22)	-
Bulk density	g/cm³	1.43 ± 0.15 (19)	1.53 ± 0.14 (30)	1.75 ± 0.27 (35)	-
Porosity	m³/m³	0.46 ± 0.06 (19)	0.42 ± 0.05 (30)	0.34 ± 0.10 (35)	-

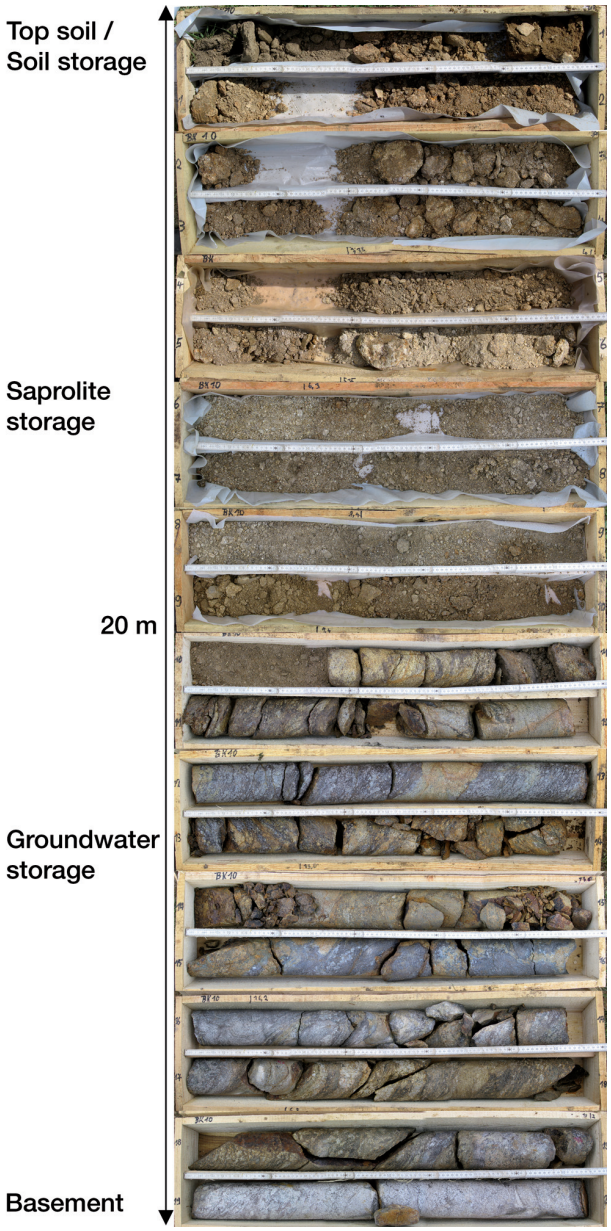

the loss-on-ignition method with a muffle furnace, (3) the bulk density by weight and volume of the sample, (4) the particle density with a gas pycnometer and (5) the porosity from the bulk and particle density. Based on these results and hydrological instrumentation techniques, the underground is characterized and classified into different geological zones that are related to the following hydrological storage components: (1) the top soil storage (0.0-0.3 m), (2) the soil storage (0.3-1.25 m), (3) the saprolite storage (1.25-11.0 m) and (4) the groundwater zone (11.0-19.0 m) (see Figure 3.2 and Table 3.1). In this study, "groundwater zone" refers to the saturated subsurface zone where water is free to move under the influence of gravity and is associated with the fractured zone. The three other storages belong to the vadose zone where water flow is mainly controlled by gradients of the capillary potential.

3.3 Snow storage

The snow mass and height are measured using a snow monitoring system consisting of a snow pillow and an ultrasonic distance sensor [*Sommer*, 2007; 2008]. The snow pillow measures the snow load – the snow water equivalent – using a pressure transducer and the ultrasonic sensor measures the snow depth. The snow height record was inspected visually and clear outliers were replaced with adjacent interpolated measurements. Snow water equivalent values were only allowed if the snow

Figure 3.2: Core of borehole BK10 and the corresponding hydrological storage components: 1) the top soil storage (0.0-0.3 m), 2) the soil storage (0.3-1.25 m), 3) the vadose saprolite storage (1.25-11.0 m) and 4) the saturated groundwater zone (11.0-19.0 m). Note that the abrupt transition at the depth of ~10 m is due to a change in the drilling technique from pile-driving to diamond core drilling (length of one core box is 1 m).

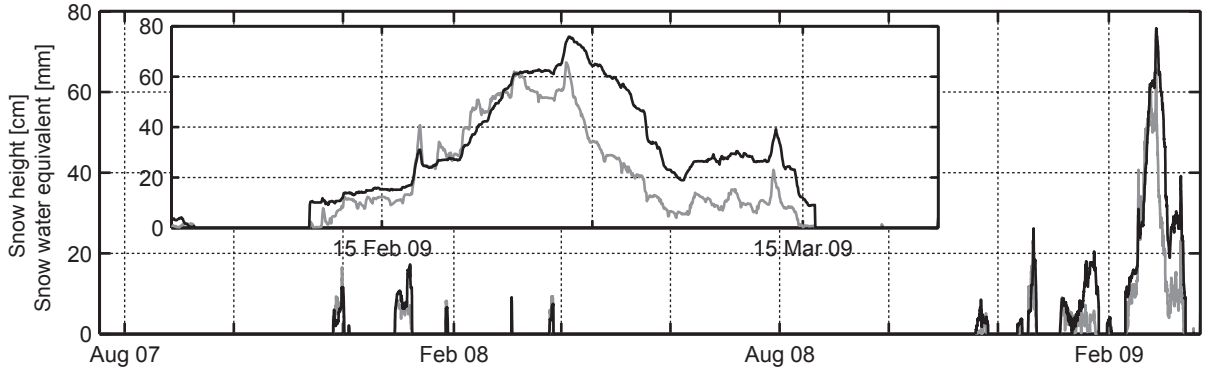

Figure 3.3: Seasonal variation of snow height (grey line) and snow water equivalent (black line) for the whole study period and for the snow event during February/March 2009.

height was greater than zero because the snow pillow measurements are influenced by seasonal temperature variations due to the expansion of trapped air bubbles in the water-glycol mixture of the snow pillow. Figure 3.3 shows the time series of the snow height and snow water equivalent. Nearly no snow was observed during the winter of 2007/08. On 27 February 2009, a maximum snow height of around 656 mm and a corresponding snow water equivalent of 75 mm were measured. From here, snowmelt started and lasted until 16 March 2009.

3.4 Top soil and soil storage

The soil is made up of gravelly sandy loamy brown soils (Cambisols), with an Ap/IIBv/IIIfBt/IVCv horizon sequence in the immediate vicinity of the SG. The top soil moisture between 0.0 and 0.3 m was measured by 18 0.3 m long 3-rod Time Domain Reflectometry (TDR) probes. Soil moisture between 0.3 and 2.0 m depth was monitored in three different soil pits (PSG, PMast and PInt). PSG and PMast consisted of TDR probes at depths of 0.3, 0.4, 0.6, 1.0, 1.5 and 2.0 m and had a distance to the SG of 6 and 17 m, respectively. PInt comprised two TDR profiles (PInt1 and PInt2) at a distance of 17 m to the SG and of 1 m to each other (Figure 3.1). In this soil pit, soil moisture was measured at 0.3, 0.4, 0.6, 1.0 and 1.5 m. 3-rod 0.075 m long TDR probes were used for all TDR profiles.

All TDR probes were connected to TDR100 time domain reflectometers, and data were generally logged every 15 minutes by a CR1000 System [*Campbell Scientific Inc.*, 2008; 2009]. The soil moisture was calculated from the dielectric permittivity using the Topp equation [*Topp et al.*, 1980] as this approach is suitable for loamy sandy soils and can be expected to be accurate enough, especially if one is mainly interested in the relative soil moisture changes as is the case in our study [*Roth et al.*, 1992]. Each time series was inspected visually and clearly anomalous measurements caused by incorrect analysis of the TDR waveform were removed. The data were resampled to one-hour intervals using a smoothing algorithm. Due to short-circuiting of the PMast probe at 1.0 m depth during installation, the probe was removed from further analysis.

The top soil moisture variation is illustrated in Figure 3.4a and the soil moisture variation at different depths in Figures 3.4b-3.4f. Temporal variations in soil moisture correspond well between all sensors. The offset in absolute values of PSG 0.6 m (Figure 3.4c) and the deviation at a depth of 1.5 m (Figure 3.4e) of the different TDR profiles may be due to different soil material or installation problems. Such offsets were not corrected in this study because we focused on the relative temporal change of water storage.

The upper sensors exhibit more pronounced weather-related variations than the lower ones. We can clearly identify a drying period of the soil in the summer of 2008 and a wetting front from the top in autumn. In summer and autumn of 2008, a decline of soil moisture occurred below 1.0 m, implying that only a little percolation occurs below this zone. The moisture decline for profile PInt is not as pronounced as for the other profiles, probably due to the higher clay/silt content. On 31 July 2008, the dry period ended with a heavy rainfall event of ~ 60 mm/2 h, reflected by a sharp increase of soil moisture. The very fast reaction of some probes up to a depth of 1.5 m indicates the activation of macropores as preferential flow paths. These macropores are most likely an immanent property of the soil, because the TDR probes were installed 0.1 m away from the soil pit wall in undisturbed soil. Also, the soil in the soil pit was highly compacted after installation so that artificial flow paths to the probes are not likely to exist. During winter (December 2007 – January 2008 and December 2008 and March 2009), markedly lower apparent soil moisture values measured at up to 0.4 m (Figure 3.4a,b) do not reflect a real decrease of soil water content, but are due to soil freezing as confirmed by soil temperature measurements. The TDR system

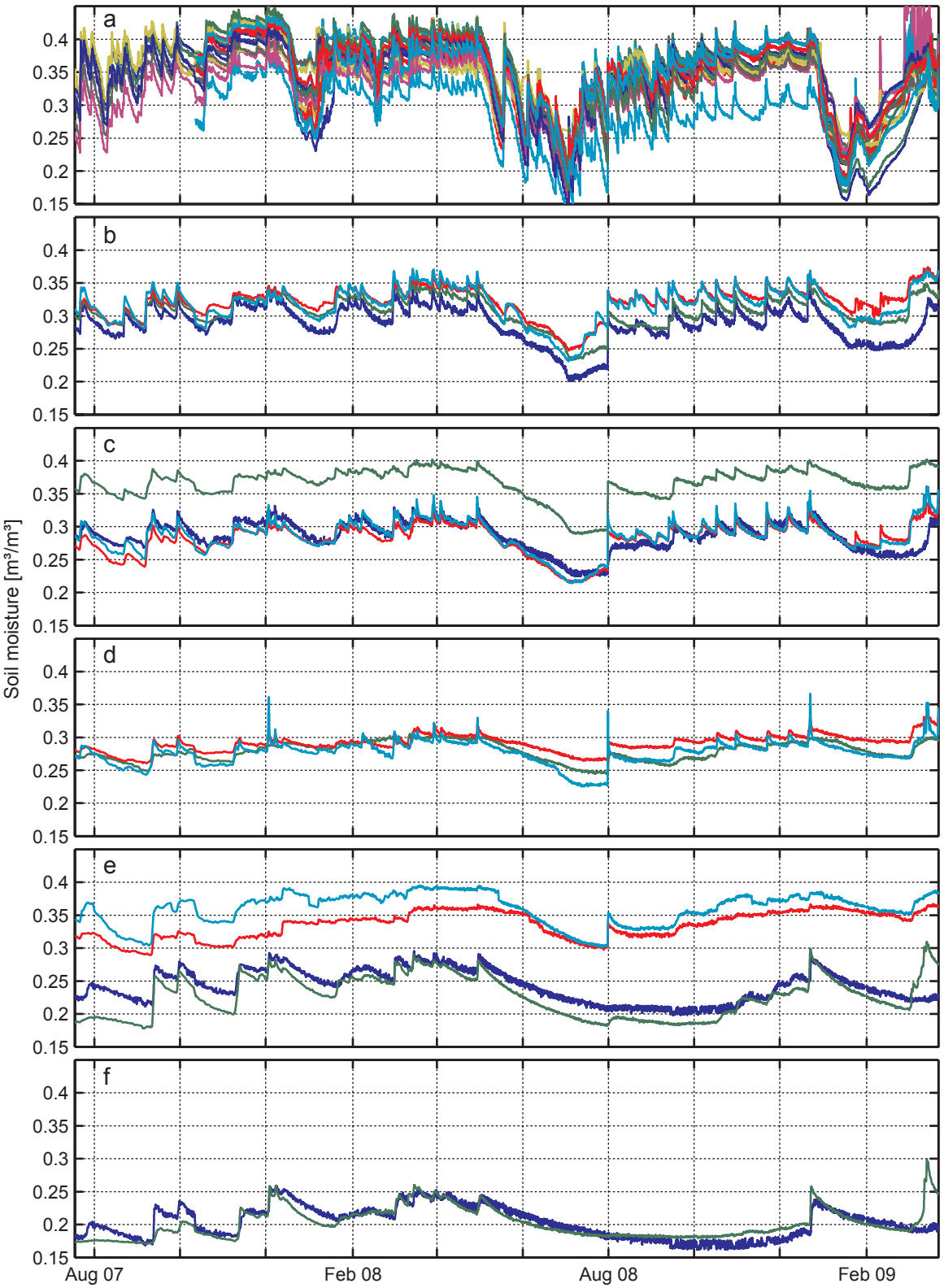

Figure 3.4: Soil moisture variation at different depths. a) Top soil moisture variations from 0.0-0.3 m measured by 18 different TDR probes (different colored lines). b) – f) Soil moisture variation at the depth of 0.4 m (b), 0.6 m (c), 1.0 m (d), 1.5 m (e) and 2.0 m (f) measured by four TDR profiles: PMast (blue line), PSG (green), PInt1 (red) and PInt2 (turquoise).

Table 3.2: Aquifer parameters estimated from a pump test by analyzing drawdown and recovery data.

Parameter	Jacob straight line method		Theis's method		Mean
	Drawdown	Recovery	Drawdown	Recovery	
T [m²/h]	9.77×10^{-2}	8.57×10^{-2}	4.95×10^{-2}	6.99×10^{-2}	7.57×10^{-2}
S_y [-]	6.30×10^{-3}	6.86×10^{-3}	1.61×10^{-2}	9.15×10^{-3}	9.61×10^{-3}
K_s [m/h]	1.40×10^{-2}	1.22×10^{-2}	7.07×10^{-3}	9.98×10^{-3}	1.08×10^{-2}

records the change in soil dielectric permittivity due to the change of the aggregate state of water. Observed soil temperature values indicate that below a depth of 0.4 m, a real decrease of soil moisture may be due to cryosuction [*Hohmann*, 1997] caused by the frozen near-surface soil horizons.

3.5 Groundwater storage

The aquifer around the Geodetic Observatory Wettzell is unconfined and is characterized by high heterogeneity. Groundwater is usually associated with the fractured zone, but may extend to the saprolite zone. The water table is highly variable over time and space. In different groundwater wells at the observatory, the water table depth varies between 4 and 15 m. It can show seasonal fluctuations as high as 4 m and a quick response to single rainfall events.

Groundwater table, electrical conductivity and temperature are monitored with multi-parameter sensors [*SEBA*, 2008] (Figure 3.5) in the boreholes close to the SG (Figure 3.1). The mean water table depth is 13.38 m (BK07) and 13.14 m (BK10) below ground surface. The groundwater table variations of both wells show a seasonal course and are very similar (correlation coefficient 0.9985). The seasonal amplitude amounts to 2.8 m. The steep rise in the groundwater table of ~2.2 m from 6 March 2009 to 20 March 2009 is caused by snowmelt water (see also Figure 3.3).

From 11 June 2008 7:00 a.m. to 13 June 2008 9:00 a.m. (Central European Time), a pump test was conducted to estimate the specific yield and to investigate the influence of the pump test on the SG measurements. In total ~12.3 m³ water were pumped from BK07, which corresponds to a constant pumping rate of 0.07 l/s. The water was drained into the sewerage 60 m away from the SG. The drawdown and the recovery of the water table after the pump was deactivated were measured in the pumping well as well as in the observation well (see also Figure 3.11).

The analysis of the pump test is based on the methods summarized by *Kruseman and de Ridder* [1990] and *Langguth and Voigt* [1980]. Based on the two bore-cores (BK07 and BK10), we set up a simplified hydrogeological model, assuming a homogeneous, isotropic and unconsolidated aquifer (highly fractured Gneiss). The aquifer basement is estimated to be at a depth of 19 m and, hence, the aquifer thickness is about 7 m and the pumping well fully penetrates the aquifer. The time-drawdown curve did not show the phenomenon of delayed water table response. Therefore, we can analyze the pump test using the method suggested by *Cooper and Jacob* [1946] and by *Theis* [1935], applying a correction of the displacement data using the approach of *Jacob* [1944]. Both approaches were used to estimate the transmissivity (T), the saturated hydraulic conductivity (K_s) and the storativity (S) from the drawdown and recovery data, taking into account that these approaches are only valid under the assumptions listed above and by *Kruseman and de Ridder* [1990]. The straight line method is valid because the

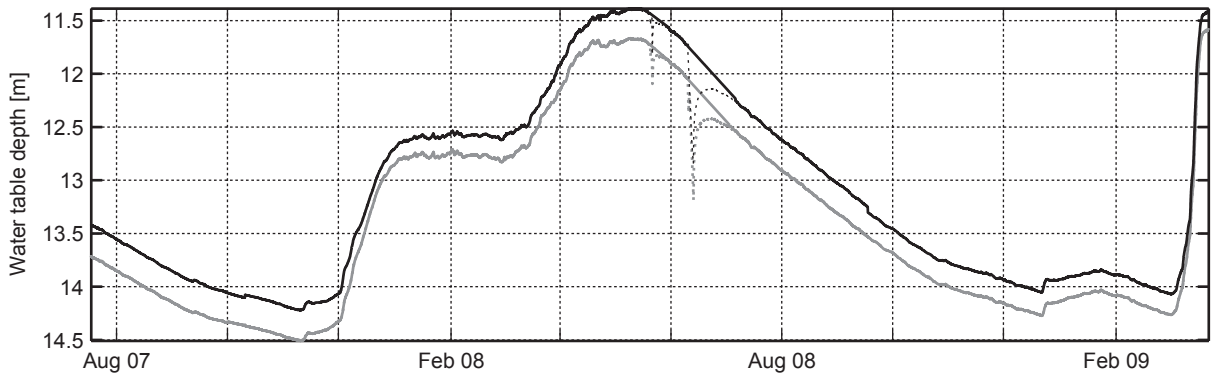

Figure 3.5: Water table depth variations of the two monitoring wells BK07 (grey line) and BK10 (black line). Dotted lines are raw and solid lines pump test corrected data.

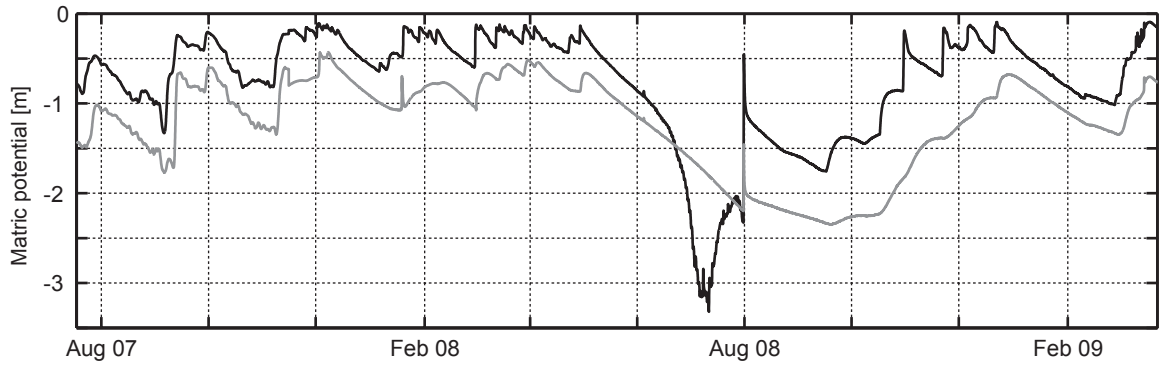

Figure 3.6: Seasonal variation of matric potential measured by tensiometers in ~1.0 m (black line) and ~1.4 m depth (grey line).

precondition that $t >= 3.8(S/T)r^2$ applies to the pump test, where r is the radial distance between pumping and observation well [m], and t the pump duration [h] [*TGL*, 1974]. The results of the pump test are presented in Table 3.2.

In unconfined aquifers, the storativity is essentially equal to the specific yield (S_y) which refers to the drainable porosity. The estimated specific yield ranges from 6.30×10^{-3} to 1.61×10^{-2} and is in line with literature values for fractured igneous rocks [e.g. *Maréchal et al.*, 2004]. For the fractured zone of the Bavarian Forest, *Rubbert* [2008] estimated the specific yield to range between 5×10^{-4} and 2×10^{-2}. Assuming that during the snowmelt event in February/March 2009 all water stored in the snow cover (75 mm) flows into the groundwater storage and causes a water table rise of 2.2 m there, S_y can be estimated to be 3.41×10^{-2}. This value reflects the upper boundary for S_y, because it is likely that not all snow water reaches the groundwater. For example, surface runoff or accumulation of snow water in the vadose zone can also occur.

Depending on the method used, hydraulic conductivity varies from 7.07×10^{-3} to 1.40×10^{-2} m/h. Assuming steady-state flow conditions at the end of the pump test, hydraulic conductivity was estimated at 2.93×10^{-2} m/h based on Thiem's method. These values are of the same order of magnitude and correspond to the hydraulic conductivity values of the Upper-Palatinate-Bavarian-Forest region [*Büttner et al.*, 2003; *Rubbert*, 2008]. *Raum* [2002] conducted tracer experiments about 1 km away from the study area. He estimated that the "maximum distance velocity (v_{max})" for six different flow paths ranges between 1.83×10^{-1} and 1.52×10^{1} m/h. Assuming that the mean distance velocity is half of v_{max}, we can estimate K_s based on the hydraulic gradient and the estimated mean specific yield to range from 1.36×10^{-2} to 9.74×10^{-1} m/h. These values are one magnitude greater than the estimated hydraulic conductivity and represent the upper range of the estimated K_s values, since these are derived from v_{max}.

3.6 Saprolite storage

The saprolite zone consists mainly of Grus (weathered Gneiss) at depths between 1.3 and 11.0 m (see Figure 3.2). This is generally a zone of high heterogeneity [*Rubbert*, 2008], including quartz veins and float blocks.

Direct measurements of WSC were not possible because the high rock content (Table 3.1) and float blocks prevent the installation of soil moisture probes, access tubes or soil pits in this zone. We therefore estimated the WSC in the saprolite zone $\Delta S_{Saprolite}$ [m/h] by estimating the upper and lower boundary flux

$$\Delta S_{Saporlite} = q_P - q_R \tag{3.1}$$

where the deep percolation (q_P [m/h]) refers to the water flux from the soil to the saprolite storage and the groundwater recharge (q_R [m/h]) is the flux from the saprolite to the groundwater storage.

3.6.1 Deep percolation

For the estimation of the upper boundary flux – the deep percolation flux (q_P) [m/h] – we used the Buckingham-Darcy law [*Buckingham*, 1907]

$$q_p = K(h)\left(\frac{dh}{dz}+1\right) \tag{3.2}$$

where $K(h)$ is the hydraulic conductivity [m/h], h is the matric pressure head [m] and z is the vertical distance. The matric pressure head gradient dh/dz is estimated from tensiometer measurements at depths of ~1.0 and ~1.4 m (TS1 tensiometers, manufactured by UMS Munich). The tensiometer measurements started on 15 November 2007 03:00 p.m. Between 18 July 2007 and 15 November 2007, matric pressure head values were derived from TDR measurements at the appropriate depth using the van Genuchten relationship derived from the tensiometers and TDR measurements. Figure 3.6 shows the time series for the tensiometer observations. The dry period of

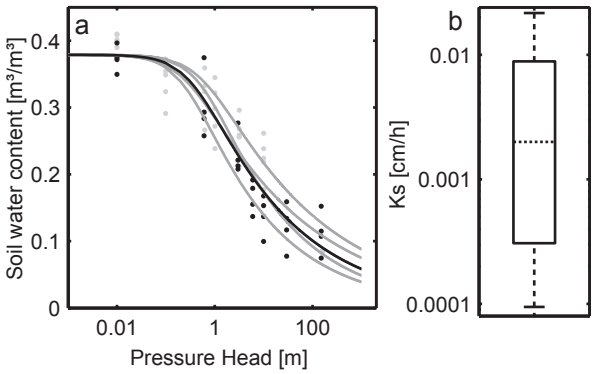

Figure 3.7: (a) Measured water retention data using borehole (black dots) and soil pit (grey dots) samples. Black line is the predicted van Genuchten model and grey lines are the model variations. (b) Box plot of the measured saturated hydraulic conductivity (see Table 3.4) (dashed line: median; black box: lower and upper quartile; whiskers: lower and upper extreme values within 1.5 times the interquartile range).

the summer of 2008 is associated with a strong decline in the matric pressure head. On 31 July 2008, a steep rise in the matric pressure head is caused by a heavy rainfall event of around 60 mm within 2 hours.

The estimation of *K(h)* is based on the Mualem-van Genuchten model [*Mualem*, 1976 ; *van Genuchten*, 1980], where the hydraulic conductivity is computed as

$$K(h) = K_s S_e^{\,l}[1-(1-S_e^{\frac{n}{(n-1)}})^{1-\frac{1}{n}}]^2 \tag{3.3}$$

where S_e is the effective saturation

$$S_e = \frac{\theta(h)-\theta_r}{\theta_s-\theta_r} \tag{3.4}$$

and *θ(h)* is the water retention curve

$$\theta(h) = \theta_r + \frac{\theta_s-\theta_r}{\left[1+\left|\alpha h\right|^n\right]^{1-\frac{1}{n}}} \tag{3.5}$$

The parameter *l* is the pore connectivity, in this study assumed to be 0.5 [Mualem, 1976]. The parameter α is the inverse of the air entry pressure [cm^{-1}], *n* is the pore size distribution index and θ_r and θ_s are the residual and the saturated water content, respectively [m³/m³].

All van Genuchten parameters were derived by fitting the water retention curve to water retention data, which were estimated using undisturbed soil samples obtained during drilling (number of samples: 4, depth: 1.1-6.1 m) and from the soil pit PMast (number of samples: 5, depth: 0.6-1.4 m) (see Figure 3.7). The influence of each sample on the predicted parameter set was assessed by successively excluding one sample after another and fitting the retention curve to the remaining water retention data. The mean and the standard deviation are calculated from these nine different realizations, assuming a normal distribution of the four parameters. Finally, four different scenarios were modeled by calculating the mean μ plus and minus two times the standard deviation σ for parameters α and *n*, resulting in a total of four permutations of α and *n* (Table 3.3).

Table 3.3: Predicted parameters, mean and standard deviation of the van Genuchten models

Parameter	θ_r	θ_s	α	n
Predicted	0.00	0.38	2.64	1.23
Mean	0.00	0.38	2.63	1.24
Standard Deviation	0.01	0.00	0.50	0.02
μ + 2 σ	0.01	0.38	3.63	1.28
μ - 2 σ	-	0.38	1.63	1.20

Table 3.4: Measured hydraulic conductivity values [m/h]

	Soil pit PMast	Drilling	Permeameter
	7.92×10^{-4}	1.09×10^{-4}	9.44×10^{-5}
	1.54×10^{-3}	1.73×10^{-4}	2.21×10^{-4}
	2.92×10^{-3}	2.50×10^{-4}	2.54×10^{-4}
	4.54×10^{-3}	3.02×10^{-4}	3.13×10^{-4}
	7.67×10^{-3}	1.01×10^{-3}	1.08×10^{-3}
	1.01×10^{-2}	1.56×10^{-3}	2.00×10^{-3}
	1.13×10^{-2}	2.00×10^{-3}	3.44×10^{-3}
	1.35×10^{-2}	2.15×10^{-3}	5.63×10^{-3}
		$2.60\times10^{-1\#}$	1.68×10^{-2}
			1.75×10^{-2}
			1.81×10^{-2}
			2.17×10^{-2}
			$1.14\times10^{-1\#}$
			$1.70\times10^{-1\#}$
			$4.24\times10^{-1\#}$
Count	8	8	12
Median	6.10×10^{-3}	6.57×10^{-4}	2.72×10^{-3}
		2.00×10^{-3}	

[#] Outlier removed from further analysis

We estimated the saturated hydraulic conductivity K_s from 9 core samples (depth: 1.10-6.35 m) and 8 samples from the soil pit PMast (depth: 0.6-1.4 m). Additionally, we measured in-situ 15 K_s values with a constant head well permeameter at different depths ranging from 0.6 to 2.2 m. Figure 3.7 and Table 3.4 show the measured K_s values. The estimated K_s values vary over several orders of magnitude. Four measurements were identified to be influenced by macropore flow and were removed from further analysis. The Buckingham-Darcy approach con-

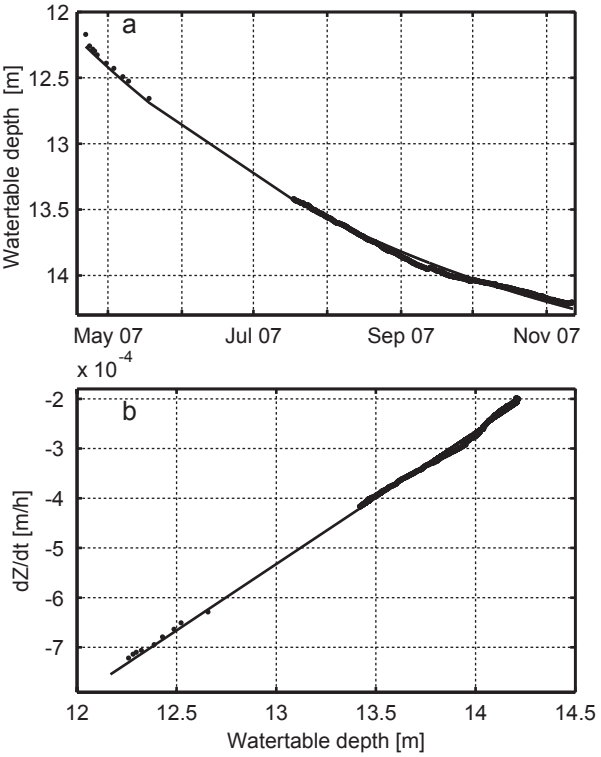

Figure 3.8: Recession curve of the water table depth (a) and estimated Master Recession Curve (b)

siders only soil matric flow, assuming that all other K_s values stand for flow in the soil matrix. We combined all samples from the different measurement techniques to increase the sample size because no significant differences could be observed between the different sample/measurement techniques. The distribution of K_s tends to show a non-Gaussian distribution (see Figure 3.7b), so we chose the median as a robust estimator and calculated the median of K_s to be 2.00×10^{-3} m/h. This value is within the range of the estimated K_s of the weathered zone [*Rubbert*, 2008], but is one magnitude lower than the K_s for the soil texture Sl3 (mean bulk density) of 1.75×10^{-2} m/h or for Su2 (high bulk density) of 2.67×10^{-2} m/h according to the German Institute for Standardization [*DIN*, 1998].

The deep percolation is calculated based on Equation 3.2 using the predicted van Genuchten model, the median K_s value and time series of the tensiometers. For the German hydrological year of 2008 (1 November 2007 – 31 October 2008), the deep percolation amounts to 173 mm. These values are in line with the estimated GW recharge of 130-190 mm/a for the area around the study area [*Apel et al.*, 1996], but lower than the groundwater recharge of 210-300 mm/a estimated by *Krásný and Sharp* [2007] for lower mountain ranges of the Bohemian Massif (mean annual precipitation of 800-1000 mm) and significantly lower than the estimated deep percolation rate of 909 mm/a in the study area of Markungsgraben in the National Park Bavarian Forest, which is ~50 km away [*Bittersohl et al.*, 2004]. This much higher percolation rate can be explained by higher annual precipitation of 1748 mm/a, but still more than half of the precipitation percolates deep into the ground. In this study, the deep percolation amounts to ~20 % of the precipitation, which corresponds to the groundwater recharge rates estimated by *Krásný and Sharp* [2007] for Centro-European mountain ranges. Land-use change or a high interflow rate could represent other explanations for the very high deep percolation rate of the Markungsgraben. *Haarhoff* [1989], for instance, estimated the groundwater recharge for the same area to be between 150 and 200 mm/a for a mean annual precipitation of 1000-1400 mm. Therefore, we must be aware that there may be a significant difference between deep percolation and groundwater recharge due to lateral fluxes in the soil or saprolite zone.

3.6.2 Groundwater recharge

The estimation of the lower boundary flux – the groundwater recharge q_R [m/h] – is based on the Water Table Fluctuation method (WTF) [*Healy and Cook*, 2002; *Sophocleous*, 1991] combined with the Master Recession Curve (MRC) [*Delin et al.*, 2007; *Heppner and Nimmo*, 2005], where the recharge is calculated as

$$q_R = S_Y \Delta Z_{WT} + q_D(Z_{WT}) \tag{3.6}$$

with ΔZ_{WT} being the water table rise [m] and $q_D(Z_{WT})$ the groundwater discharge [m/h] at the corresponding water table depth. A characteristic water table decline hydrograph – an MRC – generally exists for each site. The MRC was developed by plotting the water table depth against the water table decline data for the period from 23 April 2007 to 5 November 2008 (Figure 3.8). By assuming that no groundwater recharge occurred during this period, we estimated the discharge by the following linear MRC

$$q_D(Z_{WT}) = S_Y(aZ_{WT} + b) \tag{3.7}$$

where a and b were estimated to be 0.002668 h^{-1} and -0.004001 m/h, respectively.

Using the minimum, mean and maximum specific yields (see Table 3.2) and the mean of both groundwater time series, we can estimate the cumulative groundwater recharge for the hydrological year of 2008 to be 50, 77 and 130 mm respectively. These values are significantly lower than the estimated deep percolation and the cited groundwater recharge rates. The specific yield is estimated as a mean value over the whole aquifer thickness, but frequently, the specific yield decreases with increasing depth, and so the specific yield in the zone where the groundwater fluctuation occurs may be underestimated. This might be reflected by the parameter S_y being estimated from the snowmelt event, which corresponds to a groundwater recharge of 293 mm. In addition, only

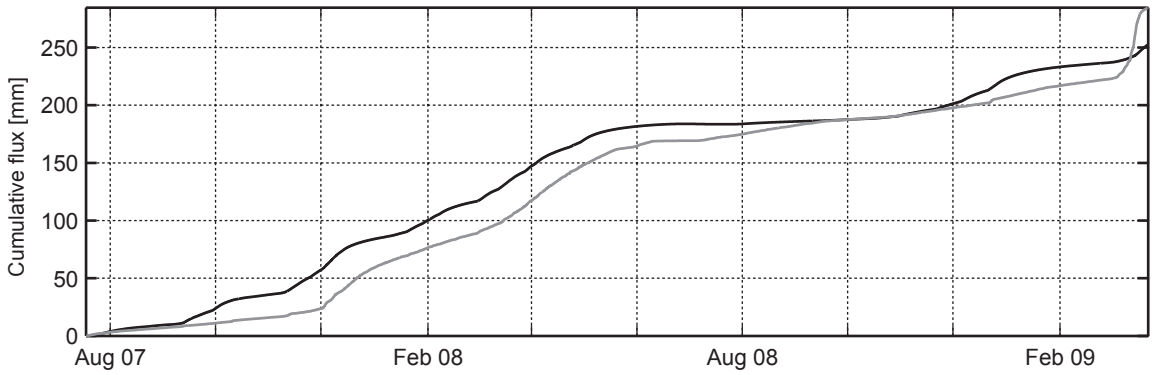

Figure 3.9: Seasonal variation of cumulative deep percolation (black line) and groundwater recharge (grey line).

discharge in the groundwater zone is considered and interflow or saprolite flow are neglected. But interflow as well as the flow in the transition between fractured and weathered zone may be of major importance [*Cho et al.*, 2003].

3.6.3 Water storage change in the saprolite zone

The deep percolation and groundwater recharge is highly dependent on the estimated K_s and S_y [e.g. *Healy and Cook*, 2002; *Hubbell et al.*, 2004; *Nimmo et al.*, 1994; *Risser at al.*, 2009]. Here, we are interested in the seasonal WSC in the saprolite zone, rather than in the absolute values of deep percolation and groundwater recharge. We will assume that on 1 November 2008, WSC in the saprolite zone are zero and that the cumulative q_P equals q_R. Because the estimated q_P is closer to the literature values than q_R, we will correct q_R to match q_P by using a S_y of 0.024, which is in the estimated range of S_y. Figure 3.9 shows the seasonal variation of cumulative deep percolation and groundwater recharge. The seasonal courses of both curves correspond well, with a time lag for the groundwater recharge compared to the deep percolation. At the end of February 2009, the cumulative groundwater recharge exceeded the cumulative deep percolation, something that is not physically possible. This effect is closely related to snowmelt (see Figure 3.3). During snowmelt, the soil is nearly saturated, which implies that preferential flow paths are activated and can contribute significantly to deep percolation [e.g. *French et al.*, 2002; *Stähli et al.*, 2004], and may even be intensified by partly frozen soils [e.g. *Stähli et al.*, 1996]. As mentioned previously, preferential flow is not represented by the Buckingham-Darcy approach, which therefore fails under these conditions. As no correction was made here, this limitation has to be taken into account in the analysis of the saprolite gravity response.

To assess the influence of the estimated van Genuchten parameters K_s and S_y on the WSC in the saprolite zone, we calculated the deep percolation and the corresponding groundwater recharge for each of the four van Genuchten models and all measured K_s, with the prerequisite that the cumulative deep percolation cannot exceed the cumulative precipitation during the study period. These different realizations for each time step were used to calculate the minimum and maximum saprolite WSC.

3.7 Gravity and water storage change

3.7.1 SG residuals

The major sources of temporal gravity variations are the tides of the solid Earth, ocean tide loading, changes in the atmosphere and polar motion. These effects are modeled and removed from the signal after pre-processing of the raw data. The pre-processing comprises correction of the sensor's drift, signal conversion by a scale factor and careful removal of spikes and disturbances (e.g. due to earthquakes). Scale factor and drift rate are reliably obtained by combining SG measurements with collocated absolute gravity measurements [*Wziontek et al.*, 2009a]. In this way, the scale factor is determined with a relative precision of better than 5 ppt. The almost linear instrumental drift of present SGs does not exceed 5.0 μGal/a, and the accuracy of its determination depends directly on the quality and repetition rate of the absolute gravity measurements. With two observation periods per year at the station Wettzell, the drift is determined with an accuracy of better than 0.5 μGal/a.

The variation of the tidal potential due to sun, moon and planets is described by precise tidal models [*Hartmann and Wenzel*, 1995; *Tamura*, 1987]. The elastic response of the solid Earth to the resulting forces is obtained by a harmonic analysis of the gravity signal up to monthly tides after atmospheric effects have been removed using a simple barometric admittance function. The effect of polar motion [*Wahr*, 1985] is calculated based on the pole coordinates as provided by the International Earth Rota-

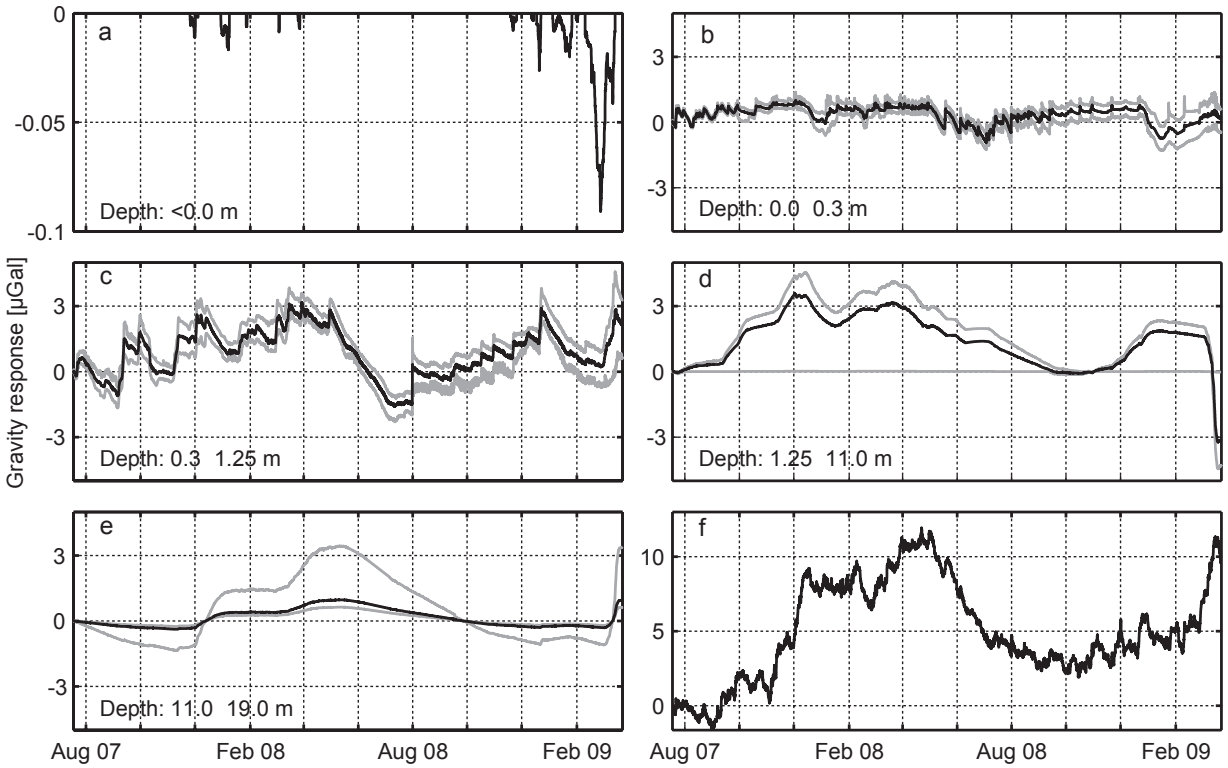

Figure 3.10: Temporal changes of mean gravity response (black line) due to WSC in the snow layer (a), the top soil zone (b), the soil zone (c), the saprolite zone (d) and the groundwater storage (e) and the measured SG residuals (f). Grey lines are the estimated minimum and maximum gravity response.

tion and Reference Systems Service (IERS) together with an adequate assumption of the elastic response of the Earth. We then performed a tidal analysis up to monthly tides. The accuracy of the SG residuals obtained can be estimated roughly with 0.1 µGal for short-term variations (1 to 30 days) and 0.5 µGal for inter-annual variations.

3.7.2 Gravity response

The gravity response of the different WSC is calculated based on the approach presented by *Creutzfeldt et al.* [2008] for a square with a side length of 4 km and the SG located in its center (Figure 3.1). We developed a spatially nested discretization domain and used the DEM to distribute the estimated WSC along the topography. The spatial resolution (Δxy = 0.25, 2.50, 10.00 m) of the DEM varies with the domain radius (R = 50, 500, 2000 m) (R: half the side length of the domain square). The z component of gravity change due to areal homogenous WSC is calculated for each body and time step using the MacMillan equation [*MacMillan*, 1958] presented by *Leirião et al.* [2009]

$$\Delta g = G\Delta\rho\Delta x\Delta y\Delta z \left[-\frac{z}{d^3}-\frac{5}{24}\frac{\left(\alpha x^2+\beta y^2+\omega z^2\right)z}{d^7}+\frac{1}{12}\frac{\omega z}{d^5}\right] \quad (3.8)$$

with $\alpha = 2\Delta x^2-\Delta y^2-\Delta z^2$, $\beta = -\Delta x^2+2\Delta y^2-\Delta z^2$, $\omega = -\Delta x^2-\Delta y^2+2\Delta z^2$ and $d=\sqrt{x^2+y^2+z^2}$. Variables x, y and z are the center coordinates of an elementary body relative to the sensor [m]. Δx, Δy and Δz are the side lengths of a rectangular body ($\Delta xy = \Delta x = \Delta y$) [m], G is the gravitational constant (Nm²/kg²) and $\Delta\rho$ is the density change in an elementary body (kg/m³), which is directly related to the WSC. The total hydrological gravity effect – the gravity response – is derived by the summation of all gravity changes in each elementary body, caused by the estimated water mass changes in the model domain.

The SG building has a significant influence on the gravity response [*Creutzfeldt et al.*, 2008]. We assume that neither in the foundation nor in the base plate of the SG building WSC occur. When taking into account the umbrella effect of the SG building inhibiting infiltration of rainfall into the soil, no WSC occur below the base plate of the SG building in the top soil storage. For the soil storage, we calculated the average gravity response both for cases excluding and including mass variations below

Table 3.5: Correlation coefficient between time series of water storage components and the SG residuals. Mean, max. and min. are the gravity responses due to the mean, maximum and minimum estimated WSC, respectively.

	Mean	Max.	Min.
Snow	-0.09	-	-
Top soil storage	0.09	0.25	-0.01
Soil storage	0.64	0.65	0.61
Saprolite storage	0.49	0.64	-0.18
Groundwater storage	0.71	0.73	0.62
Total storage	0.73	0.88	0.61

the base plate. Snow accumulates on the roof of the SG building and precipitation that runs off the roof is routed away from the SG. Therefore, the effect of water redistribution from the roof to the tank is not accounted for.

For each water storage component, namely snow, top soil zone, soil zone, saprolite zone and groundwater storage, the respective relative gravity response was calculated independently, using 18 July 2007 as the reference date (Figure 3.10). As a measure of uncertainty for water storage, we calculated the minimum, mean and maximum WSC for the upper soil and the soil storage for each time step, based on the data of all available soil moisture probes. The minimum, mean and maximum saprolite zone WSC were derived as described in section 3.6 Saprolite storage. The minimum, mean and maximum groundwater gravity responses were derived using the specific yields 6.30×10^{-3}, 9.61×10^{-3} and 3.41×10^{-2}, respectively, and the mean water table depth, which was corrected for the pump test. Finally, we estimated the total minimum, mean and maximum gravity response by summing up the minimum, mean and maximum gravity response for each time step independently.

Figure 3.10 shows the gravity response of the different water storage components. Except for snow, the gravity response of all other components is of the same order of magnitude. The gravity response of the snow storage is negative because snow mass accumulates mainly above the SG sensor in its immediate vicinity. At larger distances, snow also accumulates below the SG sensor so that the snow masses compensate each other and the gravity response of snow becomes negligible. Nonetheless, as pointed out in the previous sections, snow is an important factor as it significantly influences the other storage components via flow processes driven by snowmelt.

Storage change in the top soil and the resulting gravity response are generally closely related to precipitation and do not show pronounced seasonal dynamics. During winter, the apparent decline of the gravity response for both soil storages is not only due to a change of soil moisture but due to the change of permittivity caused by the soil freezing, as explained above.

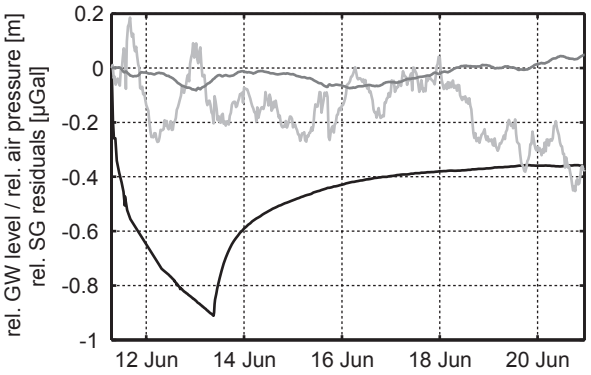

Figure 3.11: Time series during pump test of corrected relative groundwater displacement in meters (black line), relative SG residuals in µGal (light grey line) and relative air pressure in meter of water (grey line).

WSC time series in the soil, in the saprolite and in the groundwater zone, exhibit a similar seasonal pattern. As discussed in the previous section, the overall deep percolation might be underestimated with the present approach. This could cause an underestimation of the saprolite storage influence on the total gravity response. The sharp decline of the gravity response in the saprolite zone at the end of the study period is most likely due to methodological reasons, because the effect of macropores is only considered at the lower boundary, as explained in the 3.6 Saprolite storage section.

3.7.3 Comparison of gravity response and SG residuals

Figure 3.10 shows the gravity response of the different water storage components compared with the SG residuals. The time series of deeper WSC components such as groundwater, saprolite and soil storage show a similar seasonal behavior as the SG residuals, something which is also expressed by high correlation coefficients (Table 3.5). The highest correlation, however, was found for the gravity response integrated over all storage components.

However, single hydrological state variables also show a significantly high correlation with the SG residuals. For example, the correlation coefficients between the time series of two TDR soil moisture measurements at 2 m depth and the SG residuals are 0.65 and 0.79 (see also Figure 3.4f and 3.10f). Focusing on the relationship between SG residuals and groundwater level alone would result in a regression coefficient of 2.69 µGal gravity response per meter groundwater change (coefficient of determination = 0.51). Based on the Bouguer slab approximation, where a 1 m water change in an infinitely extended slab causes a gravity change of 41.92 µGal, this regression slope corresponds to a specific yield of

Table 3.6: Regression coefficient, standard error, t value, p value and performance criteria of the multiple linear regression model for time series of SG residuals and the gravity response of the different water storages for the entire study period.

Variable	Regression Coefficient	Standard Error	t value	p value
Intercept	2.42	0.02	145.10	<0.001
Groundwater storage	5.02	0.02	208.00	<0.001
Soil storage	1.56	0.01	137.80	<0.001
Saprolite storage	0.43	0.01	46.23	<0.001
Top soil storage	-0.58	0.03	-19.86	<0.001
Snow	-71.17	0.96	-73.92	<0.001
Standard deviation of error: 1.135			Multiple R^2: 0.88	
F-statistic 21544 on 5 and 14748 degrees of freedom, p-Value: 0				

6.42×10^{-2}. *Harnisch and Harnisch* [2006; 2002] estimated the regression coefficient as being in the range of 2.48 and 9.33 μGal/m based on a groundwater well at a distance of 200 m to the SG. This would result in a specific yield between 5.91×10^{-2} and 2.23×10^{-1}. As they already pointed out, interpreting this regression coefficient in a physical way is problematic and only valid if the correlation between groundwater and other water storages can be neglected or the water mass variations in all other storages are small compared to the groundwater mass variation.

These assumptions are not fulfilled for the Wettzell site. Strong interaction between different water storages exists and the SG residuals depend on different WSC components. For example, a rise of the groundwater level occurs after accumulation of water in the vadose zone or melting of the snow water. A multiple linear regression showed that all variables have a statistically significant predictive capability for SG residuals (p-value < 0.001). The development of the model was studied by including/excluding different WSC components step-by-step. Finally, variables were included in the model step-by-step to explain as much of the variability as possible in each individual step. Studying the step-by-step development of the statistical model, groundwater explains 51 % of the variability in the SG residuals' time series. By including soil moisture in the model, the coefficient of determination increased to 0.80. Upon adding the saprolite zone storage and the top soil zone storage, the coefficient of determination was estimated to be 0.82 and 0.83 respectively. Finally, the coefficient of determination increased to 0.88 upon inclusion of the snow storage. The parameters of the final model are shown in Table 3.6. While snow came out as the third most important component in terms of explained variability, it was placed in the last position, because here it compensates for the methodological shortcomings of estimating the saprolite storage change (March 2009), which is also reflected by a large negative regression coefficient (Table 3.6).

Despite the high coefficient of determination, the total estimated mean gravity response is smaller than the SG residuals. This is also reflected in Figure 3.12, where the total gravity response of all different water storages is compared to the SG residuals together with the minimum and maximum gravity response for each time step as a measure of uncertainty as explained above. For the study period, the range of minimum and maximum estimated gravity response amounts to 14 μGal. This value is very similar to the range of the observed SG residuals. Given that a water mass change of 1 m amounts to a gravity response of 52 μGal (due to topography) [*Creutzfeldt et al.*, 2008], the gravity range of 14 μGal corresponds to a total water storage change of 272 mm around the gravimeter between the driest and wettest conditions recorded in the observation period.

The time series of total WSC and SG residuals exhibit similar dynamics both at the seasonal scale and for individual periods or events. Short peaks related to discrete rainfall correspond well in time (for example, during the recession period from May 2008 to July 2008), whereas differences exist in the absolute value, e.g. the gravity increase for the largest rainfall event on 31 July 2008 is higher for the gravity response (1.9-2.9 μGal) than for the SG residuals (1.4 μGal). The seasonal correlation of the curves is expressed by a correlation coefficient ranging from 0.61 to 0.88 (Table 3.5). The maximum gravity response estimated based on the assumed uncertainty of the observation data correlates better with the SG residuals than the mean or the minimum gravity response (Figure 3.12). One possible explanation is that local WSC have been underestimated by the hydrological methods. As another explanation, the parts of the differences between the estimated gravity response and the SG residuals may be due to the effect of large-scale hydrological variations when assuming a strong correlation between

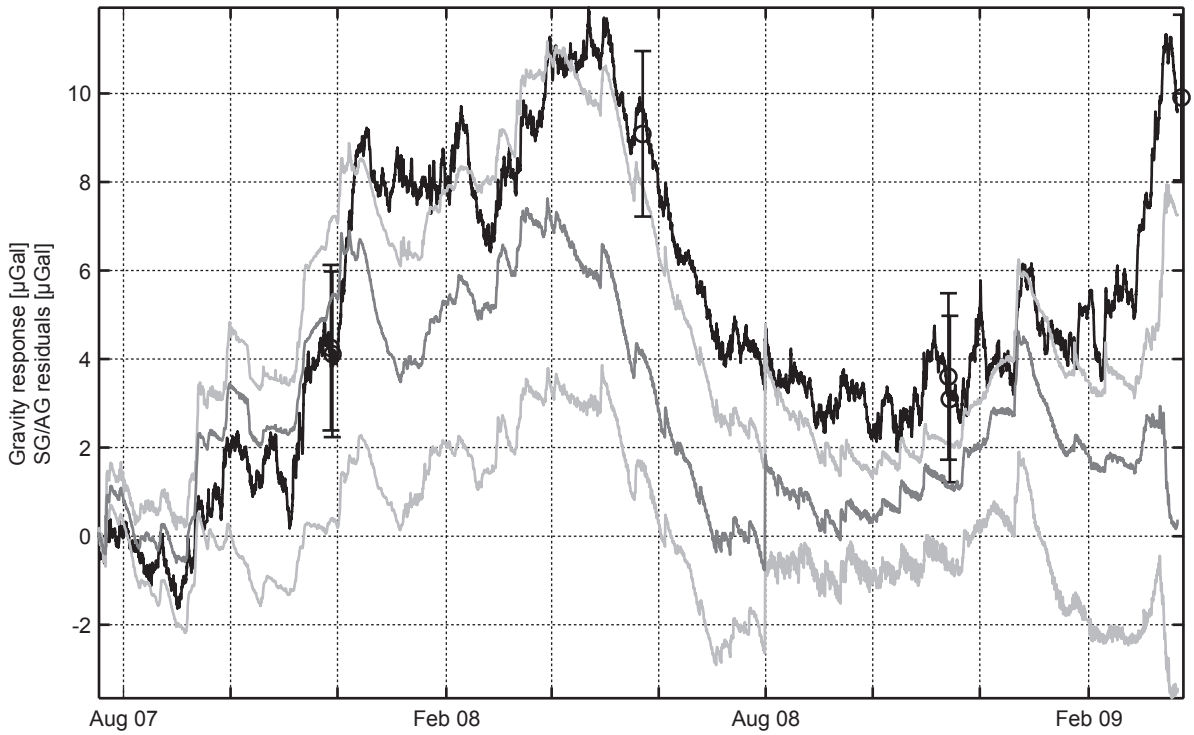

Figure 3.12: SG residuals (black line) and total gravity response as sum of all water storage components (dark grey line). Light grey lines are the minimum and maximum estimated gravity response. Absolute gravity (AG) residuals and their uncertainty are displayed as circles with error bars.

the local and large-scale WSC. As shown by *Wziontek et al.* [2009c], most of the hydrological large-scale effect is generated in a zone with a radius of 200 km up to 10,000 km around the SG and may amount to a few µGal. Nevertheless, it cannot be expected that large-scale variations will significantly contribute to the event-scale variations of the SG signal. For example, the steep rise of the SG residuals by about 6 µGal from 27 February 2009 to 20 March 2009 was most likely caused by local WSC due to the snowmelt and water mass redistribution in the soil. This provides additional evidence that the local gravity response tends to be underestimated.

An analysis of the SG residuals during the pump test reveals that the SG residuals do not show a clear correlation with the groundwater table displacement. In the beginning, a gravity rise of ~0.2 µGal can be observed, followed by a decline of ~0.4 µGal and another rise of ~0.4 µGal (Figure 3.11). This ambivalent response of the SG residuals is difficult to interpret because the gravity response depends on the specific yield as well as on the hydraulic conductivity of the aquifer as pointed out by *Blainey* [2007]. In general, the results support that the drainable porosity is small, but it is not possible to draw the conclusion that the overall gravity effect of groundwater table variations is negligible because the water level depression cone is of limited spatial extent causing water mass variations that have barely any gravity effect for this specific case. Also *Harnisch and Harnisch* [2006; 2002] did not find a clear relation for a pump test conducted at a distance of 250 m. They observed a decline of 1 µGal in the SG residuals with a time lag of 12 hours and assumed this decline to be caused by the groundwater displacement.

3.8 Discussion

As illustrated in Figure 3.10 and Figure 3.12, the estimation of local WSC and its gravity response is associated with considerable uncertainties. This study considers only specific aspects within a broad set of uncertainties in both hydrological and gravimetric procedures: (1) measurement accuracy (sensor calibration, resolution of device, etc.), (2) assumptions and simplifications in the structural model of the subsurface, (3) hydro(geo)logical parameter estimation, (4) spatial variability, (5) calculation of the gravity response (impact of, e.g., topography and SG building) and (6) processing of the SG residuals.

Points 2 to 5 are the most critical aspects in this study. Errors in representing hydrological processes are mainly associated with the saprolite zone because only matric flow is considered, neglecting preferential flow as well as lateral fluxes in the saprolite or the periglacial weathering cover. For the estimation of fluxes in the saprolite zone, data from different sources (TDR probes, tensiometers, pressure transducer) correspond well in terms of their

seasonal variations, but the quantification of total WSC in the saprolite zone is associated with a high level of uncertainty. The estimation of effective soil hydraulic parameters as well as aquifer parameters is still a challenging task.

Concerning spatial variability, Figures 3.4, 3.5 and 3.10 and Table 3.1 provide preliminary evidence that supports the validity of the 1D approach adopted in this study because heterogeneity is much more pronounced with depth than with area, especially when considering the near field effect of local WSC on the SG residuals. However, the spatial variability at larger distances along the hillslope with potentially different soil moisture and groundwater regimes is not considered here. In addition, the soil moisture dynamics below the SG building are not known exactly, even though this zone has a high influence on the SG measurements.

The uncertainties arising from the estimation of WSC on the local scale by classical hydrological methods point to the potential use of precise temporal gravity measurements in hydrology. In general, the advantage as well as disadvantage of gravity measurements is their integrative character. On the one hand, this makes them capable of integrating a small catchment-scale hydrological response, similar in nature to discharge measurements [*Hasan et al.*, 2008]. Thus, they might be especially useful in areas far away from the river such as headwaters where no adequate measurement technique is available to estimate local WSC and integrative catchment dynamics. In this study, for example, we assume that over a one year period, the WSC in the saprolite zone are zero. However, the positive trend of the SG residuals compared to the total hydrological gravity response may be an indication that water accumulates over this period in the saprolite zone. On the other hand, due to the integrative character of gravity measurements, it is difficult to unambiguously identify the source of the gravimeter signal. This makes a unique interpretation for individual storage components challenging or even impossible if no complementary information is available.

Favourable conditions for a hydrological interpretation of gravimetric data prevail where WSC occur either above or below the gravimeter. This applies to the gravimeter in Wettzell, where most of the WSC occur below the gravimeter. This is in contrast to SGs installed at underground locations where local water storage may change above and below the gravimeter so that local WSC may compensate for each other to some extent in the gravimeter signal. This may imply that large-scale WSC make a relatively larger contribution to the SG signal. Additionally, in the direct surroundings of the SG, the hydrological system should be kept as simple as possible, (i.e. avoiding stone or earth cover or artificial drainage systems close to the gravimeter that are difficult to interpret). The uncertainties discussed above indicate that it may be difficult to completely remove the local hydrological effect from gravity data, (i.e. providing SG residuals that are free from local "hydrological noise" and that could be used for geodetic and large-scale applications such as validation of satellite gravity data [e.g. *Weise et al.*, 2009] or of large-scale hydrological models).

In view of the potential applications and limitations of gravity measurements and towards a broader evaluation of their value for hydrological applications, further research is needed on quantifying hydrological processes and state variables including their spatial variability around SGs. At the Wettzell site, studies using additional soil moisture and groundwater sensors, a lysimeter, tracer tests, permanent electrical resistivity (ERT) surveys and a second SG are under progress to better describe processes such as evapotranspiration, deep percolation, preferential or saprolite flow and their relation to gravity data. The evaluation will benefit by combining hydrological and geophysical data in a joint or coupled hydrogeophysical inversion [*Ferré et al.*, 2009], whereas spatial gravity changes caused by WSC can be resolved by repeated observations with relative gravimeters [*Naujoks et al.*, 2008]. Finally, we also suggest performing detailed hydrological analyses of all relevant water storage components at other SG stations in order to extend the evaluation and learn from different environmental settings.

3.9 Conclusions

In this study, we present a comprehensive observation-based approach for the estimation of total local water storage, composed of the components snow, soil moisture, saprolite and groundwater storage. Continuous time series of WSC in each component were estimated, including their possible range of uncertainty by minimum and maximum storage values. Nevertheless, not all sources of uncertainty could be addressed in this study.

For each storage component, the gravity response was calculated considering the spatial distribution of water masses around the SG. The results were compared to the SG gravity observations. Except for the small effect of the snow storage, the gravity response of the different storage components is of the same order of magnitude. A linear regression model showed that all storage changes estimated from hydrological observations have a significant predictive capability for the SG gravity signal. Some hydrological state variables as well as single storage components correlate well with the SG residuals. However, a strong correlation does not necessarily imply a physical relation (direct effect of water masses on the SG) but may indicate only that a particular observable variable is a reasonable indicator for part of the storage changes in the area surrounding the SG.

Comparing the total gravity response of the WSC to the

SG residuals shows similarities on the event scale as well as on the seasonal time scale. A large part of the gravity signal can be explained by local WSC. An uncertainty analysis based on the observation data showed that the maximum gravity response correlates better with the SG residuals than the mean or the minimum estimated gravity response. Therefore, we argue that the local hydrological gravity effect tends to be underestimated in this study, since large-scale hydrological mass variations can contribute only a few μGal on the seasonal timescale to the total gravity signal.

Estimating local WSC is associated with uncertainties (measurement errors, model assumptions, parameter estimation, process quantification and spatial variability) and demonstrates the limitations of conventional hydrological instruments to quantify local WSC. This demonstrates the shortcomings of providing a gravity signal free of local "hydrological noise". It highlights that the signal separation process is an iterative process and that different disciplines have to work together closely.

The disadvantage as well as the advantage of gravity measurements is their integrative nature. It makes gravity observations difficult to interpret, and therefore, extreme caution should be applied when interpreting a gravity signal for hydrological studies, especially if only a single parameter or a single water storage component is studied. Nevertheless, gravity measurements can provide unique data for hydrological studies and thus have a high potential to improve water balance studies and catchment characterization by estimating the storage term, for example, in order to set up storage-discharge functions [*Kirchner*, 2009].

Acknowledgement. This work has been supported by the Deutsche Forschungsgemeinschaft (German Research Foundation) within the Priority Program SPP 1257 'Mass transport and mass distribution in the system Earth', project TASMAGOG. We want to thank the editor John Selker, the associate editor Frederick Day-Lewis, the reviewer Ty Ferré, the reviewer Michel van Camp and one anonymous reviewer for the thoughtful comments that significantly improved the study.

Chapter 4:

Reducing local hydrology from high precision gravity measurements: A lysimeter-based approach

Reducing local hydrology from high precision gravity measurements: A lysimeter-based approach

Abstract

Temporal gravimeter observations, used in geodesy and geophysics to study the Earth's gravity field variations, are influenced by local water storage changes (WSC). At the Geodetic Observatory Wettzell (Germany), WSC in the snow pack, top soil, unsaturated saprolite and fractured aquifer are all important terms of the local water budget. In this study we present the first comparison of lysimeter and gravimeter measurements. Lysimeter data are used to estimate WSC at the field scale in combination with complementary observations and a hydrological 1D model. From these estimated WSC we calculate the hydrological gravity response. The results are compared to other methods used in the past to correct temporal gravity observations for the local hydrological influence. Lysimeter measurements significantly improve the independent estimation of WSC and thus provide a better way of reducing the local hydrological effect from gravimeter measurements. We find that the gravity residuals are caused to a larger extent by local WSC than previously stated. At sites where temporal gravity observations are used for geophysical studies beyond local hydrology, the installation of a lysimeter is recommended.

Published as:

Creutzfeldt, B., A. Güntner, H. Wziontek, and B. Merz (2010), Reducing local hydrology from high precision gravity measurements: a lysimeter-based approach, Geophysical Journal International, 183(1), 178-187, http://dx.doi.org/10.1111/j.1365-246X.2010.04742.x.

[Author's note: The manuscript underwent modifications during the review process after this document was compiled. Please check the journal for the final version.]

4.1 Introduction

Ground-based temporal gravity observations are gaining importance in a wide range of geophysical research issues. Gravimeter observations have been used to study long-term geodynamic processes like for example post-glacial rebound [e.g. *Lambert et al.*, 2006; *Sato et al.*, 2006; *Steffen et al.*, 2009], processes in the Earth's mantle and core [e.g. *Imanishi et al.*, 2004; *Shiomi*, 2008], natural hazards like for example gravity changes associated with earthquakes and volcanism [e.g. *Battaglia et al.*, 2008; *Nawa et al.*, 2009], reservoir-monitoring applications like for example hydrocarbon and geothermal exploration, and carbon sequestration, [e.g. *Brady et al.*, 2008; *Sugihara and Ishido*, 2008], and the comparison of ground-based with satellite gravity measurements like for example comparison with GRACE [e.g. *Neumeyer et al.*, 2008; *Weise et al.*, 2009]. To study relative gravity variations in time, superconducting gravimeters (SG) [*Goodkind*, 1999] are currently the best performing gravimeters in terms of precision and temporal resolution. Advances in atom interferometry promise the time-continuous application of absolute gravity measurements in the future [*Angelis et al.*, 2009; *Peters et al.*, 2001].

Ground-based temporal gravimetric observations are influenced by up to tens of μGal by natural local water storage changes (WSC) like changes in groundwater, soil moisture, snow, or surface water storage [*Bonatz*, 1967; *Bower and Courtier*, 1998; *Crossley and Xu*, 1998; *Hasan et al.*, 2008; *Lambert and Beaumont*, 1977; *Mäkinen and Tattari*, 1988; *Pool*, 2008]. WSC affect temporal gravity measurements on the event and seasonal time scale, but can also show long-term changes due to natural and human-induced trends [e.g. *Rodell et al.*, 2009]. The hydrological effect is an intrinsic feature of ground-based temporal gravity measurements and can mask the geodetic/geophysical phenomena of interest. Therefore, it has to be removed from the gravimeter signal.

Different approaches have been developed to correct for the hydrological influence in gravity measurements. We can distinguish between empirical approaches, which establish a statistical relationship between hydrological and gravity data [*Battaglia et al.*, 2008; *Harnisch and Harnisch*, 2002; *Imanishi et al.*, 2006; *Lambert and Beaumont*, 1977] and physically-based approaches, which calculate the hydrological gravity response from WSC [*Creutzfeldt et al.*, 2008; *Hokkanen et al.*, 2006; *Virtanen*, 2001]. Some approaches are mainly based on observation data [*Longuevergne et al.*, 2009; *Van Camp et al.*, 2006] whereas other approaches rely on hydrological models [*Kazama and Okubo*, 2009; *Naujoks et al.*, 2009] to estimate the local WSC. Furthermore, we can distinguish between approaches, which estimate the effect of local WSC independently from gravity measurements [*Creutzfeldt et al.*, 2010a] and approaches, which calibrate the data or model to match the gravity signal [*Hasan et al.*, 2008; *Lampitelli and Francis*, 2010]. Finally, the large-scale hydrological gravity effect on gravimeter observations [*Llubes et al.*, 2004; *Neumeyer et al.*, 2008; *Wziontek et al.*, 2009c] is considered before [*Jacob et al.*, 2008; *Longuevergne et al.*, 2009] or after focusing on local WSC [*Hasan et al.*, 2008; *Weise et al.*, 2009]. No standard procedure for reducing the hydrological effect has been introduced up to now as suggested by *Harnisch and Harnisch* [2006]. For studies using temporal gravity observations to investigate geophysical phenomena beyond local hydrology, a standardised approach is needed to independently estimate local WSC and remove the hydrological gravity response from gravimeter measurements. However, estimating local WSC from independent observations or models is associated with a high level of uncertainty, making signal reduction a challenging task [*Creutzfeldt et al.*, 2010a].

In hydrology, weighable lysimeters can be considered very accurate devices to measure precipitation and deep drainage and they are, in fact, the only device to directly measure the actual evapotranspiration [*Meissner et al.*, 2007; *Tolk and Evett*, 2009; *WMO*, 2008; *Yang et al.*, 2000]. By continuously recording the mass of a soil monolith, lysimeters provide us with an accurate measurement of the soil moisture change. The Geodetic Observatory Wettzell [*Schlüter et al.*, 2007] is the only place where both gravimetric monitoring systems – a state-of-the-art lysimeter and a dual sphere SG – operate in parallel at a distance of around 40 m. The aim of this study is to use the lysimeter as an independent monitoring device to correct temporal high precision land-based gravity measurements for the influence of local WSC without performing any calibration against the gravimeter residuals. We will compare this lysimeter-based approach to other methods reported in the literature for correcting the gravity signal for hydrological influence, i.e., a statistics-based approach, a model-based and a data-based approach.

4.2 Data and method

4.2.1 Data

In this study temporal gravity variations were observed by the GWR SG CD029 at the Geodetic Observatory Wettzell (Figure 4.1). Apart from an instrumental drift, SGs are high precision instruments with a noise level of 5 $(nm/s^2/Hz)^2$. This corresponds, for example, to a level of 0.02 μGal during a period of 100 s [*Banka and Crossley*, 1999; *Van Camp et al.*, 2005]. After the elimination of spikes, disturbances and offsets during pre-processing, the SG data were combined with absolute gravity measurements to determine scale factor and instrumental drift [*Wziontek et al.*, 2009a]. Then, the gravity effects of known non-hydrological effects, i.e. solid Earth tides, ocean tide loading and polar motion [*Hinderer et al.*,

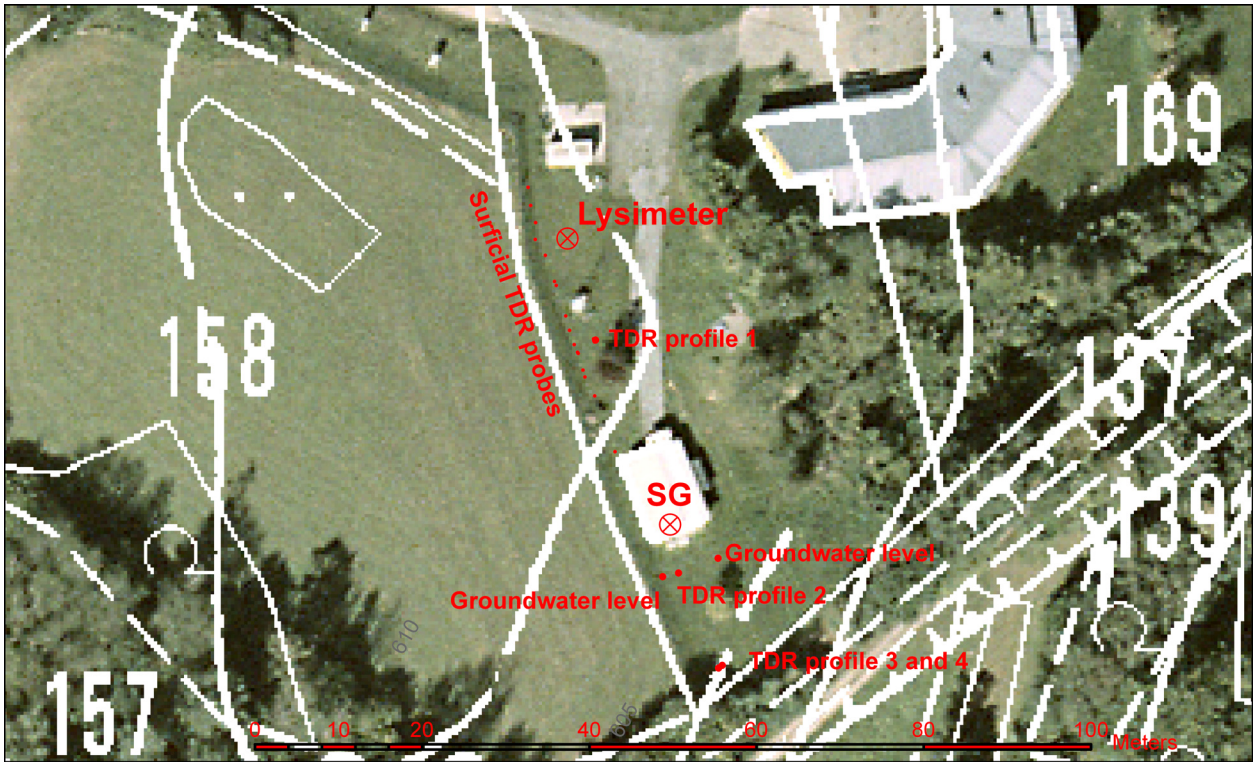

Figure 4.1: Lysimeter, SG and different hydrological sensors in combination with an ortho-image of the study site (white lines: contour map and land register map).

2007] as well as mass changes in the atmosphere [*Klügel and Wziontek*, 2009] were modelled and removed from the SG data. The remaining signal is hereinafter referred to as 'SG residuals'.

At the Geodetic Observatory Wettzell, a hydrological monitoring system was installed to observe the water in different storages and hydrological fluxes [*Creutzfeldt et al.*, 2010a; *Creutzfeldt et al.*, 2010b]. Precipitation was measured by two heated tipping bucket rain gauges. Evapotranspiration was estimated based on air temperature, relative humidity, wind speed and global radiation data. Snow height and snow water equivalent was measured by an ultrasonic height sensor and a snow pillow. Soil moisture sensors based on the Time Domain Reflectometry (TDR) technique measure the top soil moisture (0.0-0.3 m). Soil moisture up to a depth of 2.0 m was monitored with TDR sensors installed in 4 different soil profiles. Next to the SG building, the groundwater level was recorded in two boreholes (Figure 4.1).

In July 2007, a UMS lysimeter with a 1.5 m deep undisturbed soil monolith and a surface area of 1 m² was installed to measure the gravimetric change in snow and soil water. Similar water regime and drainage conditions in the lysimeter and in the field (e.g. no capillary barrier) were achieved by suction control of the lower lysimeter boundary. At the lower boundary, a tensiometer in the lysimeter and another one in the corresponding depth in the field measure the soil matric potential. The matric potential measured in the field was applied via a suction cup rake and a bidirectional pump to the lower boundary of the lysimeter by pumping water into a drainage water tank or into the monolith. The monolith and the drainage water tank were placed on a high precision scale for continuous mass recording. The reader is referred to the study of *von Unold und Fank* [2008] for a detailed description

Precipitation, actual evapotranspiration and deep drainage were estimated from the lysimeter monolith and the drainage water weight, assuming that during a sample interval (1 min) either evapotranspiration or precipitation occurs. Precipitation, actual evapotranspiration and deep drainage can be estimated with an accuracy of 0.01 mm as stated by the manufacturer, but the accuracy is reduced due to wind effects on the weight measurements. Nonetheless, lysimeters measure precipitation more precisely than the common precipitation gauge because lysimeter measurements are not affected by the well-know wind field effects and wetting losses of precipitation gauges [*Allerup*, 1997; *Richter*, 1995].

The snow water equivalent estimated by the snow pillow was subtracted from the lysimeter weight to distinguish between mass changes in the snow and soil storage because a mass change in the snow storage has a different gravity effect than a mass change in the soil [*Creutzfeldt*

et al., 2008]. For the study period from 30 July 2008 to 30 July 2009, all data were processed to one hour intervals. The mean was calculated for parameters being measured several times (groundwater level, soil moisture in the same depth).

4.2.2 Lysimeter-based approach

Figure 4.2 shows the study design of the lysimeter-based approach to estimate the total local WSC defined as

$$WSC_{local} = \Delta S_{Snow} + \Delta S_{Soil} + \Delta S_{Saprolite} + \Delta S_{GW} \quad (4.1)$$

for the Geodetic Observatory Wettzell. WSC in the snow and soil storage ($\Delta S_{Snow} + \Delta S_{Soil}$) depend on the precipitation (P), the actual evapotranspiration (ETa) and the deep drainage (D)

$$\Delta S_{Snow} + \Delta S_{Soil} = P - ETa - D \quad (4.2)$$

The water balance equation for the saprolite and groundwater storage ($\Delta S_{Saprolite} + \Delta S_{GW}$) is expressed in its general term as

$$\Delta S_{Saprolite} + \Delta S_{GW} = D - Q \quad (4.3)$$

where D is the deep drainage and Q the groundwater discharge. Up to a depth of 1.5 m, the lysimeter directly measured $\Delta S_{Snow} + \Delta S_{Soil}$. $\Delta S_{Saprolite} + \Delta S_{GW}$ was estimated based on the lysimeter deep drainage (here equals D) and groundwater level measurements. The vertical water redistribution below the lysimeter and the groundwater discharge (Q) were estimated with the hydrological model HYDRUS 1D [*Šimůnek et al.*, 2008]. Water flow in the subsurface was described by the van Genuchten-Mualem soil hydraulic model [*Mualem*, 1976; *van Genuchten*, 1980], with the following parameters: residual water content (θ_r), saturated water content (θ_s), inverse of the air entry pressure (α), pore size distribution index (n), pore connectivity (l) and saturated hydraulic conductivity (K_s) (Table 4.1). In this study we use the parameter set estimated in *Creutzfeldt et al.* [2010a] from field and laboratory measurements. The depth below the lysimeter was divided into the saprolite (1.5 – 11.0 m) and the fractured bedrock zone (11.0 -19.0 m). For the saprolite zone, the soil hydraulic parameters (θ_r, θ_s, α, n) were estimated from water retention measurements of undisturbed soil samples and K_s from laboratory and field measurements. The same parameter values for θ_r, α and n were applied for the fractured zone because taking and analysing undisturbed soil samples for the fractured zone is challenging [*Katsura et al.*, 2005]. We assume that fractures are filled with the same material as the saprolite zone. Based on these parameters and the specific yield (S_y) of the aquifer estimated from a pump test, the parameter θ_s was derived assuming that the specific yield represents the water content between saturation and field capacity. From the pump test, the conductivity K_s was estimated for the fractured zone. For both zones, the parameter l is set to be 0.5 [*Mualem*, 1976]. In line with a gradual transition from saprolite to bedrock, the contrast of K_s and θ_s between both zones was smoothed by linear interpolation between a depth of 8.0 m and 11.0 m.

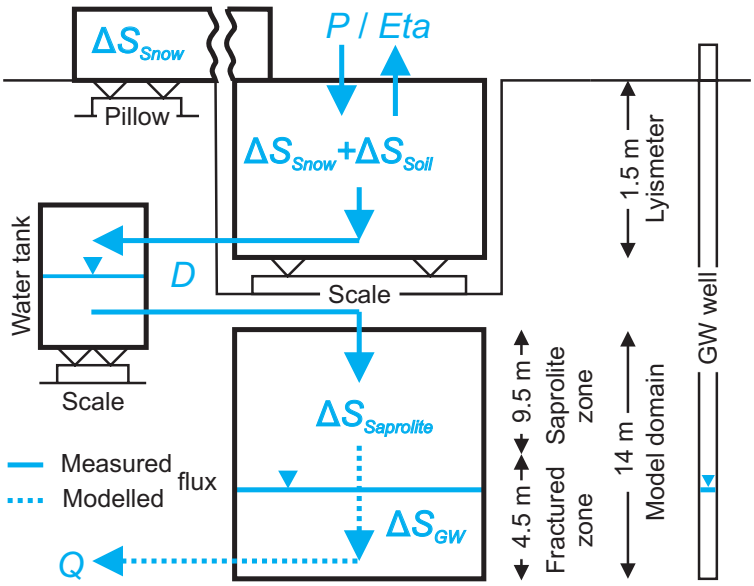

Figure 4.2: Hydrological study design. Snow water change (ΔS_{Snow}) is measured by a snow monitoring system. Snow and soil water change ($\Delta S_{Snow} + \Delta S_{Soil}$) by the lysimeter up to a depth of 1.5 m. A hydrological model is used to estimate the WSC in the saprolite and groundwater ($\Delta S_{Saprolite} + \Delta S_{GW}$) up to a depth of 15.5 m. Precipitation (P), actual evapotranspiration (ETa) and drainage (D) are directly measured fluxes (solid lines). Percolation and groundwater discharge (Q) are modelled (dotted line).

The upper boundary flux of the hydrological model was defined by the deep drainage measured with the lysimeter. The lower boundary was defined by the mean of both groundwater levels as a variable head condition. The initial moisture profile was estimated during a warm-up period starting on 18 July 2007. For this period, no lysimeter measurements were available for the upper boundary conditions. Therefore, deep drainage was derived from tensiometers based on the Buckingham-Darcy approach [*Creutzfeldt et al.*, 2010a].

The gravity response of estimated WSC was calculated from the hydrological observations and model results with a spatially nested extended point mass approach [*Leirião et al.*, 2009; *MacMillan*, 1958] presented by *Creutzfeldt et al.* [2008] for an area of 4 × 4 km around the SG in Wettzell and taking into account the spatial distribution of WSC along and below the topography. The gravity response of snow, soil water, the saprolite and groundwater storage change was calculated in relation to the beginning of the study period as the reference date. The distribution of WSC in the near field has a major influence on the estimated gravity response [*Creutzfeldt et al.*, 2008]. The effect of the SG building and foundation was considered assuming that 1) snow accumulates on the roof of the SG building, 2) no WSC occur in the foundation of the SG and the base plate of the SG building and 3) the SG building prevents infiltration of water into the ground from above (umbrella effect) but lateral fluxes may occur to some extent in the subsurface. As an approximation for the last assumption, we calculated the average gravity response for cases excluding and including mass variations below the base plate.

4.2.3 Other approaches for comparison

Following correction methods used in previous studies (see references above), we set up the statistics-based approach, which is an empirical approach. Considering the importance of various WSC components at Wettzell, we included groundwater, soil moisture in different soil depths and snow data in the analysis. A backward stepwise regression suggested that all parameters have a statistically significant predictive capability for the SG residuals, so all data were included in the model to predict the SG residuals. Table 4.2 shows the parameters and statistics for the multiple linear regression model.

The model-based approach uses the calibrated hydrological model of *Creutzfeldt et al.* [2010b] to predict WSC and the gravity response. A conceptual hydrological model was automatically calibrated against the SG residuals using precipitation, reference evapotranspiration for short canopy and snow height as input data. The gravity response from the WSC was calculated deterministically as described in the previous section, whereas uncertainties due to WSC distribution in the near field were considered as calibration factors. In this context, this is a deterministic approach, but the hydrological model parameters and the WSC distribution in the near field were calibrated against the SG residuals. The estimated gravity response is independent from the SG residuals in that this approach was calibrated for a different time period (July 2005 to 30 July 2008).

Table 4.1: Sub-surface hydraulic parameters: residual water content (θ_r), the saturated water content (θ_s), inverse of the air entry pressure (α), pore size distribution index (n), pore connectivity (l) and saturated hydraulic conductivity (K_s) [*Creutzfeldt et al.*, 2010a].

		Unit	Saprolite	Fractured bedrock
Depth	From	m	1.5	11
	To		11	19
θ_r		m^3/m^3	0	0
θ_s		m^3/m^3	0.38	0.02
α		cm^{-1}	2.64	2.64
n		-	1.23	1.23
l		-	0.5	0.5
K_s		m/h	0.002	0.0108

A third approach, the data-based approach similar to the study of *Creutzfeldt et al.* [2010a], uses snow observations, TDR soil moisture measurements and groundwater levels data to calculate the gravity effect based on the approach presented in the previous section. This is an independent and deterministic approach. The estimated specific yield from a pump-test of 1 % is used to derive the mass changes for the aquifer. In general, it is difficult to install sensors to measure WSC in the vadose zone below a depth of ~ 2 m. Hence, WSC in this zone are generally neglected. Following this and due to a lack of observations for this study period, we will not consider WSC estimated by *Creutzfeldt et al.* [2010a] for the saprolite zone, knowing that we underestimate the hydrological gravity effect. Additionally, we modified this data-based approach by simply subtracting the soil moisture gravity response from the SG residuals and then estimating the specific yield by linear regression between the remaining SG signal and groundwater level. This modified approach is a mixed form of the statistics- and data-based approach.

4.2.4 Large-scale hydrological gravity effect

The large-scale hydrological gravity effect [*Llubes et al.*, 2004; *Neumeyer et al.*, 2008] was derived based on the approach presented by *Wziontek et al.* [2009c] using

Table 4.2: Parameters, statistics and performance criteria of the multiple linear regression model for the statistics-based approach to predict the SG residuals from hydrological measurements.

Variable		Regression Coefficient	Standard Error	t value	p value
Intercept		5.71	0.27	21.09	<0.001
Groundwater		-2.02	0.01	-189.00	<0.001
Soil moisture	2.0 m	20.06	1.00	20.09	<0.001
	1.5 m	25.67	1.24	20.66	<0.001
	1.0 m	53.03	2.18	24.36	<0.001
	0.6 m	-82.51	2.76	-29.88	<0.001
	0.4 m	73.40	2.03	36.22	<0.001
	0.3 - 0.0 m	-4.97	0.34	-14.43	<0.001
Snow		58.77	0.65	89.83	<0.001
Estimate of std. dev. of error: 0.61452				Multiple R^2: 0.952	
f-statistic 21610 on 8 and 8751 degrees of freedom				p-Value: 0	

WSC simulated by global hydrological models. To account for uncertainties of global hydrological models, we used the WaterGAP Global Hydrology Model (WGHM) [*Döll et al.*, 2003] and four different land surface models (CLM, MOSAIC, NOAH and VIC) of the Global Land Data Assimilation System (GLDAS) [*Rodell*, 2004]. We calculated the large-scale gravity effect (excluding the near zone of less than 50 km around the SG in Wettzell) for each model in terms of Newtonian attraction and deformation due to the changing load on the Earth's surface.

4.3 Results and discussion

4.3.1 Lysimeter-based approach

In the study period, cumulative precipitation measured by the lysimeter was 1140 mm (Figure 4.3a). The actual evapotranspiration was measured to be 541 mm and deep drainage to be 591 mm. Except for the precipitation, all time series show distinct seasonal variations. Actual evapotranspiration decreases to nearly zero in winter and strongly increases with the start of the vegetation period. Water storage measured by the lysimeter (sum of soil and snow storage) starts to increase in autumn to reach a maximum at the end of February. No deep drainage is observed during winter time (January-February 2009) because soil freezing prevents soil water movement and causes an accumulation of water in the lysimeter system (Figure 4.3a). Snowmelt in February/March causes a strong decrease of the lysimeter weight and an increase of the deep drainage followed by a rise of the groundwater of ~2.2 m (Figure 4.3b).

The time series of the SG residuals and the gravity response to WSC agree well in amplitude, phase and short-term variations (Figure 4.3c). A shift between both time series exists caused by an extreme rainfall event of 64 mm/2 hours on 31 July 2008, which may have lead to a disturbance of the system during its spin-up period. The overall seasonal amplitudes for the SG residuals and the gravity response amount to 9.5 and 8.8 µGal respectively. For the lysimeter-based approach, the regression slope of 0.98 and a corresponding coefficient of determination of 0.97 reflect a good agreement in phase and magnitude of the SG residuals and the lysimeter-based approach (Table 4.3). Short-term variations in SG residuals are strongly influenced by rainfall and snowmelt events and related snow and soil moisture changes. The seasonal variations are mainly associated to WSC in the saprolite and aquifer zone. A wetting front travelling through the hydrological system causes an exponential decay of the WSC. Translated into gravity response, the recession curves tend to become linear and thus agree with the linear character of the SG residuals (Figure 4.3c).

4.3.2 Comparison to other approaches

Hydrological gravity responses estimated with the different approaches are compared in Figure 4.4. The statistics-based approach explains 95 % of the variation of the SG signal. However, the model parameters cannot be interpreted in a physical way. Due to the correlation of soil moisture measurements at different depths, soil moisture data can substitute each other in a regression analysis so that the regression coefficient can become negative (e.g. soil moisture at a depth of 0.6 m in Table 4.2). The correspondence between the model-based approach and SG residuals (97 % of explained signal variation) is also very high, but it is problematic to interpret the internal model

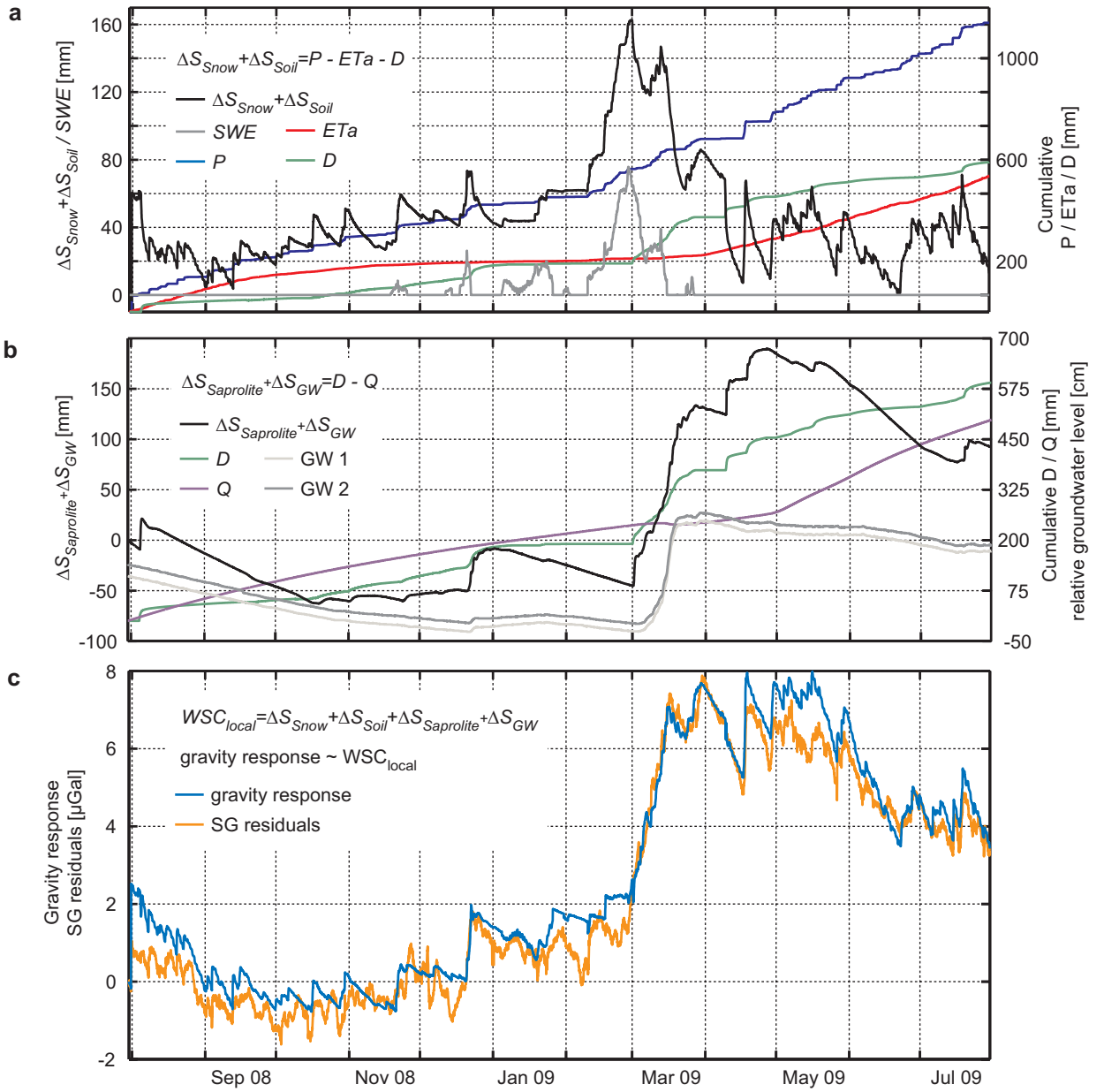

Figure 4.3: a) Time series of lysimeter weight change ($\Delta S_{Snow}+\Delta S_{Soil}$), snow water equivalent (*SWE*), cumulative precipitation (*P*), cumulative evapotranspiration (*ETa*) and cumulative drainage (*D*). b) Time series of water storage changes in the saprolite and groundwater ($\Delta S_{Saprolite}+\Delta S_{GW}$), cumulative drainage from lysimeter (*D*), cumulative groundwater discharge (*Q*), relative groundwater levels (GW 1 & GW 2; absolute groundwater table depth = 1400 - relative groundwater level [cm]). c) Time series of the SG residuals and the total hydrological gravity response derived with the lysimeter approach.

structure or individual parameter sets of these conceptual models in a physical way [*Creutzfeldt et al.*, 2010b]. The data-based approach agrees well with the SG residuals in terms of short-term variations, but using a specific yield of 1 % underestimates the seasonal variation of the SG residuals. The specific yield was estimated to be 7 % by linear regression between groundwater data and the soil moisture reduced SG signal. Using this value, the estimated gravity signal explains 89 % of the SG residuals. However, a specific yield of 7 % is unrealistically high because the estimated specific yield from a pump test was only 1 %. Significant deviations between data-based estimated gravity response and SG residuals can be identified during winter (January-March 2009). The estimated decrease of gravity response is caused by the apparent decrease of soil moisture in the top soil (Figure

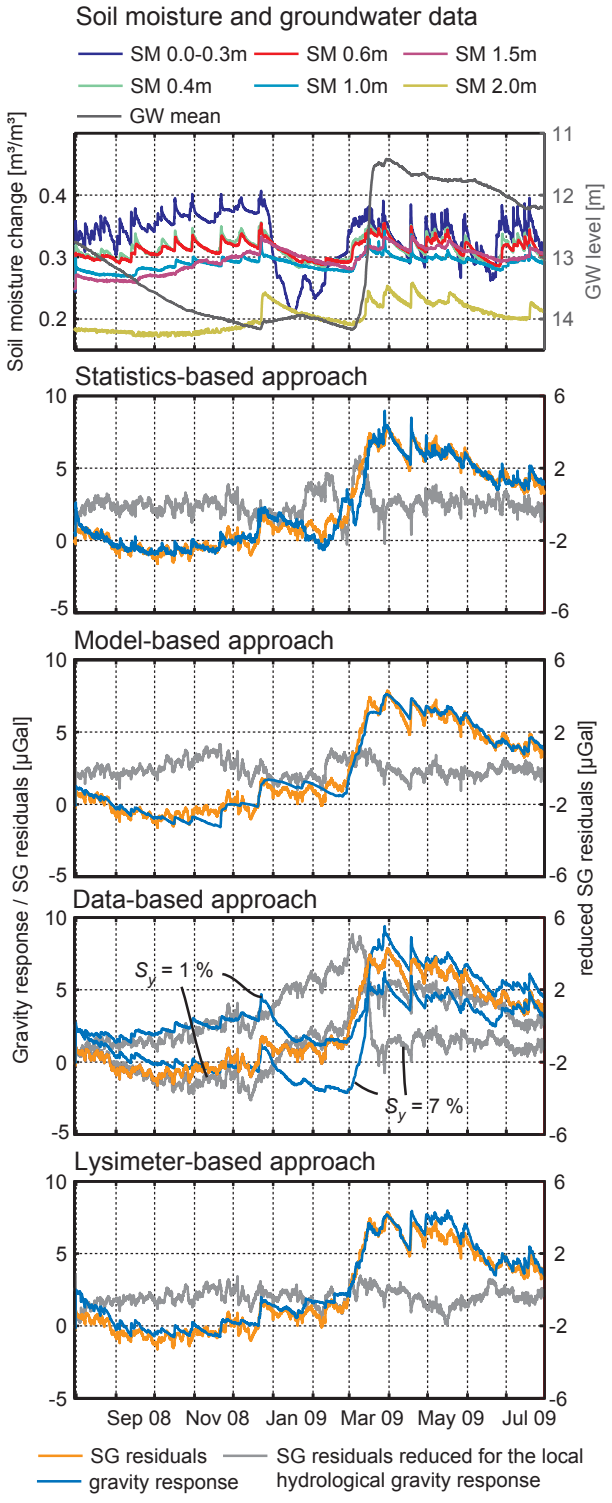

Figure 4.4: Soil moisture (SM) observed at different depth and groundwater data. Gravity response estimated based on the different approaches. SG residuals and the differences between both times series (reduced SG residuals) for each approach.

4.4a: soil moisture 0.0-0.3 m) caused by the change of the dielectric permittivity due to soil freezing. This serves to show that it is difficult to use electromagnetic methods to estimate surface soil moisture during the winter time. For the statistics-based approach, the apparent decrease of soil moisture in the top soil zone is compensated by a small regression coefficient for the top soil zone (Table 4.2).

The correlation of gravimetric time series and local WSC found in this study is higher than previously estimated for Wettzell before lysimeter data were available or for other gravity sites with less extensive hydrological observations. For Wettzell, the variability of the SG residuals explained by independently estimated WSC ranged between 37 % and 77 % and the RMSE varied between 1.57 and 5.70 µGal [*Creutzfeldt et al.*, 2010a]. Longuevergne *et al.* [2009] estimated the local hydrological gravity effect deterministically and explained 31 % (RMSE 1.55 µGal) of SG residual variations for the Strasbourg observatory (personal communication). The approach developed by *Van Camp et al.* [2006] to estimate the local hydrological gravity effect explained 53 % (RMSE 1.02 µGal) of SG residual variations for the geodynamic station in Membach (time series extended to 2009; personal communication). For the SG at the Geodynamic Observatory Moxa, variations of the SG residuals explained by local WSC that had been fitted against the SG residuals ranged between 77 % [*Krause et al.*, 2009] and 80 % [*Hasan et al.*, 2008], whereas *Naujoks et al.* [2009] showed that seasonal variations of the SG residuals of Moxa become visible only after reducing the signal for the local hydrological gravity effect. In the study of *Lampitelli and Francis* [2010], a conceptual model was calibrated against SG residuals, which explained 77 % of the variation of the SG residuals at the Walferdange Underground Laboratory for Geodynamics.

One explanation for the higher correspondence is that lysimeters are considered to be an accurate method to quantify near-surface hydrological flux and storage variations. A higher representativeness is given due to a sampling volume of the lysimeter that is larger by a factor of 1500 compared to electromagnetic (EM) soil moisture sensors (with an assumed sampling volume of 1000 cm³). EM sensors in access tubes have often been used in previous studies, but the accuracy, variability and physical significance of these EM sensors as field soil moisture measurements have been called into question [*Evett et al.*, 2009; *Mazahrih et al.*, 2008]. The present approach combining the lysimeter measurements with a well-constrained physically-based model and complementary data for deeper zones suggests that the derived WSC are as close to reality as we can get nowadays in terms of estimating total WSC at the field scale. Nonetheless, the estimated hydrological gravity response is associated with uncertainties arising from hydrological

Table 4.3: Statistical comparison of SG residuals and the different approaches to estimate the hydrological gravity response and the standard deviation of the reduced SG residuals

Approach	RMSE	Coefficient of correlation	Coefficient of determination	Slope (SG vs. approach)	Standard deviation
Lysimeter-based	0.615	0.987	0.975	0.982	0.44
Statistics-based	0.614	0.976	0.952	0.952	0.61
Model-based	0.473	0.986	0.973	1.01	0.47
Data-based (S_y = 1.0 %)	2.079	0.816	0.666	0.333	1.98
Data-based (S_y = 7.0 %)	1.556	0.891	0.793	1.079	1.56

Table 4.4: Correlation coefficient and the corresponding p-value (in brackets) of the SG residuals reduced for the local hydrological gravity response and the large-scale hydrological gravity effect.

	WGHM	GLDAS CLM	GLDAS MOSAIC	GLDAS NOAH	GLDAS VIC
Lysimeter-based	0.26 (0.41)	0.27 (0.42)	0.14 (0.66)	0.20 (0.53)	0.13 (0.68)
Statistics-based	0.54 (0.07)	0.54 (0.07)	0.45 (0.14)	0.50 (0.10)	0.44 (0.15)
Model-based	0.14 (0.66)	0.13 (0.69)	-0.04 (0.91)	0.06 (0.85)	-0.03 (0.92)
Data-based (S_y = 1 %)	0.50 (0.10)	0.47 (0.12)	0.75 (<0.00)	0.60 (0.04)	0.72 (0.01)
Data-based (S_y = 7 %)	0.75 (0.04)	0.76 (<0.00)	0.51 (0.09)	0.65 (0.02)	0.51 (0.09)

measurement accuracy, assumptions and simplifications in the structural model of the subsurface, hydro(geo) logical parameter estimation, spatial variability of WSC, distribution of WSC in the near field (e.g. below the SG building) and processing of the SG residuals. They were not evaluated in this study. In this uncertainty chain, the distribution of WSC in the near field is considered to have the largest influence on the results.

Another explanation for the higher correlation between the estimated gravity response and SG residuals is that WSC occur almost exclusively below the SG at the Wettzell station (except for snow). This implies that vertical gravity effects are unidirectional only. At SG sites where water mass variations can occur below and above the sensor, their effect might partially cancel each other out and hydrological flow processes, i.e. vertical processes leading to water mass redistribution from above (negative gravity effect) to below (positive gravity effect) the gravimeter are very important. This makes the SG signal interpretation more complicated because hydrological flow processes have to be quantified.

4.3.3 Comparison to the large-scale hydrological gravity effect

Figure 4.5 shows the SG residuals reduced for the local hydrological gravity response (hereinafter referred to as 'reduced SG residuals') in comparison to the modelled large-scale hydrological gravity effect. The reduced SG residuals may reveal other geophysical gravity effects as discussed in the introduction. For the Geodetic Observatory Wettzell, it can be assumed that reduced SG residuals will mainly be caused by large-scale hydrological mass variations because, for a start, all other geophysical signals can be considered to be very small at this station. Using the data-based approach for the local hydrological reduction, the reduced SG residuals show seasonal variations and are significantly correlated (p-value < 0.05) to the large-scale hydrological gravity effect of the hydrological models WGHM, GLDAS CLM and GLDAS NOAH, but not GLDAS MOSAIC and GLDAS VIC (Table 4.4). The data-based approach with a specific yield of 7 % is correlated only to the global hydrological models because the apparent decline of soil moisture due to soil freezing adds a 'seasonal' component to the reduced SG residuals.

The statistics- or model-based approaches explain nearly all of the SG residuals and therefore, the reduced SG residuals are not significantly correlated to the large-scale hydrological effect. The higher correlation coefficient for the statistics-based approach is again due to soil freezing. The poor correlation is not surprising because both approaches were calibrated to best fit the SG data. This finding generally calls into question the benefits of these types of local hydrological reduction when the goal is to study other geophysical processes based on the reduced SG residuals. The calibration to the SG data may accidently remove parts (or all) of the signal of interest, in particular if the reduction method is flexible enough to be adjusted to complex SG residual time series. This is the case in this study, where both the multi-linear regression and the conceptual hydrological model have enough parameters, i.e. degrees of freedom, to be efficiently adjusted to the SG signal.

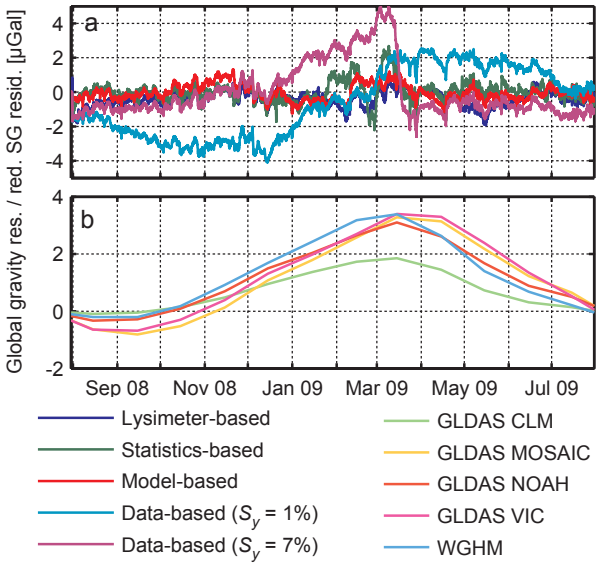

Figure 4.5: SG residuals reduced for the local hydrological gravity response using different approaches (a) in comparison to the large-scale hydrological gravity effect estimated using the different hydrological models (b).

No significant correlation exists between the reduced SG residuals of the lysimeter-based approach and the modelled large-scale hydrological gravity effect (Table 4.4). The standard deviation of the reduced SG residuals is small with less than 0.5 µGal, which is even smaller than for the calibrated approaches. This is surprising because the lysimeter-based reduction was derived completely independent from the SG data. Two explanations exist as to why both signals are not correlated. On the one hand, the local hydrological gravity effect might be overestimated. This could result from uncertainties in estimating the WSC distribution in the near field. In particular, it could not be determined to which extent the observed WSC in the natural environment around the SG building apply to the zone below the base plate of the building. Errors in estimating this contribution, however, would affect the amplitude of the gravity response but not the signal shape or its phase. Thus, assuming a smaller local hydrological gravity effect implies that parts of the observed seasonal trend of about 4 µGal in the SG residuals between the start and the end of the study period would remain unexplained (Figure 4.3c). They cannot be explained by the large-scale hydrological gravity changes because the simulated signal of the global hydrological models are zero over the one year study period (Figure 4.5b). Also the short-term variations (e.g. decrease of SG residuals in the beginning of April 2009) can not be explained by the large-scale hydrological gravity effect. Both facts give some evidence that possibly the local hydrological gravity effect is not overestimated by the lysimeter-based approach.

On the other hand, we might not observe a correlation between the reduced SG residuals and the large-scale hydrological gravity effect due to high uncertainties in the quantification of the large-scale hydrological gravity effect. For example, we estimated the seasonal amplitude of the large-scale hydrological effect for the GLDAS CLM to be 2 µGal and for GLDAS NOAH to be 4 µGal (Figure 4.5b). This is in line with the statement of *Neumeyer et al.* [2008] that the uncertainties from models in estimating the global hydrological effect are in the same range as the signal itself. Additionally, opinions about the importance of the regional and global effect as well as of the large-scale hydrological attraction disagree in literature [*Breili and Pettersen*, 2009; *Crossley et al.*, 2004; *Jacob et al.*, 2008; *Llubes et al.*, 2004; *Neumeyer et al.*, 2008; *Weise et al.*, 2009; *Wziontek et al.*, 2009c]. These uncertainties also question the possible approach of subtracting the large-scale hydrological effect from SG residuals before focusing on the local hydrological signals.

From this discussion of the correlation between local and large-scale gravity effect, we may speculate that, based on the results of the lysimeter-based approach, the large-scale hydrological gravity effect on the SG tends to be smaller than estimated in this study. However, this is not consistent with the observation that global hydrological models tend to under-predict water storage variations when evaluated with time-variable gravity data of the GRACE satellite mission [*Güntner*, 2008]. In summary, one may argue that a remaining key question is the 'scaling problem' caused by uncertainties due to WSC distribution in the near field of a few meters around the SG. The impact of constructions, soil sealing and drainage will make the very near water storage and transport dynamics considerably different from the local water regime under more natural conditions in larger distances around the building and, hence, has to be more carefully addressed to enhance the value of SG data.

4.4 Conclusions

In this study, lysimeter and gravimeter measurements are compared for the first time. Lysimeter measurements in combination with a well-constrained 1D hydrological model and additional observation data (soil hydraulic and groundwater data) are used to estimate total local WSC and the corresponding hydrological gravity effect for the Geodetic Observatory Wettzell.

The results of the lysimeter-based approach were evaluated in comparison to a statistics-based, a model-based and a data-based approach, which represent methods used in previous studies to correct for the local hydrological gravity effect. Approaches calibrated against the SG residuals (statistics- and model-based approach) can explain 95-97 % of the variation of the SG residuals, but it is very difficult to interpret the fitted model as well as

the remaining unexplained part of the SG residuals. Any additional non-hydrological gravity signal of interest may have partly been removed due to the fitting procedure. Thus, the benefit of these approaches for geophysics and geodesy can be questioned.

Therefore, it is necessary to estimate the local hydrological gravity effect independently from the gravimeter measurements. The data-based approach shows the limitations of using only snow, groundwater and near-surface soil moisture data to estimate the total WSC at the field scale. High uncertainties associated with the estimation of hydrological fluxes and specific yield may above all hinder the estimation of WSC in deeper subsurface zones. But WSC in the groundwater and in particular in the unsaturated saprolite zone are especially important components of the seasonal and long-term water storage budget. Short-term variations in the SG residuals can largely be explained by snow mass and near-surface soil moisture changes related to precipitation and snowmelt events. When trying to estimate these changes, uncertainties arise from technical problems of EM sensors, e.g. the failure of EM sensors during frost. Lysimeters, in contrast, allow for the direct and precise estimation of precipitation, evapotranspiration, deep drainage and soil moisture change and for an indirect estimation of WSC in the deep vadose and aquifer zone. Furthermore, lysimeters can also measure WSC during periods of frost and snowmelt provided that the effect of snow bridges is considered.

At sites where temporal gravity observations are undertaken, the installation of a state-of-the-art lysimeter (weighable, suction-controlled and monolith-filled) is recommended in case the gravity signal should be corrected for local WSC. The installation of a lysimeter seems to be justified in view of the very high cost of high precision temporal gravity observations (lysimeters cost less than ~1/10 of an SG). The lysimeter should be combined with a site-specific hydrological observation strategy to monitor total WSC at the field scale.

The gravity response of the lysimeter-based estimated total WSC is in very good agreement with the SG residuals, implying that the gravity residuals are caused to a larger extent by local WSC than previously stated. This highlights the importance of considering the effect of local WSC in all storage components of ground-based temporal gravity observations on the event and seasonal timescales, but long-term WSC might also exist. Hence, extreme caution should be applied when interpreting gravity residuals in terms of large-scale hydrological variation. For example, the direct comparison of gravimeter measurements with GRACE data [*Andersen et al.*, 2005] is only valid if local and regional WSC are similar in phase and amplitude. Geophysical processes can be masked by local hydrological mass transfer processes, but a lysimeter-based approach can accurately estimate the WSC to correct the temporal gravity signal for the hydrological gravity effect and can provide us with the possibility of studying these variations of the Earth's gravity field with ground-based temporal gravity observations.

Acknowledgement. The authors wish to thank the editor Michel Diament, the reviewer Michel Van Camp and one anonymous reviewer for their constructive comments which significantly improved the manuscript. This work has been supported by the Deutsche Forschungsgemeinschaft (German Research Foundation) within the Priority Program SPP 1257 'Mass transport and mass distribution in the system Earth', project TASMAGOG.

Chapter 5:

The benefits of gravimeter observations for modelling water storage changes at the field scale

The benefits of gravimeter observations for modelling water storage changes at the field scale

Abstract

Water storage is the fundamental state variable of hydrological systems. However, comprehensive data on total water storage changes (WSC) are practically inaccessible by hydrological measurement techniques at the field or catchment scale, and hydrological models are highly uncertain in representing the storage term due to the lack of adequate validation or calibration data. In this study, we assess the benefit of temporal gravimeter measurements for modelling WSC at the field scale. A simple conceptual hydrological model is calibrated and evaluated against records of a superconducting gravimeter, soil moisture and groundwater time series. The model is validated against independently estimated WSC data. Using gravimeter data as a calibration constraint improves the model results substantially in terms of predictive capability and variation of the behavioural model runs. Thanks to their capacity to integrate over different storage components and a larger area, gravimeters provide generalised information on total WSC that is useful to constrain the overall status of the hydrological system in a model. The general problem of specifying the internal model structure or individual parameter sets can, however, not be solved with gravimeters alone.

Published as:

Creutzfeldt, B., A. Güntner, S. Vorogushyn, and B. Merz (2010), The benefits of gravimeter observations for modelling water storage changes at the field scale, Hydrol. Earth Syst. Sci., 14, 1715-1730, http://dx.doi.org/10.5194/hess-14-1715-2010.

[Author's note: The manuscript underwent modifications during the review process after this document was compiled. Please check the journal for the final version.]

5.1 Introduction

In hydrology, the measurement of the water storage term in the *only hydrological equation* [*Blöschl*, 2005] – the water balance equation – is still a challenging task at all scales. Therefore, catchments are characterised by the output – in general the discharge – using the storage-output relationship to draw conclusions on the storage of an area. However, as *Beven* [2005] states „… we do not have the investigative measurement techniques necessary to be secure about what form these [storage-output; note from the author] relationships should take … except by seeing which functions might be appropriate in reproducing the discharges at the catchment outlet (where we can take a measurement)."

Progress in observation techniques has improved the estimation of water storages at various scales. At the global scale, GRACE [*Tapley et al.*, 2004] gives us the unique opportunity to estimate water storage changes (see *Ramillien et al.* [2008] for a review) and to improve macro-scale hydrological models [*Güntner*, 2008; *Lo et al.*, 2010; *Werth et al.*, 2009a; *Zaitchik et al.*, 2008]. At the field scale, water storage and its changes are generally estimated by point measurements, but high spatial and temporal variability makes the estimation of water storages difficult. Different techniques and strategies have been developed to overcome these problems, e.g. gathering many soil moisture measurements and inter-/extrapolating them by geostatistics [e.g. *Western et al.*, 2002] or ground penetrating radar measurements [e.g. *Huisman et al.*, 2002; *Huisman et al.*, 2003], the use of spatial TDR soil moisture measurements [e.g. *Graeff et al.*, 2010] or of high-precision lysimeters [e.g. *von Unold and Fank*, 2008] and the development of cosmic ray neutron probes [*Zreda et al.* 2008]. In general, these techniques are limited to the estimation of near-surface water storages. Neutron probes, electromagnetic sensors or (cross-borehole) geophysics in boreholes allow the estimation of water storages in deeper zones, but the temporal as well as the spatial resolution (depth and area) is limited. Further limitations such as high inaccuracies of electromagnetic sensors in access tubes [e.g. *Evett et al.*, 2009] make the estimation of subsurface WSC at the field scale a challenging task, especially for deeper zones.

Ground-based temporal gravity measurements using absolute or relative gravimeters are influenced by local WSC [e.g. *Abe et al.*, 2006; *Amalvict et al.*, 2004; *Bonatz*, 1967; *Bower and Courtier*, 1998; *Boy and Hinderer*, 2006; *Crossley et al.*, 1998; *Jacob et al.*, 2008; *Kroner and Jahr*, 2006; *Llubes et al.*, 2004; *Longuevergne et al.*, 2009; *Meurers et al.*, 2006; *Naujoks et al.*, 2008; *Pool and Eychaner*, 1995; *Van Camp et al.*, 2006]. The effect of WSC on gravity measurements does not only depend on the topography around the gravity sensor but is also a function of the vertical distribution of mass change below the sensor [*Creutzfeldt et al.*, 2008]. Different studies showed that local WSC within a radius of 50 to 150 m around the gravimeter are of primary interest for the local hydrological effect on temporal gravity measurements [e.g. *Hasan et al.*, 2008; *Hokkanen et al.*, 2006; *Kazama and Okubo*, 2009; *Naujoks et al.*, 2008; *Van Camp et al.*, 2006]. The gravity time series thus primarily reflect WSC on the field scale, but the exact sampling volume is difficult to define.

Consequently, the question arises: How can we use temporal gravity measurements for hydrological applications? Different studies focus on the interpretation of the gravity signal by single storage components (e.g. surface water [*Bonatz and Sperling*, 1995; *Lampitelli and Francis*, 2010], snow [*Breili and Pettersen*, 2009], soil moisture [*Van Camp et al.*, 2006] or groundwater [*Harnisch and Harnisch*, 2006; *Takemoto et al.*, 2002]) or by estimation of different subsurface properties (e.g. porosity [*Jacob et al.*, 2009], fractures [*Hokkanen et al.*, 2007], block content [*Van Camp et al.*, 2006] or specific yield [*Pool and Eychaner*, 1995]). The unambiguous identification of the exact source of the gravimeter signal is difficult or even impossible if no additional information is available implying that the estimation of single parameters representing the storages or properties is associated with a high uncertainty [*Creutzfeldt et al.*, 2010a; *Pool*, 2008]. *Blainey* [2007], for example, pointed out that the estimation of hydraulic conductivity and specific yield by gravity data alone was likely to be unacceptably inaccurate and imprecise.

Temporal gravimeter measurements result in an integral signal. Hence, one may adopt a holistic perspective by considering temporal gravimeter measurements as an integral signal of the hydrological system status similar in nature to discharge measurements [*Hasan et al.*, 2008]. More precisely, temporal gravity data can be a direct measure of the change of the system status – the change of water storages – whereas discharge is a measure for the catchment response. The latter requires assumptions about the storage-output relationship to characterise the system status.

In the absence of adequate observation data, the only and frequently used alternative to comprehensively characterise the hydrological system status is by applying hydrological models. Many different hydrological models have been developed ranging from simple, lumped and conceptual models to complex, distributed and physically-based ones. Typically, measured input fluxes are used to drive a model. The model parameters are calibrated to match the observed output fluxes, usually river discharge. This approach leaves the model with a considerable uncertainty in representing the status of a complex hydrological system because the relationship between the system response and its status may not be unique (hysteresis) [*Spence et al.*, 2009] and/or many different parameter sets may result in similar system responses

[equifinality problem after *Beven and Binley*, 1992].

In this study, instead of calibrating a hydrological model against output fluxes, we use information about the change of the integral system status for model calibration. The aim is to investigate the benefit of temporal gravimeter measurements for hydrological modeling as an integrative measure of the water storage term. Gravimeter observations are assessed in comparison to classical hydrological point measurements (groundwater and soil moisture) using the different data sets as calibration constraints. We apply a simple conceptual model that comprises a set of connected linear storages with a limited number of free parameters as a typical example of hydrological models widely used in catchment modelling.

5.2 Study area and data

5.2.1 Study area

The study area is located in the Bavarian Forest, a mid mountain range in the Southeast of Germany (Figure 5.1). The area is characterised by flat highlands with grassland and fields and steep long slopes dominated by forestry. The study area surrounds the Geodetic Observatory Wettzell operated by the Federal Agency for Cartography and Geodesy [*Schlüter et al.*, 2007].

The observatory is mainly surrounded by grassland with single bushes. The geology is made up of gneiss and the bedrock seamlessly merges into the weather saprolite layer. *Creutzfeldt et al.* [2010a] classified the underground of the direct gravimeter surrounding into the following four different zones: (1) soil zone with mainly loamy-sandy brown soils (Cambisols), (2) saprolite zone consisting of grus (weathered gneiss), (3) fractured zone and (4) the basement zone.

5.2.2 Gravity data

The dual-sphere superconducting gravimeter (SG) CD029 of the Geodetic Observatory Wettzell, which is part of the Global Geodynamics Project (GGP) network [*Crossley et al.*, 1999; *Crossley and Hinderer*, 2009], measures the temporal variation of the Earth's gravity field. The scale factor and the instrumental drift of the SG were determined by absolute gravity measurements [*Wziontek et al.*, 2009a]. Temporal variations of the Earth's gravity field are mainly influenced by tides of the solid Earth, ocean loading effects, mass changes in the atmosphere and polar motion. These gravity effects have to be removed to reveal the hydrological signal in gravimeter measurements. A tidal analysis was performed to remove the solid Earth tides and ocean loading effects. Atmospheric effects were removed by three-dimensional modelling of atmospheric mass changes [*Klügel and Wziontek*, 2009]. The pole coordinates as provided by the International Earth Rotation and Reference Systems

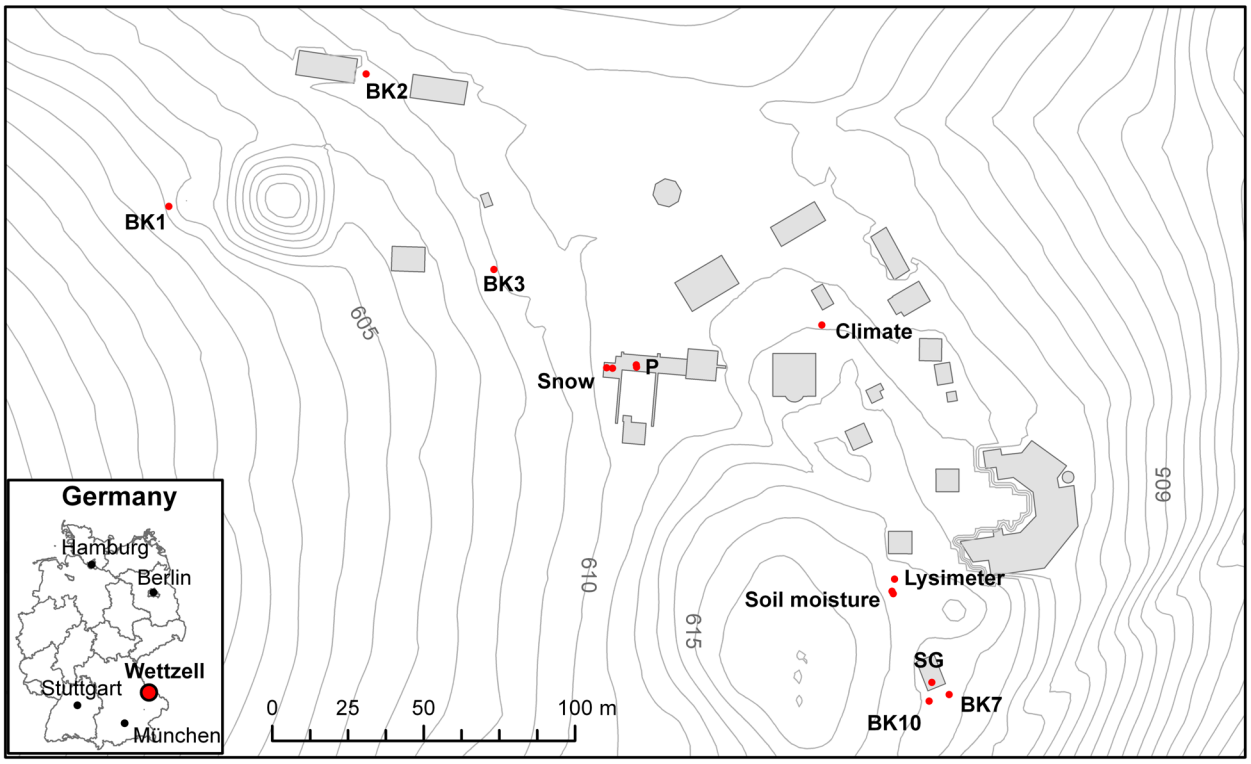

Figure 5.1: Study area with the different hydrological sensors and the topography represented by contour lines (distance 1 m). Location of Wettzell in Germany and some major cities are displayed in the inset map.

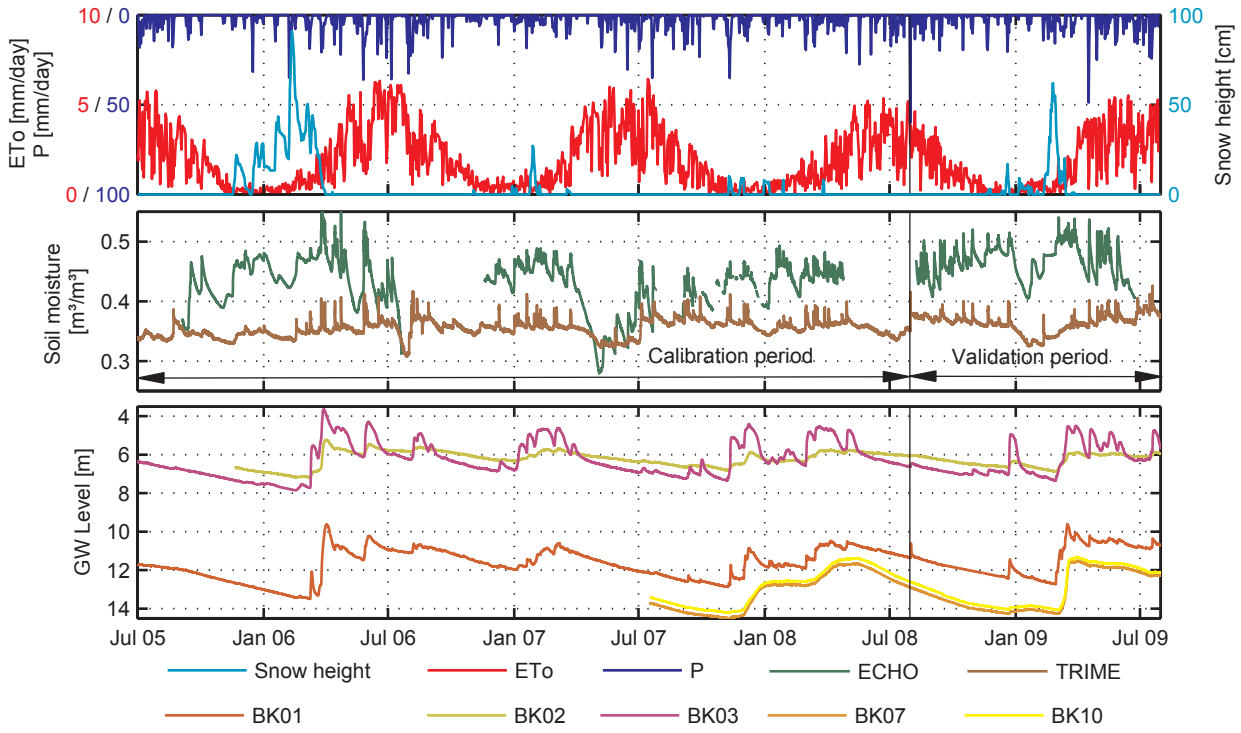

Figure 5.2: Time series of input and calibration data. Time series of daily precipitation (*P*), daily reference evapotranspiration (*ETo*) and snow height (top). Time series of soil moisture (middle) and groundwater data (bottom).

Service (IERS) were used to calculate the effect of polar motion. For details on the SG instrument and the data processing, the interested reader is referred to *Hinderer et al.* [2007].

SG residuals were derived by removing the different gravity effects from the SG signal. These residuals are considered to be caused by hydrological mass variation, because all other possible effects on temporal gravimeter measurements are assumed to be negligible for Wettzell (e.g. post-glacial rebound or processes in the Earth's mantle and core). For the SG Wettzell, *Creutzfeldt et al.* [2008] showed that between 52 % and 80 % of the local hydrological gravity signal is generated within a radius of 50 m around the SG, and 90 % of the signal comes from an area within a radius of around 1000 m. A high correlation of independently estimated WSC in this area and SG residuals (coefficient of determination: 0.97; corresponding slope: 1.06) proved that a major part of the gravity residuals is generated by WSC in this area [*Creutzfeldt et al.*, 2010c]. In the present study, the large-scale hydrological effect on gravimeters [e.g. *Llubes et al.*, 2004; *Weise et al.*, 2009] is not considered due to the dominant local hydrological influence and high uncertainties in the modelling of large-scale WSC [e.g. *Werth et al.*, 2009b]. The SG signal was not corrected for the global hydrological effect because different hydrological models show that the estimated gravity effect due to large-scale WSC lies in the same order of magnitude as the differences between different models [*Neumeyer et al.*, 2008; *Wziontek et al.*, 2009b].

5.2.3 Meteorological data

Meteorological data – air temperature, relative humidity, wind speed and global radiation – were recorded at the Geodetic Observatory Wettzell (Table 5.1 and Figure 5.1) and were processed to hourly time series for the whole study period from 01 July 2005 to 31 July 2009. A few data gaps in the time series were filled using the nearby climate station Allmannsdorf at a distance of 6 km and an altitude of 557 m [*LfL*, 2009]. The reference evapotranspiration for short grass canopy was calculated from the climate data based on the Penman-Monteith equation from the American Society of Civil Engineering [*Allen et al.*, 2005].

Precipitation was measured by two heated tipping bucket rain gauges (Figure 5.1, Table 5.1). The differences of the total precipitation were less then 1 % for both gauges for the study period, so the mean of both gauges was used for further analysis. The precipitation was corrected for wind effect and wetting losses, acknowledging the well-known undercatch of unshielded heated tipping gauges [*Allerup*, 1997; *Richter*, 1995].

Since August 2007, a snow monitoring system consisting of a snow pillow and an ultrasonic snow depth sensor is measuring snow depth and the snow water equivalent

(SWE) (Figure 5.1, Table 5.1). Before the installation, the snow depth was derived from two snow depth gauge stations close to the observatory (Prackenbach-Moosbach: distance 8 km, altitude 505 m; Viechtach-Bühling: distance 3 km, altitude 662 m). Figure 5.2 shows the records of precipitation, reference evapotranspiration and snow height.

5.2.4 Hydrological / water storage data

For the whole study period from 01 July 2005 to 31 July 2009, soil moisture and groundwater data were recorded. Soil moisture was measured with a capacitance (ECHO) and 'pseudo TDR' sensor (TRIME) at a depth of 0.5 m. Groundwater level data were available from 3 different boreholes (BK1, BK2, BK3) using a relative pressure transducer. Since mid-2007, additional boreholes have been drilled and equipped with multi-parameter sensors, but of these, only boreholes BK7 and BK10 close to the SG are relevant for this study (Figure 5.1, Figure 5.2, Table 5.1).

For the period from 30 July 2008 to 30 July 2009, independently estimated WSC were available from *Creutzfeldt et al.* [2010c]. In this study, WSC were derived from lysimeter measurements in combination with complementary hydrological observations and a hydrological 1D model for the SG site. WSC up to a depth of 1.5 m, precipitation, actual evapotranspiration and deep drainage were estimated by a monolith-filled, suction-controlled and weighable lysimeter [*von Unold and Fank*, 2008]. WSC below the lysimeter in the deep vadose zones, the saprolite zone, and in the groundwater were estimated by the deep drainage of the lysimeter and the groundwater level. Water redistribution in the saprolite and groundwater zone and the groundwater discharge were calculated using the physically-based hydrological model HYDRUS 1D [*Šimůnek et al.*, 2008]. The underground was classified into the saprolite (thickness 9.5 m) and the fractured (thickness 4.5 m) zone and was parameterised based on measurements of water retention and of saturated hydraulic conductivity and on pump tests [*Creutzfeldt et al.*, 2010a]. Deep drainage measurements from the lysimeter were used to define the upper boundary flux of the hydrological model. The lower boundary was defined by the groundwater level (BK07 and BK10) as variable head conditions. This approach developed for the SG site was transferred to the other groundwater sites (BK1, BK2, BK3). The underground model was adjusted and the corresponding groundwater level data were used as the lower model boundary. The underground was classified based on the cores from the corresponding boreholes. At the BK1 site, the thickness of the saprolite (9.0 m) and fractured (3.0 m) zone was comparable to the SG site. For the BK2 and BK3 sites the thickness of the saprolite zone was only 4.5 m and 3 m respectively. The fractured zone thickness was estimated to be 5.5 m for BK2 and 3.0 m for BK3. Finally, for the four sites, namely SG, BK1, BK2 and BK3, WSC were estimated for the period from 30 July 2008 to 30 July 2009 (Figure 5.1).

Table 5.1: Measured variable and the corresponding devices/sensors at the Geodetic Observatory Wettzell.

Measured variable	Unit	Sensor/Device
Relative gravity	µGal	GWR SG CD029
Absolute gravity	µGal	Micro-g LaCoste FG5
Wind direction	deg.	Lambrecht 14512 G3
Wind speed	m s^{-1}	Lambrecht 14512 G3
Air temperature	°C	Lambrecht 809 MU
Relative air humidity	%,	Lambrecht 809 MU
Precipitation	mm	L-Tec tipping gauge
Global radiation	W/m²	Kipp&Zonen CM11
Snow depth	mm	Sommer USH-8
SWE	mm	Sommer snow pillow
Soil moist. (TRIME)	m³/m³	IMKO TRIME-EZ
Soil moist. (ECHO)	m³/m³	Decagon EC-10
Groundwater	m	SEBA MDS-Dipper-3
Groundwater	m	SEBA MDS-Dipper-T

In order to quantify near-surface hydrological flux and storage processes, lysimeters are considered to be a very accurate method [e.g. *Howell*, 2004; *Tolk and Evett*, 2009; *Yang et al.*, 2000]. In combination with a well-constrained physically-based model and complementary data for the deeper zones, this suggests that the derived WSC are as close as we can get to reality nowadays in terms of estimating total WSC. In this context, we assume that the estimated WSC from the multi-method and multi-site approach presented above can henceforth serve as validation data at the field scale.

5.3 Hydrological modelling

5.3.1 Model structure

For the estimation of WSC, a simple conceptual hydrological model was set up with the prerequisite to account for both parameter parsimony and adequate representation of hydrological processes. On the one hand, the model should be as simple as possible with a few parameters only. On the other hand, the model must represent the different hydrological storage components and water fluxes

Table 5.2: Parameters of the hydrological model and for the estimation of the gravity response and their lower and upper bounds.

Parameter	Description	Unit	Min.	Max.
Hydrological parameters				
Pcorr	Precipitation correction parameter	-	0.9	1.15
FC	Field capacity	mm	50	300
LP	Threshold for reduction of ETo	-	0.5	1.0
alpha	Shape coefficient	-	0	0.2
k_{Soil}	Recession coefficient for top soil storage	h	0	3000
$k_{Saprolite}$	Recession coefficient for saprolite storage	h	50	5500
k_{GW}	Recession coefficient for groundwater	h	50	5500
Gravity response parameters				
gSWE	Factor for snow gravity response	µGal	$-3.9\times10^{-6}\times SWE^2$	$-0.0009\times SWE$
gSM	Factor for top soil gravity response	µGal	0.026	0.015
gV_{Soil}	Factor for soil gravity response	µGal	0.035	0.017
$gV_{Saprolite}$	Factor for saprolite gravity response	µGal	0.050	0.014
gV_{GW}	Factor for groundwater gravity response	µGal	0.049	

between them, because the gravity response depends on where and in which storage WSC occur in relation to the gravimeter [*Creutzfeldt et al.*, 2008]. The model is based on the HBV model [*Bergström*, 1992; *Seibert*, 2005] but has been adapted and modified to reflect storages and fundamental mechanisms of the study area. Based on the underground classification, the model considers WSC in the snow, soil, saprolite and groundwater storages. It consists of a snow (*SS*), top soil (*SM*) (depth: 0.0-0.5 m), soil (V_{Soil}) (depth: 0.0-1.0 m), saprolite ($V_{Saprolite}$) (depth: 1.0-13.0 m), and groundwater module (V_{GW}) (depth: 13.0-16.0 m). The model uses hourly precipitation, reference evapotranspiration and snow height as input data and estimates the WSC in the different storages.

The snow water equivalent was computed based on the snow depth and precipitation data. During periods with a snow height greater than zero, we assumed that all precipitation had fallen as snow (*SIn*). We also assumed that a decline of snow depth was caused by snowmelt (*SOut*), whereas the snowmelt amount was proportionally estimated in relation to the snow depth decline. For each time step, the snow storage is

$$SS_{(t)} = SS_{(t_0)} + SIn_{(t)} - SOut_{(t)} \tag{5.1}$$

where t_0 is the time step preceding t. Precipitation and snowmelt (P) were partitioned into the top soil and soil module based on the factor *alpha*. The top soil storage was a simple bucket storage with a maximum storage capacity of *FC*. The top soil moisture was calculated as

$$SM_{(t)} = SM_{(t_0)} + P_{(t)} \cdot (1 - alpha) - ETa_{(t)} \tag{5.2}$$

Excess water (q_{excess}) was directly routed into the soil storage V_{Soil}. The actual evapotranspiration (*ETa*) was calculated based on the reference evapotranspiration (*ETo*) as follows

$$ETa_{(t)} = \begin{cases} ETo_{(t)} & for \quad \dfrac{SM_{(t_0)}}{FC} > LP \\ ETo_{(t)} \dfrac{SM(t_0)}{FC \cdot LP} & for \quad \dfrac{SM_{(t_0)}}{FC} \le LP \end{cases} \tag{5.3}$$

where *LP* is the threshold reducing the reference evapotranspiration depending on the soil moisture. The input into the soil storage was determined by

$$I_{(t)} = P_{(t)} \cdot alpha + q_{excess} \tag{5.4}$$

and the outflow by

$$Q_{Soil(t)} = Q_{Soil(t_0)} e^{-(t-t_0)/k_{Soil}} + I_{(t)} \left[1 - e^{-(t-t_0)/k_{Soil}} \right] \tag{5.5}$$

where k_{Soil} is the storage coefficient of the soil storage [h]. The soil storage (V_{Soil}) was calculated

$$V_{Soil(t)} = k_{Soil} \cdot Q_{Soil(t)} \tag{5.6}$$

The outflow and water storage of the saprolite ($V_{Saprolite}$) and groundwater (V_{GW}) were estimated analogously to Eq. (5) and Eq. (6) using the outflow of the upper storage as input.

Three model parameters represented the interaction of atmosphere and soil (*FC, LP and alpha*). The other three parameters controlled the water storage in soil, saprolite and groundwater (k_{Soil}, $k_{Saprolite}$ *and* k_{GW}). A multiplication factor for precipitation correction (*Pcorr*) was introduced to account for possible differences of precipitation measured by the tipping bucket rain gauge and lysimeter.

Table 5.3: The different calibrated models based on the different data sources and the site type.

Models	Data set: SG	Groundwater: BK1	Groundwater: BK2	Groundwater: BK3	Soil moist.: ECHO	Soil moist.: TRIME	Site type
SG	x						Deep vadose zone
SGECHO	x				x		Deep vadose zone
SGTRIME	x					x	Deep vadose zone
BK1		x					Shallow vadose zone
BK1ECHO		x			x		Shallow vadose zone
BK1TRIME		x				x	Shallow vadose zone
BK2			x				Shallow vadose zone
BK2ECHO			x		x		Shallow vadose zone
BK2TRIME			x			x	Shallow vadose zone
BK3				x			Shallow vadose zone
BK3ECHO				x	x		Shallow vadose zone
BK3TRIME				x		x	Shallow vadose zone
ECHO					x		Shallow vadose zone
TRIME						x	Shallow vadose zone

5.3.2 Gravity response

WSC can be compared to temporal gravity measurements either by calculating the Newtonian gravity effect of WSC on gravimeter measurements (forward problem) or by deriving masses of WSC from temporal gravity measurements (inverse problem). Here, we pursued the solution of the forward problem avoiding problems associated with inversion, e.g. multiple solutions. The influence of WSC on gravimeter measurements – the gravity response – was calculated based on the approach presented by *Creutzfeldt et al.* [2008] for a square with a side length of 4 km and the SG located in its centre. In this approach, a spatially nested discretisation domain was developed. A high-precision DEM was used to distribute the estimated WSC along the topography and to discretise the continuous landscape into elementary bodies. For each elementary body the gravity effect was calculated based on a modified point mass equation [*Leirião et al.*, 2009; *MacMillan*, 1958]. The gravity response for each different storage component was derived by summation of all gravity changes in each elementary body in the corresponding storage zone of the model domain. By doing this, we derived a 'WSC to gravity response conversion factor' for each storage component.

The surrounding and subsurface structures in the vicinity of the gravimeter have a major influence on the relationship between WSC and gravity residuals. However, we do not exactly know what happens below the gravimeter building, which prevents infiltration of water into the soil (umbrella effect). Hence, uncertainties arise for the physical solution of the forward problem. For each storage component, we estimated the physically possible upper and lower bounds of the 'WSC to gravity response conversion factor' to take into account these uncertainties. Therefore, we looked at both possibilities in that we first calculated the gravity effect assuming that WSC can occur below the gravimeter building and then, as a second possibility, excluded mass variations below the base plate. These uncertainties only apply for the storage components *SM*, V_{Soil} and $V_{Saprolite}$, because snow accumulates on the roof of the SG building and free gravity-driven groundwater flow is not affected by the SG building. Furthermore, we assumed for *SM* and V_{Soil} storages that WSC occur neither in the concrete foundation nor in the base plate of the SG building [*Creutzfeldt et al.*, 2008]. This implies that three additional parameters have to be estimated to derive the gravity response from WSC in the *SM*, V_{Soil} and $V_{Saprolite}$ storage (Table 5.2). These parameters were considered to also account for the precipitation redistribution from the SG roof to the drainage tank at a distance of ~20 m from the SG.

5.3.3 Assessment of model performance

We distinguished between calibration, evaluation and validation process. The automated calibration of the hydrological model was based on the GLUE method developed by *Beven and Binley* [1992]. 50 000 Monte Carlo runs were performed with different parameter sets. The parameter sets were sampled assuming uniform distribution between the lower and upper bounds. For initial model runs, the parameter range was chosen based on previous studies [*Merz et al.*, 2009; *Seibert*, 1996], but they were adjusted so that the parameter for the behavioural model runs were only limited by physical properties.

In the GLUE approach, the definition of behavioural model runs is based on a threshold value for the performance indices. Here, the correlation coefficient (R) was used as a performance index of the relative temporal dynamics in the simulated time series. Using R avoids the need to get absolute water storage data from the observations by deriving the specific yield of the aquifer and estimating the field capacity of the soil or calibrating the soil moisture sensors. In this study, we defined the top 0.1 % of the model runs as behavioural model runs. This allows for a better quantitative comparison of the different calibrated models [*Juston et al.*, 2009].

The performance of each single model run was evaluated by comparing modelled to measured data. Firstly, we compared the modelled gravity response to the SG residuals. Secondly, the performance of each model run

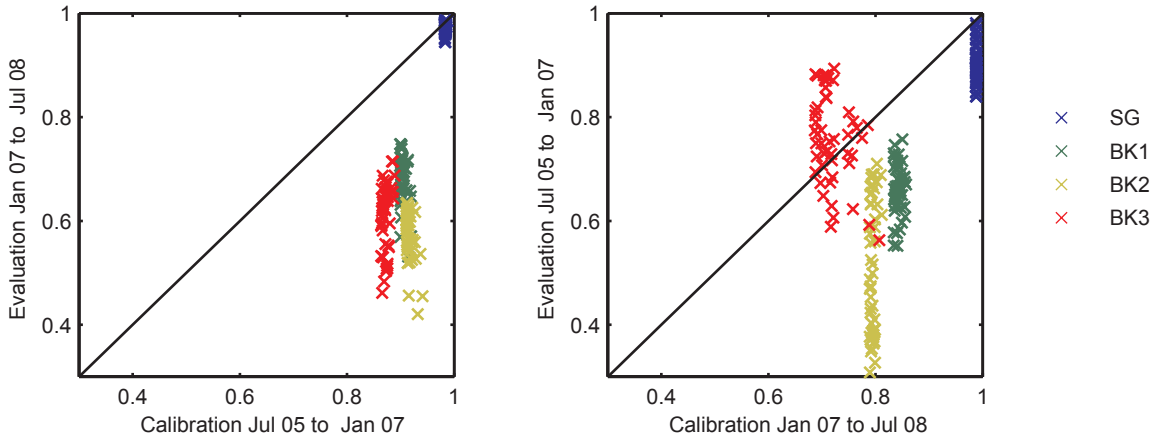

Figure 5.3: Model performance of four models for the calibration versus the evaluation periods. Here the correlation coefficient is used as a performance index.

was evaluated by comparing WSC in the *SM* storage and the V_{GW} storage to the soil moisture (ECHO, TRIME) and groundwater measurements (BK1, BK2, BK3). Thirdly, a multi-criteria calibration was performed based on soil moisture and groundwater data on the one hand and soil moisture and gravity data on the other. The mean of the different performance indices was used to allow a direct comparison to single-criteria calibrated models. In total, 14 different calibrated models were derived (Table 5.3). Each of these models consisted of 50 behavioural model runs.

The model performance was tested using two different strategies: the evaluation and the validation of the model. For model evaluation, we applied a split-sample test according to *Klemes* [1986b]. The record was split into two parts of equal duration from 01 July 2005 to 31 December 2006 and from 01 January 2007 to 01 July 2008. The model was calibrated for the first period and the performance was evaluated using the data from the second period. Then the periods were swapped and the model was calibrated for the second period and evaluated for the first period. A warm-up period of 2 years was used prior to every simulation. Finally, the model performance was evaluated by comparing the performance indices for the different calibration/evaluation periods. The model can be considered acceptable if the model performs similarly well for both periods.

The split-sample test is a classical hydrological model test, which is a necessary rather than a sufficient testing scheme allowing to asses the capability of the model to make accurate predictions also for periods outside the calibration period [*Refsgaard and Knudsen*, 1996]. Using SG as calibration constraint, this test can prove the model adequacy to represent the SG residuals also outside the calibration period. However, temporal gravity data do not directly measure the WSC in mm but express the influence of WSC in change of gravity. Hence, a second strategy for testing the model with independent data, the model validation, was implemented. The WSC from the lysimeter approach for the different sites (see section Data) were used as the validation data. Based on the available data, the study period was divided into a calibration period (from 01 July 2005 to 30 July 2008) and a validation period (from 30 July 2008 to 31 July 2009). Different models were calibrated against gravimeter, groundwater and/or soil moisture data as described above. The models were validated by independently measured WSC. The modelled and measured results were compared using the *R*, the standard deviation and the centred root-mean-square differences (*RMSD*) [*Taylor*, 2001]. The model validation with independent data allows gaining credibility in the novel measurement method to serve as calibration/validation data for hydrological modelling.

Finally, the modelled hydrological gravity response (SG model) is compared to the SG residuals for the whole study period. For this comparison the Nash-Sutcliffe coefficient [*Nash and Sutcliffe*, 1970] was used as a performance index to constrain the 'WSC to gravity response conversion factors'.

5.4 Results and discussion

5.4.1 Model evaluation

Focusing on the performance of the behavioural model sets (top 0.1 % simulations) during the calibration/evaluation period, differences between the models calibrated against different data sources could be identified. For the calibration period, using groundwater or/and soil moisture as calibration constraints, the maximum achieved performance indices were smaller and the range of the performance indices was larger than for models calibrated against SG data (Table 5.4). As a reason for this, one could argue that more parameters are available to

Table 5.4: Range of performance indices for the different calibration/evaluation periods for the models calibrated against the different data sources.

Period	Calibration 2005-2006	Evaluation 2007-2008	Calibration 2007-2008	Evaluation 2005-2006
SG	0.98-0.99	0.94-0.99	0.99-0.99	0.84-0.98
BK1	0.90-0.92	0.53-0.75	0.83-0.86	0.55-0.76
BK2	0.91-0.94	0.42-0.63	0.80-0.81	0.31-0.71
BK3	0.86-0.88	0.46-0.71	0.67-0.81	0.56-0.89
ECHO	0.80-0.81	0.76-0.82	0.88-0.89	0.81-0.81
TRIME	0.51-0.52	0.53-0.60	0.53-0.60	0.51-0.52
SGECHO	0.87-0.88	0.76-0.93	0.95-0.95	0.71-0.80
BK1ECHO	0.84-0.85	0.63-0.82	0.87-0.88	0.67-0.77
BK2ECHO	0.84-0.85	0.57-0.77	0.83-0.84	0.51-0.75
BK3ECHO	0.81-0.83	0.63-0.81	0.79-0.84	0.60-0.82
SGTRIME	0.77-0.79	0.72-0.81	0.87-0.87	0.64-0.70
BK1TRIME	0.72-0.80	0.50-0.74	0.77-0.78	0.54-0.66
BK2TRIME	0.72-0.79	0.49-0.69	0.73-0.76	0.40-0.65
BK3TRIME	0.70-0.80	0.51-0.73	0.69-0.74	0.52-0.68

match the SG record than to fit the model to the other observation data. The larger degree of freedom may cause better calibration performance. This could be true for soil moisture where only four parameters can be calibrated to match the observation. But all model parameters influence the groundwater part of the model because V_{GW} is the last component in the storage cascade. Hence, the same parameter amount is available to fit the model to the groundwater record as to match the SG observations. The three 'WSC to gravity response conversion factors' are of minor importance for the temporal reproduction of the SG residuals because they only influence the amplitude of the signal.

Figure 5.3 and Table 5.4 summarise the comparison of the model performance during the calibration versus the evaluation periods. The differences of the performance index between the calibration and evolution period are higher for models calibrated against groundwater or soil moisture than for models using SG data as calibration constraint. This pattern is persistent also for the multi-objective calibrated models. The model evaluation shows that the model predicts the temporal behaviour of the SG residuals in a better way than the temporal variation of the groundwater or soil moisture for the calibration and evaluation period. For the independent evaluation period, the model performance for groundwater and/or soil moisture models deteriorates more than for SG models.

One explanation for the difference in model performance and predictive capability is that point measurements of WSC are a product of complex processes such as preferential flow, root water uptake, soil freezing/thawing or lateral flow. Furthermore, WSC vary in space due to spatial heterogeneity of landscape features. Hence, differences of modelled and measured records exist because these detailed processes or the spatial variability of WSC could not be represented by the generalised and simplified conceptual model. Since they integrate over different storages and a larger area, SG measurements can resolve neither the detailed and complex processes nor the high spatial variability of WSC. SGs capture a generalised and simplified signal, which is in accordance with the nature of conceptual models. Not surprisingly, the performance and predictive capability is better for the generalised and simplified signal than for a complex and variable signal.

Due to the integral character of SG measurements, it remains difficult to make statements about internal model structures or to differentiate between single parameter sets. Soil moisture and/or groundwater data permit the evaluation of internal model components. For example, the model performance of BK2 reaches up to 0.94 for one calibration period, whereas the maximum model performance is only 0.81 for the other calibration. Soil moisture measurements are another example. For one soil moisture sensor, the model performance is as high as 0.89, whereas for the other sensor, the maximum performance index was only 0.60. Still, it remains difficult to evaluate whether the differences are due to parameterisation problems, structural model errors or spatial variability (neglecting observation data errors). SG data, on the contrary, permit the evaluation of the total model because they represent the water storage status instead of evaluating single model parameters or the internal structure.

The model evaluation shows that using SG data as calibration constraints improves the model performance and

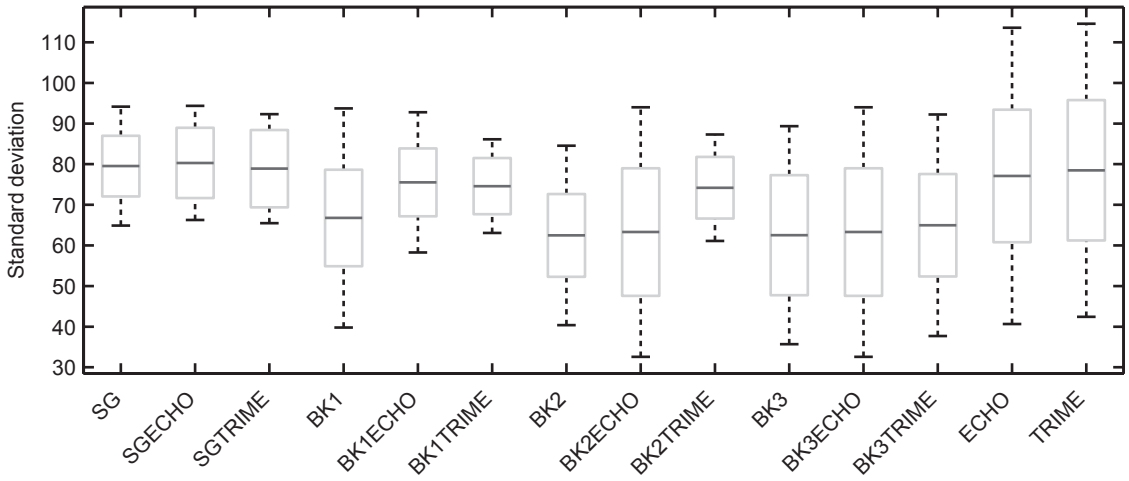

Figure 5.4: Performance of the different models for the calibration period. The median of the box plot is a measure of the signal amplitude (the standard deviation of the mean signal). The box and whiskers represent the scattering of the standard deviation of the behavioural model runs computed at each time step. (The standard deviation of the mean signal was added to the standard deviation of the behavioural model runs at each time step).

the predictive capability. In this context, SG measurements can improve the evaluation of the model results substantially. Nonetheless, different parameter sets can give the identical fit to the calibration data, raising the issue of getting the right answers for the wrong reasons.

5.4.2 Model validation

The model was calibrated for the period from 01 July 2005 to 30 July 2008 using again SG, groundwater and soil moisture data to constrain model parameters. For the calibration period, the performance of each model was assessed in terms of the variation of behavioural model runs. Here, this variation is expressed as the standard deviation of the behavioural model runs computed at each time step. In general, the variation of the behavioural model runs correlates positively with the signal amplitude. Here, the signal amplitude is expressed as the standard deviation of the mean time series. Figure 5.4 summarises the performance of the different models in a box plot for the calibration period. Using SG data to constrain the model parameters reveals that the variation of the behavioural model runs is relatively small in comparison to the other groundwater/soil moisture data. Neither variation nor amplitude change when additional information is included.

The model based on BK1 data shows that including soil moisture data into the calibration process reduces the variation of the model runs and increases the total amplitude. For the BK2 model, soil moisture data can increase (BK2ECHO) or decrease (BK2TRIME) the variation of behavioural model runs. Soil moisture data do not affect the variation or amplitude of the BK3 model significantly, but the scattering of the behavioural model runs is relatively large. The behavioural model runs show the maximum variation for models using soil moisture data as the only calibration constraint.

SG data can characterise the whole hydrological system because the inclusion of additional data does not change the model results in terms of variations of behavioural model runs and total signal amplitude. In contrast to this, soil moisture or groundwater data can be used to calibrate single model components directly, whereas including additional data can have a significant effect on the model results.

Focusing on the validation data in Figure 5.5, two different site types can be distinguished (Table 5.3). The seasonal amplitude of WSC of the sites SG and BK1 is larger than that of sites BK2 and BK3, something which is also reflected by the standard deviation of the measured time series which amounts to 86 mm for the SG site and to 102 mm for the BK1 site but is only as high as 67 mm and 57 mm for BK2 and BK3 respectively. The two site types differ not only in the seasonal amplitude but also in temporal dynamics. At the sites SG and BK1, we can identify a later and stronger increase of water storage during the snowmelt event from February to March 2009, whereas the recession of water storages is faster for the sites BK2 and BK3 (Figure 5.5). These differences are caused by the varying thickness of the vadose zone at the different sites. For BK2 and BK3, the groundwater depth varies between 4 and 8 m, whereas for SG and BK1, the groundwater depth amounts to up to 14.5 m (Figure 5.2).

Figure 5.5 compares the modelled and measured WSC.

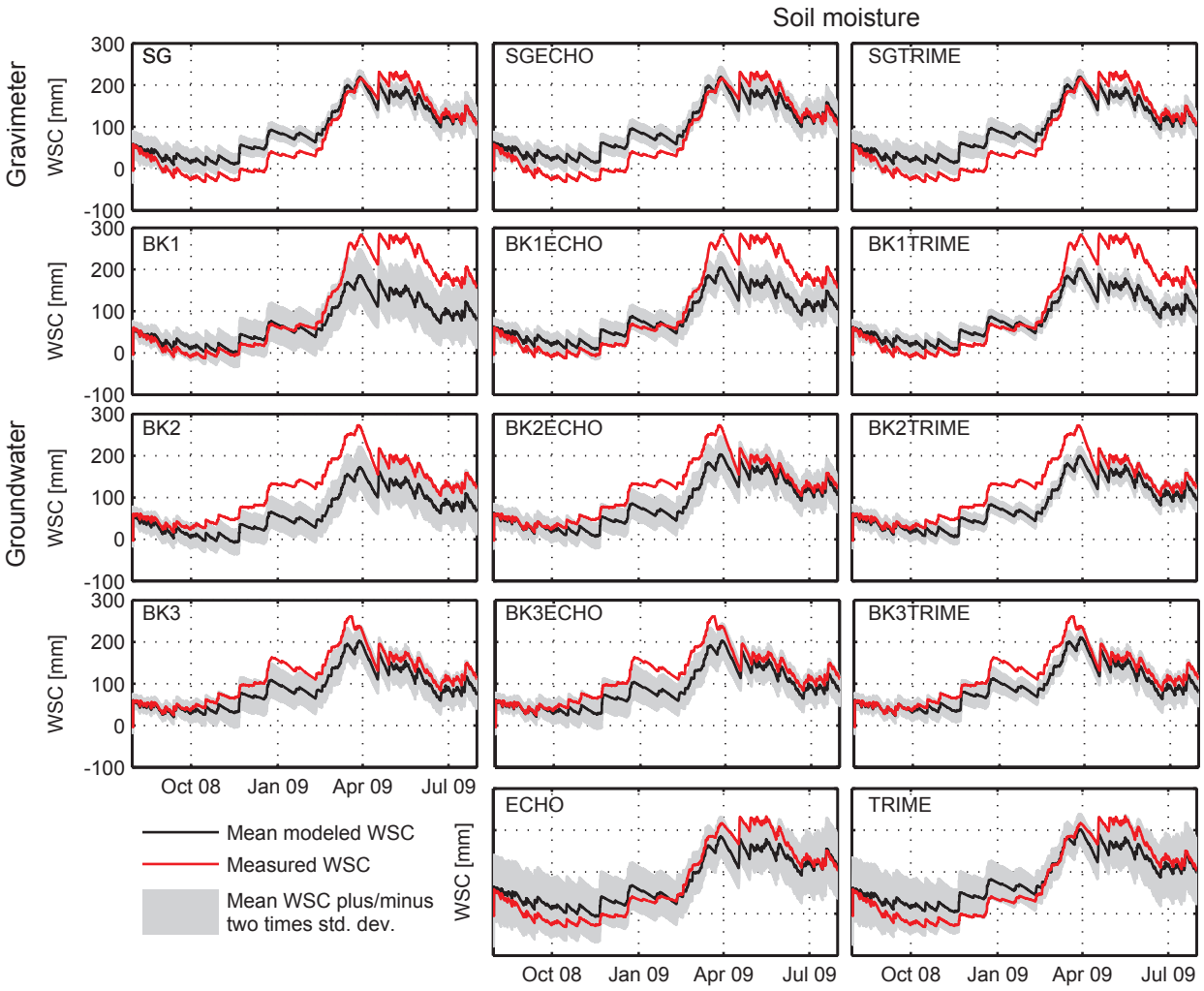

Figure 5.5: Measured versus modelled WSC for the validation period of July 2008 to July 2009.

The modelled mean WSC and the uncertainty bands (expressed as plus/minus two times the standard deviation) are displayed in combination with the validation dataset. The same picture applies to the validation and the calibration period. In general, the variation of behavioural models runs is larger for models calibrated against groundwater than for the SG models. All models underpredict the seasonal amplitude of the measured WSC. Most of the models reproduce the temporal variations of WSC well and agree on the event scale as well as on the seasonal scale.

The variation of the behavioural model sets, the differences in amplitude and temporal variation, are graphically summarised in Taylor diagrams [*Taylor*, 2001]. This is illustrated for the SG model and for two different site types (BK1 and BK3) (Figure 5.6). The Taylor diagram can show how well the modelled pattern matches the observations in terms of R, *RMSD* and standard deviation. The standard deviation of the modelled WSC for BK1 ranges between 43 and 65 mm and is clearly smaller than the observed one, but the correlation coefficient can be as high as 0.99. Contrary to model BK1, the differences for BK3 are smaller in terms of observed and modelled standard deviation, whereas the observed and modelled WSC has a smaller correlation coefficient. This pattern is consistent for the different site types. The models for deeper vadose zone sites agree better with the measured WSC in terms of temporal dynamics (higher R). For shallower sites, the models fit the total signal amplitude in a better way (smaller *RMSD*). The results of the SG model lie between these two different characteristics. For the sake of completeness, Table 5.5 also shows the Taylor statistics for the other models.

The validation shows that hydrological models constrained by temporal gravimeter data only, can reasonably predict the measured WSC in terms of amplitude and temporal dynamics. Hence, temporal gravimeter data can be used to estimate WSC, even though WSC are measured in change of gravity and not in millimetre of water.

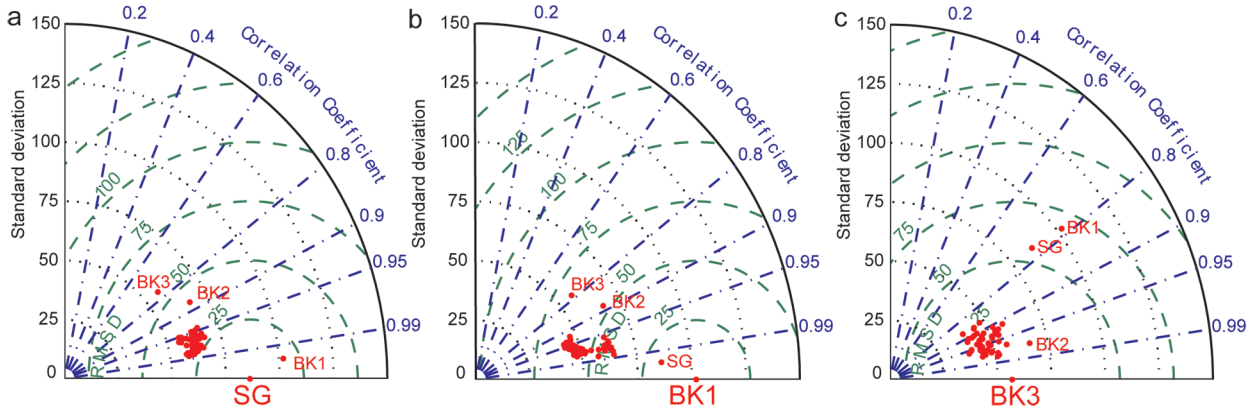

Figure 5.6: Taylor diagrams [*Taylor*, 2001] comparing measured and modelled WSC for the models SG (a), BK1 (b) and BK3 (c). Each figure also contains the measured WSC for the other sites.

5.4.3 Water storage changes

When we compare the modelled hydrological gravity response (SG model) to the SG residuals for the whole study period, we find that both signals show similarities in terms of amplitude, interannual, seasonal and short-term variations (Figure 5.7). The maximum amplitudes of the SG residuals and the gravity response amount to 15.24 and 14.35 µGal respectively. This is caused by a maximum WSC of 342 mm. These numbers are in line with the seasonal gravity variations of 10 to 15 µGal for the Durzon karst system in France estimated by *Jacob et al.* [2008]. They are caused by a seasonal WSC of 240-360 mm. The *RMSD* varies between 0.89 and 1.16 µGal. For the SG residuals and the gravity response, the regression slope of 0.96-1.25 and a corresponding coefficient of determination of 0.90-0.95 reflect a good agreement in phase and amplitude of both time series. The correlation coefficient of SG residuals and gravity response ranges between 0.95-0.97.

Table 5.5: Statistics of the model validation against WSC data.

Models	*Std*	*R*	*RMSD*
SG	55.45-67.41	0.94-0.99	25.31-37.29
SGECHO	53.80-66.10	0.95-0.99	25.16-38.53
SGTRIME	52.85-67.16	0.91-0.99	26.35-41.21
BK1	43.34-64.80	0.92-0.99	39.57-63.06
BK1ECH0	48.69-64.80	0.96-0.99	39.41-55.86
BK1TRIME	47.53-62.81	0.96-0.99	41.34-57.37
BK2	42.92-64.80	0.87-0.97	17.29-34.53
BK2ECHO	48.69-66.55	0.89-0.96	19.41-32.13
BK2TRIME	47.53-62.80	0.88-0.96	19.81-32.87
BK3	38.43-57.18	0.87-0.98	11.89-29.93
BK3ECHO	38.43-57.17	0.86-0.98	12.74-28.93
BK3TRIME	39.21-56.28	0.89-0.98	11.99-27.73
ECHO	52.23-61.43	0.91-0.98	27.13-41.81
TRIME	47.03-65.35	0.78-0.99	26.72-58.01

By focusing on the system state in comparison with the meteorological driving forces, a clear response of WSC can be observed in relation to the input/output fluxes (compare Figure 5.2). The different time series show weather-related characteristics and a seasonal course. Similar temporal characteristics can be identified in the hydrological gravity response, the SG residuals and the modelled WSC. High deviations in absolute value as well as in temporal dynamics for groundwater and soil moisture data make it difficult to identify the system response to the meteorological conditions. In Figure 5.2, a high variability between the different groundwater levels highlights the problem of single point measurements. It raises the issue of choosing "representative" sites for hydrological measurements, in particular for these complex geological settings. The differences of soil moisture measurements may not only reflect the spatial variability of soil moisture but can also be due to the soil moisture technique used, highlighting general problems in measuring soil moisture in the vadose zone [e.g. *Chow et al.*, 2009; *Evett et al.*, 2009; *Saito et al.*, 2009]. Furthermore, WSC in the deep vadose zone may differ significantly from the top soil moisture, but no measurements are available for this zone. SG measurements integrate over the different hydrological storage components and the sampling volume is several orders of magnitude larger than for the point measurements. SG observations allow for the identification of whole hydrological system responses to the driving forces.

5.5 Conclusions

This study investigates the use of temporal gravity measurements as an integrative measure of the hydro-

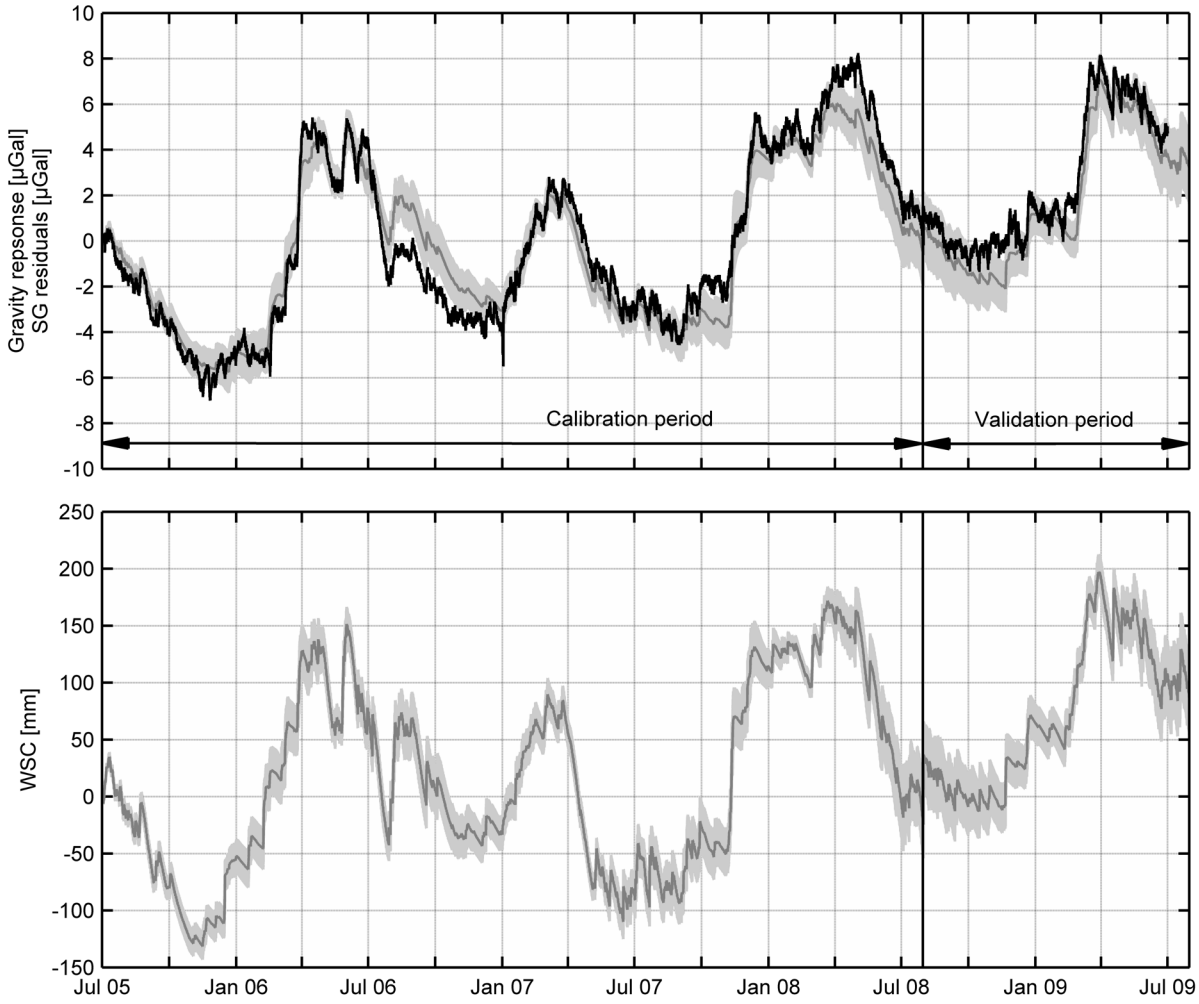

Figure 5.7: SG residuals (black line) and modelled gravity response (grey band) (top). Modelled water storage change (bottom). The model was calibrated against the SG residuals for the period of 01 July 2005 to 30 July 2008.

logical system state. The benefits of gravimeters when it comes to measuring WSC were assessed also in comparison to classical hydrological point measurements (groundwater and soil moisture). To estimate local WSC, a simple conceptual hydrological model was set up. This is the first study in which a model has been calibrated and evaluated using temporal gravimeter data as the only calibration/evaluation constraint. The model was also calibrated against groundwater and soil moisture data and combinations of observation data sets. Using SG measurements as calibration constraints improved the model results substantially in terms of the model fit to the calibration data, the predictive capability and the variation of the behavioural model runs. For the SG model, the variations of the behavioural model runs and the amplitude do not change when additional calibration data are included. They do however change for models calibrated against groundwater data when soil moisture is included.

SG observations are generalised and simplified measurements because they integrate over different storages and a larger area. In this context, they are in accordance with the nature of strongly generalised and simplified models (conceptual models). Furthermore, SG data can help hydrologists to find out which simplifications and generalisations are the right ones to describe the overall system state [*Kirchner*, 2009]. SG time series can characterise the hydrological system as a whole, whereas groundwater and soil moisture only permit the evaluation of model components. In this context, the 'right answers for wrong reasons' issue remains because it is difficult to assess the internal model structure or single parameter sets using only gravimeter data. Gravimeter records can help finding the right answer, in this case total WSC, instead of evaluating whether the reasons (model structures/parameters) are right or wrong but not knowing the right answer.

The results of different models were validated using independently estimated WSC based on a state-of-the-

art lysimeter and complementary observations. Some models predicted the amplitude of measured WSC in a better way and others showed a higher agreement with temporal dynamics. The results of SG models lie between these two different characteristics. In principle, the model validation with independent data proves that gravimeters can serve as a novel measurement method to observe WSC. Rather than solving the inverse problem, WSC are derived from a hydrological model of which the gravity response is calibrated against the SG (forward problem).

The high variability of groundwater and soil moisture data raises the issue of representativeness of point measurements. SG measurements integrate over different hydrological storages and larger volumes and thus permit the identification of the system response to the driving meteorological forces. Hence, temporal gravimeter observations may reveal some system characteristics like maximum total storage capacity, which could not be observed in soil moisture and/or groundwater data.

In this context, they are comparable to discharge measurements [*Hasan et al.*, 2008]. The disadvantages of gravimeters are that it is difficult to unambiguously identify the signal source and that the sampling volume and the radius of influence change over time [*Creutzfeldt et al.*, 2008; *Creutzfeldt et al.*, 2010a]. These downsides also apply to a certain extent to discharge measurements where the area contributing to runoff may change over time or the source is difficult to define (e.g. event/pre-event water). This study shows additional similarities between gravimeter and discharge measurements because due to the integral character of gravimeters, it is difficult to constrain internal model structures or single parameters solely based on one method as already highlighted by *Mroczkowski et al.* [1997] for discharge measurements. Nonetheless, gravimeter measurements can be complementary to discharge observations. They can help to characterise the catchment status above the outlet point and thus to define storage-output relationships. This provides a valuable contribution towards a better general understanding of catchment dynamics and towards constraining hydrological models.

Acknowledgements. The authors are sincerely grateful to the section National Reference Systems for Gravity and to the section Geodetic Observatory Wettzell of the Federal Agency for Cartography and Geodesy (BKG) for providing us with the data. The study was financial supported by the Deutsche Forschungsgemeinschaft (German Research Foundation) within the Priority Program SPP 1257 ‘Mass transport and mass distribution in the system Earth’, project TASMAGOG is greatly appreciated.

Chapter 6:

Discussion, conclusions and outlook

Discussion, conclusions and outlook

6.1 Summary of achievements

The objective of this study was to investigate the relationship between hydrological mass variations and temporal gravity measurements in order to reduce the interfering hydrological signal from temporal gravity measurements and to explore the value of temporal gravity measurements for hydrology. To study this objective, a cross-disciplinary approach was developed which integrates measurements and modeling. The main findings with regard to the research questions (see Chapter 1) are as follows:

1. How is the gravitational signal influenced by water mass as a spatiotemporal variable continuum in the landscape?

To investigate the relationship between hydrological mass variations and temporal gravity measurements, a forward model to calculate the gravity response of the water storage variable in space and time was developed and a spatially nested discretization domain was suggested. The complex hydrological system was represented in a simplified model and the gravity response due to 4D hydrological variations was simulated by manipulating this model. Although the relationship between hydrological mass variations and temporal gravity measurements is based on well-known physical laws, this study showed that simulating the influence of WSC on gravity measurements is necessary to understand the relationship of WSC and temporal gravity measurements. This applies to both the static distribution of hydrological mass in space as well as the dynamic mass redistribution over time.

2. How can we estimate the local hydrological gravity effect and reduce the interfering hydrological signal from the gravity signal?

To understand the influence of local WSC on temporal gravity measurements and in order to reduce the interfering hydrological signal from gravity measurements, this study showed that it is necessary to estimate local WSC independently in all relevant water storage compartments. A comprehensive monitoring system was designed and installed to measure hydrological variations in all potentially relevant water storages, which were identified during the simulation. WSC were directly measured and, where not directly measurable, WSC were derived using analytically-based approaches. The results of the data-based approach showed that WSC in the snow pack, top soil, unsaturated saprolite and fractured aquifer are all important terms of the local water budget and, hence, have to be estimated for the reduction of the interfering local hydrological signal. High uncertainties of the quantification of local WSC demonstrated the limitations of measuring local WSC using point measurements.

Therefore, an innovative approach combining lysimeter measurements with complementary data (soil physics, groundwater) and a physically-based hydrological model was developed. The benefits of the lysimeter-based approach were assessed in comparison to other approaches used in the past to correct for the local hydrological influence. The lysimeter-based approach significantly improved the independent estimation of WSC and thus provided a better way of reducing the local hydrological effect from gravimeter measurements. The lysimeter-based approach showed that the gravity residuals are caused to a larger extent by local WSC than previously stated. At sites where temporal gravity observations are used for geophysical studies beyond local hydrology, the installation of a lysimeter is recommended.

3. Can gravimeters serve as a novel measurement instrument for hydrology and, hence, allow for a better characterization of the hydrological system?

At the Geodetic Observatory Wettzell, the gravimeter residuals can be considered to be mainly caused by local WSC based on the previous results so that the local hydrological information content of gravimeter residuals is larger than previously estimated. However, due to the integrative character of gravity measurements, it is difficult to unambiguously identify the source of the gravimeter signal and, hence, to estimate single hydrological parameters from gravimeter measurements. In this study, the gravimeter signal was used to characterize the hydrological system as a whole, integrating over all different WSC. In this context, they are similar in nature to runoff measurements and allow for the characterization of the hydrological system. Gravimeters can serve as a novel measurement instrument for hydrology to observe the water storage term in the water balance equation at the field scale.

6.2 Discussion and directions of further research

During the investigation of the relationship between hydrological mass variations and temporal gravity measurements with the aim of reducing the interfering hydrological signal from temporal gravity measurements and of exploring the value of temporal gravity measurements for hydrology, different aspects arose, which need further discussion and can provide directions for further research.

6.2.1 Simulating the gravity signal

It is necessary to simulate 'how the gravimeter sees changes in a complex hydrological system' to understand the influence of hydrological mass variations on temporal gravity measurements. This study suggests a nested discretization of the model domain because it strikes a balance between high discretization in the near field and calculation time; both are prerequisites for gravity modeling. From a geodetic perspective, the use of homogeneous polyhedra seems to be more suitable for gravity modeling, not least because they are more flexible than rectangular homogeneous prisms [*Petrović and Skiba*, 2001; *Tsoulis et al.*, 2003]. Hydrologists, on the contrary, work predominantly with raster-based data or software (e.g., DEM, common GIS software, layer-based vertical discretization of the subsurface), so rectangular homogeneous prisms are more suitable for hydrological gravity modeling. A nested model discretization is especially useful for investigating the gravity response of SGs caused by WSC.

Simulating the relationship between hydrological mass variations and temporal gravity measurements should become a standard because it is a prerequisite in order to understand and interpret the gravity residuals. The development of a standard software to calculate the gravity effect from hydrological mass variations is strongly recommended. This software should integrate spatial as well as temporal information. Based on information about the topography and the near field, a conversion factor should be derived for each elementary body in the simulation domain. Instead of neglecting the volume dimension of the elementary body (as done in this study), an approach should be used that integrates over each volume element. This might increase the calculation time but is not critical because for each elementary body, the 'WSC to gravity response conversion factor' has to be calculated only once. Different complexity levels about WSC data should be integrated by the software, ranging from single time series of snow, soil moisture or groundwater up to the calculation of the gravity response from spatially distributed time-variable 4D WSC data. Finally, this software should also allow for the calculation of the large-scale hydrological gravity effect (deformation and attraction term) from different global hydrological models.

A user-friendly software commonly used by the community would be a first step towards a standardized approach to treat the hydrological gravity effect in gravimeter observation at all stations in a similar way. A standardized approach is a prerequisite if the different gravimeters are to be compared. In addition, a common approach could also clarify some definition uncertainties that still exist among scientists in this field, for example, to which spatial domain the notation of local, regional or global gravity effects applies.

6.2.2 Gravity measurements for hydrology

This study showed that gravimeters can serve as a novel measurement instrument for hydrology. Still, practical aspects limit the application of gravimeters for hydrology. SGs are the state-of-the-art relative gravimeters with a temporal resolution of ~1 sec and an accuracy of ~0.1 µGal. However, they are cost-intensive in acquisition and operation. In general, they need a good infrastructure and are operated at a fixed location, although first attempts are made to take SGs into the field [*Wilson et al.*, 2007]. The new SG generation – the *iGrav*™ SG – will improve the applicability of SGs in terms of portability, low drift and usability [*GWR*, 2009]. Absolute gravimeters (FG5 and A10 [*LaCoste*, 2010a; b]) are stable concerning the temporal drift and have the advantage of being portable. The accuracy and temporal resolution is not as high as for SGs [*Schmerge and Francis*, 2006], but they have already been used to study the relationship of gravity and hydrology [*Jacob et al.*, 2008; *Jacob et al.*, 2009]. Spring-based gravimeters are relative gravimeters, portable and relatively inexpensive. In the context of WSC, they are used on a campaign-basis to map spatial variation of gravity changes in comparison to a reference point. In general, gravity changes above 10-15 µGal can be detected by these gravimeters, and with very high effort, the detection limit can be lowered to ~2 µGal [*Brady et al.*, 2008; *Chapman et al.*, 2008; *Gettings et al.*, 2008; *Naujoks et al.*, 2008; *Pool*, 2008]. For the sake of completeness, we would like to mention that advances in atom interferometry promise to improve the reliability of absolute gravity measurements and will be available for the geophysical community in the future [*Angelis et al.*, 2009; *Peters et al.*, 2001]. Hence, technical advances in gravimeter technology are necessary in terms of portability, precision and cost-efficiency to tap the full potential of gravimeter measurements for hydrological applications and to make them routinely available to the hydrological community.

6.2.3 The near field problem

WSC in the near field (i.e., in the order of several meters around the gravimeter) have a large influence on gravimeter measurements, but it is difficult to determine their effect because the gravimeter measurement place has in turn an impact on the WSC. Consequently, WSC in the near field differ from WSC at larger distances where they are more easily measurable.

Different strategies can be implemented to tackle the near-field problem: 1) the construction impact on the hydrological system should be minimized so that WSC in the near-field are comparable to WSC at larger distances; 2) WSC in the near-field should be measured so that differences in the hydrological regime can be identified; 3) the gravity effect of WSC should be unidirectional to make the interpretation of the gravity signal easier; and 4) the distance between the gravimeter and the closest WSC should be maximized so that no WSC occur in the near-field.

At first glance, some strategies may contradict each other, which would call for a balanced approach. However, all of these strategies have to be implemented before and during the construction of a gravimeter measurement place implying that hydrologists should be consulted and involved as early as during the site selection, planning and construction process. The simulation of the influence of WSC on temporal gravimeter observations should be carried out during each of these phases so that the near-field effect of WSC can be minimized and the estimation of WSC in the near-field can be optimised.

The near-field problem is more of a practical than a scientific problem. Nonetheless, it is one of the key problems regarding WSC and temporal gravity measurements and will determine success or failure in terms of the reduction of the interfering hydrological signal and in terms of the hydrological interpretation of the gravity measurements. The near field problem needs much more attention in the future.

6.2.4 Transferability to other gravity measurement sites

In this study, the hydrological effects on SG measurements of the Geodetic Observatory Wettzell were estimated to reduce the interfering hydrological signal from gravity measurements and to explore the potential of gravimeter measurements for hydrology. Hence, the question is: What can we learn from this case study at the Geodetic Observatory Wettzell for other temporal gravity measurement sites? Are the results transferable?

This study showed that the gravity residuals are caused to a larger extent by local WSC than previously stated, highlighting the importance of appropriately estimating local WSC at temporal gravity measurement sites. The local WSC are a key component of temporal gravity measurements and a standard approach is required to determine the local hydrological gravity effect in temporal gravimeter measurements.

The presented lysimeter-based approach can serve as a standard procedure for the reduction of the hydrological effect at sites where continuous or frequent gravity measurements are conducted. Complementary measurements should be appropriately adjusted to measure WSC in all relevant storages. For SG sites, the installation of a lysimeter is recommended.

At sites with a lower temporal sampling interval like, for example, sites where AG measurements are conducted only once or twice a year, this approach may be difficult to implement because of high costs due to the installation and maintenance of lysimeters. Nonetheless, for these sites it is also crucial to consider local WSC and thus, WSC should be measured directly. Neutron probes may be an appropriate alternative to lysimeter measurements. They are an accurate tool to measure soil moisture profiles in campaign-based intervals, and these measurements can then be combined with the continuous measurements of soil moisture probes, groundwater level probes and precipitation gauges. The neutron probe-based approach can be used for the reduction of local WSC in absolute gravity measurement. Furthermore, neutron probes (contrary to other moisture probes) can also measure WSC in deeper zones below the lysimeter so that they can serve as a calibration and validation dataset in the lysimeter-based approach since no continuous measurements are possible by neutron probes.

This study further showed that due to the integrative character of gravity measurements, it is difficult to unambiguously identify the source of the gravimeter signal. This makes a unique interpretation of individual storage components or parameters challenging or even impossible if no complementary information is available. Furthermore, extreme caution should be applied when interpreting the gravity residuals, which are reduced from local hydrological influence in terms of other effects, e.g., large-scale hydrological variation. Due to the fact that the major part of the gravity residuals is caused by local WSC, the gravity residuals can be used to study the local hydrological system. Thanks to their capacity to integrate over different storage components and a larger area, gravimeters provide generalized information on total WSC. This study showed that interpreting the gravity residuals from this perspective can provide valuable information about the hydrological system. This could prove beneficial for other sites as well.

For the hydrological interpretation of the gravity residuals and for the use of temporal gravity observation beyond local hydrology, a monitoring system is mandatory to observe the water mass variation in all relevant

water storages. The design of the measurement system that was developed here can be applied to other gravity measurement sites and, if necessary, should be adjusted to the specific hydrological conditions at other sites, including WSC in surface water for instance.

6.2.5 Spatiotemporal variability of water storages

To estimate the hydrological interfering signal and to assess the benefit of temporal gravimeter measurements for WSC modeling, water storages were assumed to be variable over depth, and the lateral variability of water storages was only considered implicitly in some uncertainty analyses. We were motivated to use this 1D approach by the fact that the hydrological system is an open and complex system and, in order to study this system, it is necessary to simplify it. For a first approximation, the 1D assumption seems to be justified because at the scale relevant for the gravimeter (50 - 80 % of the gravity signal is generated within a radius of 50 m), the variability of WSC over depth is much more important than the lateral variability of WSC. This is given because water storages are controlled by driving processes like infiltration, evaporation, plant water uptake, deep drainage, groundwater recharge or groundwater discharge, as well as by internal properties of the system such as soil hydraulic properties or macropores. At the scale relevant for the gravimeter these first order controls of water storages differ significantly over depth, whereas a lateral continuity is given for most of the processes and landscape features like precipitation, evapotranspiration, topography, geology, soil types, etc.

Nonetheless, processes and system properties vary in space with very different spatial continuities (correlation length) and control the variability of water storages. The spatial variability of boundary fluxes, internal system parameters and water storages is closely related to spatial scales because the importance of different controlling mechanisms changes with scale [*Blöschl and Sivapalan*, 1995; *Western et al.*, 2002]. To consider the lateral variability of water storages in gravity studies in the future, it is necessary to reveal the explainable variability and to explore the controlling mechanisms at the different scales. Geostatistical techniques can help to characterize the spatial patterns of water storages [*Bardossy and Lehmann*, 1998; *Entin et al.*, 2000; *Mohanty et al.*, 2000; *Western et al.*, 2002].

At the point scale, the water storages can vary at short distances and generally are a system immanent feature, which can be assumed to be randomly distributed (nugget in a variogram) [*Western et al.*, 2004]. However, also technologies and methods used to estimate water storages can invoke considerable random variability [*Evett et al.*, 2009; *Mazahrih et al.*, 2008] and can mask the explainable variability at larger scales. At the field scale, vegetation and soil hydraulic properties largely control water storage because other landscape features such as land use, geology, soil types or topography can be considered to be of rather homogenous variability [*Teuling and Troch*, 2005; *Vereecken et al.*, 2007]. At saturation state, water storages can be considered to be rather homogenous and have a high correlation length because the spatial variability of porosity is relatively small [*Corwin et al.*, 2006; *Harter and Zhang*, 1999]. For the unsaturated zone, the relation of water content and spatial variability is still under discussion. *Vereecken et al.* [2007] suggested that soil moisture variability increases during the process of drying until the variability reaches a maximum and by further drying decreases again. Other scientists [*Famiglietti et al.*, 1999; *Hupet and Vanclooster*, 2002], on the contrary, reported an increase of soil moisture with decreasing mean moisture content. At the next larger scale still relevant for gravity measurements (the hillslope scale), the distribution of water storages is linked to the topography. This correlation can be explained by the lateral redistribution of water along the topography but may also result indirectly from soil characteristics, meteorological forcings, land use and vegetation pattern, which are frequently correlated to the topography [*Brocca et al.*, 2007; *Kim*, 2009; *Merz and Plate*, 1997; *Weihermuller et al.*, 2007; *Western et al.*, 2002]. Although water storages are controlled by different factors at different scales, different studies show that the correlation between water storages and the controlling factors is not always given [*De Lannoy et al.*, 2007; *Famiglietti et al.*, 2008].

In the context of temporal gravity measurement and spatial variability, the concept of temporal stability plays an important role because for gravity measurements, we are more interested in changes of water storages than in the absolute value. The temporal stability concept is based on the assumption that spatial patterns are temporally persistent and that the relationship between spatial location and statistical measures of soil moisture are temporally invariant [*Grayson and Western*, 1998; *Kachanoski and de Jong*, 1988; *Vachaud et al.*, 1985]. Following this concept does not only allow for the determination of a sampling strategy to make a reliable estimation of area1 mean soil moisture, but due to the temporal stability, it is possible to reliably determine the temporal variations of soil moisture by a few measurements [*Brocca et al.*, 2009; *Grayson and Western*, 1998]. Due to the temporal stability of the soil moisture pattern, *Brocca et al.* [2010], for example, showed that the temporal variations of soil moisture can be reliably (accuracy of better than 1 %) estimated from 4 to 10 measurements at the field scale. For studies focusing on temporal gravity observations and WSC, this implies that temporal variations of soil moisture (only relevant for gravimeters) can be estimated

reliably using a few measurements only in case an appropriate soil moisture measurement technology is used.

Nonetheless, the developed concepts of the spatiotemporal variability of water storages should be investigated in the context of gravity measurements. For example, as a next step at the Geodetic Observatory Wettzell, the 2D spatial variability of water storages should be investigated along the hillslope because preliminary results showed that the water storage variability is mainly controlled by topography. The spatially-distributed and dynamic description of WSC along hillslopes can be addressed by an appropriate integration of the data and their spatial variability into a hydrological model [*Bronstert*, 1999; *Merz and Bárdossy*, 1998]. Additionally, the different hydrological theories about spatiotemporal variability of water storages should be evaluated in the context of gravity observations by simulating the influence of spatially variable WSC on gravity measurements as well as from the experimental perspective. The theories about the spatiotemporal variability of water storages were developed and tested based mainly on surface soil moisture data [e.g., *Brocca et al.*, 2010; *Famiglietti et al.*, 2008; *Western et al.*, 2002], but only very few studies used data from deeper water storage changes [*Kachanoski and de Jong*, 1988; *Pachepsky et al.*, 2005]. Hence, it might be problematic to apply them directly to gravity measurements because gravity measurements are also influenced by deeper WSC. At the same time, this reveals the potential of gravity measurements to test the developed theories of spatiotemporal variability in combination with different spatial scales not only for surface soil moisture but also for the whole hydrological system at the field scale.

6.2.6 Hydrological modeling and temporal gravity data

To investigate the relationship of hydrological masses and temporal gravity variations, different approaches were used in this study: one approach based on hydrological measurements only (Chapter 3), another approach, which combines hydrological measurements with a physically-based model (Chapter 4) and a third approach based on a conceptual hydrological model (Chapter 5). Why different approaches were used needs further evaluation.

Regarding the approach based on hydrological measurements only, the question may arise: Why did we not use a hydrological model to estimate the local hydrological gravity effect? A hydrological model would have explained the hydrological system more comprehensive or it could have been used to interpolate and extrapolate the hydrological observations. A hydrological model may have improved the correlation between local WSC and SG residuals and would have allowed a more comprehensive uncertainty analysis. Hydrological model parameters have to be estimated, which is generally done by calibration. But typically, the amount of available calibration data is not sufficient to constrain all free parameters in a hydrological model, leaving the model with considerable parameter uncertainty and often calling into question the predictive capacity of these calibrated models [*Beven*, 2006; *Kirchner*, 2006; *Klemes*, 1986b; *Seibert*, 2003]. Hence, using a hydrological model would not only have invoked considerable additional sources of uncertainty that result from the modeling process itself and are caused, for example, by uncertainties of the model structure and model parameters. But the use of a hydrological model would also have increased the risk of fitting the estimated local WSC to the SG residuals, where, in fact, the aim was to estimate the local hydrological gravity effect independently from gravity data. Local WSC estimated with the data-based approach were associated with high uncertainties arising from classical hydrological point measurements. Also, it is difficult to describe the whole hydrological system in a comprehensive way with measurements only. This task can only be accomplished by a hydrological model, but the model uncertainty has to be reduced, something that can be accomplished by increasing the amount of available calibration data and/or decreasing the degrees of freedom of the hydrological model.

Therefore, a more comprehensive approach was necessary to reduce the uncertainty of WSC estimation on the field scale. Consequently, an approach was developed which combines lysimeter measurements with complementary measurements and a physically-based hydrological model. Here, the model can be considered as a tool to interpolate WSC between lysimeter and groundwater measurements. Combining measurements with a hydrological model in this way has the advantage that the degrees of freedom of the hydrological model can be reduced significantly. In hydrological modeling, the actual evapotranspiration is usually derived from the potential evapotranspiration with assumptions made about the vegetation, e.g., the species, root depth distribution, the state of health and growth. The vegetation is integrated into the model based on parameters such as leaf area index, maximum root depth or root depth distribution. To derive the actual evapotranspiration from the potential evapotranspiration, these different vegetation parameters and their variation over time have to be estimated. In our study, WSC including evapotranspiration up to a depth of 1.5 m were measured instead of modeled. Thus, the estimation of the hydraulic parameters for the soil could also be avoided. Modeling the surface soil moisture, would have implied the estimation of at least five different parameters for at least three different horizons. Both examples illustrate that the lysimeter-based approach reduces the degrees of freedom of the hydrological model significantly, but the results still contain unresolved uncertainties arising from the lysimeter measurement,

the model structure and the parameters. The measured soil parameters were directly integrated into the model, neglecting the issue of effective parameters [*Blöschl and Sivapalan*, 1995]. Lysimeter measurements were not evaluated because of the missing reference measurement. TDR probes were not considered an appropriate technology to assess lysimeter measurements due to differences in the sampling volume. TDR measurements are also an indirect technology to measure soil moisture, and they are influenced by different sources of uncertainties arising, e.g., from the analysis of the transmission line or the derivation of the soil moisture content from the electric permittivity [*Robinson et al.*, 2003]. The assessment of lysimeter measurements in terms of the snow effect, 'natural conditions' and lower boundary condition is still an open question. Uncertainties arising from the model structure need to be addressed in the future. This could be done according to the framework suggested by *Butts et al.* [2004].

Finally, a hydrological model was calibrated automatically for the first time against gravity residuals. To this end, a conceptual model with only a few free model parameters was used. When calibrating and evaluating this model, single model parameters cannot be constrained using gravity residuals only because different parameter sets gave almost identical fits to the observed gravity data. The GLUE approach widely applied in hydrology was used for this task, although some criticism for the GLUE approach exists because of the subjective character and inconsistencies from a statistical point of view [*Mantovan and Todini*, 2006]. This study showed that SG observations generalize and simplify the hydrological system and, thus, they are in accordance with the nature of strongly generalized and simplified models (conceptual models). However, using conceptual models calibrated against the gravity signal for the reduction of the hydrological noise is not a good option because this may also remove parts or all of the SG signal of interest.

To sum up the discussion of hydrological modeling in the context of gravity measurements, we can say that whenever the gravity signal should be reduced from the hydrological interfering signal, a hydrological model should be applied very carefully and parameter calibration against the gravity residuals should be avoided. From the hydrological view point, physically-based models in combination with gravity data should be given a try in the future, especially for the investigation of the influence of lateral variations of WSC and for the estimation of effective parameters. In this case, more sophisticated calibration techniques should be considered also in combination with other observations to constrain internal model parameters by a multi-objective calibration scheme [e.g., Multiobjective Shuffled Complex Evolution Metropolis, *Vrugt et al.*, 2003].

6.3 Concluding outlook

I think that, from the hydrological perspective, the time for hydrological gravimeters has come – gravimeters that are specifically dedicated for hydrological monitoring and thus designed and installed to meet hydrological requirements. For hydrological gravimeters, the environmental settings should be kept as simple as possible. Disturbances of the near field should be minimized and WSC should act only unidirectionally on the gravimeter, i.e. WSC should either occur above or below the sensor of the gravimeter. Hydrological gravimeters would be especially useful to study open research questions related to the issue of storages in the context of upslope versus near-stream zone influence on discharge [*Seibert et al.*, 2003a; *Seibert et al.*, 2003b], storage dynamics and streamflow including storage-runoff-relationships [*Kirchner*, 2009; *Spence*, 2007; *Spence et al.*, 2009; *Wittenberg*, 1999], or storage states as a potential indicator of flood and drought hazards [*Reager and Famiglietti*, 2009; *Zehe et al.*, 2009].

Although the very high costs of temporal gravity measurements will limit the application of gravimeters to only a few scientific studies, I think that they are "worth their salt" and I subscribe to the statement of *Klemes* [1986a]: "it also seems obvious that search for new measurement methods that would yield areal distributions, or at least reliable areal totals or averages, of hydrologic variables such as precipitation, evapotranspiration, and soil moisture would be a much better investment for hydrology than the continuous pursuit of a perfect massage that would squeeze the nonexistent information out of the few poor anaemic point measurements […] even Lucretius Carus knew two thousand years ago that 'nil posse creari de nilo.'"

6.4 Conclusion

This cross-disciplinary study showed that the effect of local water storages on temporal gravity measurements can be independently estimated and that hydrology can benefit from temporal gravity measurements.

References

Abe, M., S. Takemoto, Y. Fukuda, T. Higashi, Y. Imanishi, S. Iwano, S. Ogasawara, Y. Kobayashi, S. Dwipa, and D. S. Kusuma (2006), Hydrological effects on the superconducting gravimeter observation in Bandung, Journal of Geodynamics, 41, 288-295.

Allen, R. G., I. A. Walter, R. L. Elliott, T. A. Howell, D. Itenfisu, M. E. Jensen, and R. L. Snyder (2005), The ASCE standardized reference evapotranspiration equation, American Society of Civil Engineers, Virginia.

Allerup, P. (1997), A comprehensive model for correcting point precipitation, Nordic hydrology, 28(1), 1-20.

Amalvict, M., J. Hinderer, J. Makinen, S. Rosat, and Y. Rogister (2004), Long-term and seasonal gravity changes at the Strasbourg station and their relation to crustal deformation and hydrology, Journal of Geodynamics, 38(3-5), 343-353.

Andersen, O. B., S. I. Seneviratne, J. Hinderer, and P. Viterbo (2005), GRACE-derived terrestrial water storage depletion associated with the 2003 European heat wave, Geophysical Research Letters, 32(L18405).

Angelis, M. d., A. Bertoldi, L. Cacciapuoti, A. Giorgini, G. Lamporesi, M. Prevedelli, G. Saccorotti, F. Sorrentino, and G. M. Tino (2009), Precision gravimetry with atomic sensors, Measurement Science and Technology(2), 022001.

Apel, R., A. Klemm, and F. Rüdiger (1996), Grundlagen zum Wasserwirtschaftlichen Rahmenplan Naab-Regen. Hydrogeologie, Bay. Geologisches Landesamt, München.

Banka, D., and D. Crossley (1999), Noise levels of superconducting gravimeters at seismic frequencies, Geophysical Journal International, 139(1), 87-97.

Bardossy, A., and W. Lehmann (1998), Spatial distribution of soil moisture in a small catchment. Part 1: geostatistical analysis, Journal of Hydrology, 206(1-2), 1-15.

Battaglia, M., J. Gottsmann, D. Carbone, and J. Fernandez (2008), 4D volcano gravimetry, Geophysics, 73(6), WA3-WA18.

Baumgartner, A., and H.-J. Liebscher (1996), Lehrbuch der Hydrologie: Allgemeine Hydrologie - Quantitative Hydrologie, Borntraeger, Berlin.

Bergström, S. (1992), The HBV model - its structure and applications, Swedish Meteorological and Hydrological Institute (SMHI), Norrköping.

Beven, K., and A. Binley (1992), The future of distributed models: Model calibration and uncertainty prediction, Hydrological Processes, 6(3), 279-298.

Beven, K. (2006), A manifesto for the equifinality thesis, Journal of Hydrology, 320(1-2), 18-36.

Beven, K. J. (2005), Rainfall-runoff modeling: Introduction, in Encyclopedia of hydrological sciences, edited by M. G. Anderson, John Wiley & Sons Ltd, Chichester.

Bittersohl, J., K. Moritz, C. Schöttl, and H. Wahler (2004), 15 Jahre Integriertes Messnetz: Stoffeintrag – Grundwasser, Methoden und Ergebnisse, Bayerisches Landesamt für Wasserwirtschaft München.

BKG (2004), ATKIS® DGM-D, edited, © Vermessungsverwaltungen der Länder und BKG (Bundesamt für Kartographie und Geodäsie).

BKG (2005), ATKIS® Basis-DLM, edited, © Vermessungsverwaltungen der Länder und BKG (Bundesamt für Kartographie und Geodäsie).

Blainey, J. B., T. P. A. Ferré, and J. T. Cordova (2007), Assessing the likely value of gravity and drawdown measurements to constrain estimates of hydraulic conductivity and specific yield during unconfined aquifer testing, Water Resources Research, 43, W12408.

Blöschl, G., and M. Sivapalan (1995), Scale issues in hydrological modelling: A review, Hydrological Processes, 9(3-4), 251-290.

Blöschl, G. (2005), On the fundamentals of hydrological sciences, in Encyclopedia of hydrological sciences, edited by M. G. Anderson, John Wiley & Sons Ltd, Chichester.

Bonatz, M. (1967), Der Gravitationseinfluss der Bodenfeuchte, Zeitschrift für Vermessungswesen, 92, 135-139.

Bonatz, M., and D. Sperling (1995), Gravitation effects at the Vianden storage power station, in Cahiers du Centre Européen de Géodynamique et de Séismologie, edited by C. Poitevin, pp. 169-180, Walferdange.

Bower, D. R., and N. Courtier (1998), Precipitation effects on gravity measurements at the Canadian Absolute Gravity Site, Physics of the Earth and Planetary Interiors, 106(3-4), 353-369.

Boy, J. P., and J. Hinderer (2006), Study of the seasonal gravity signal in superconducting gravimeter data, Journal of Geodynamics, 41, 227-233.

Brady, J. L., J. L. Hare, J. Ferguson, J. E. Seibert, F. J. Klopping, T. Chen, and T. Niebauer (2008), Results of the world's first 4D microgravity surveillance of a waterflood – Prudhoe Bay, Alaska, SPE Reservoir Evaluation & Engineering, 11(5), 824-831.

Breili, K., and B. R. Pettersen (2009), Effects of surface snow cover on gravimetric observations, Journal of Geodynamics, 48(1), 16-22.

Brocca, L., R. Morbidelli, F. Melone, and T. Moramarco (2007), Soil moisture spatial variability in experimental areas of central Italy, J. of Hydrology, 333(2-4), 356-373.

Brocca, L., F. Melone, T. Moramarco, and V. P. Singh (2009), Assimilation of observed soil moisture data in storm rainfall-runoff modeling, Journal of Hydrologic Engineering, 14(2), 153-165.

Brocca, L., F. Melone, T. Moramarco, and R. Morbidelli (2010), Spatial-temporal variability of soil moisture and its estimation across scales, Water Resources Research, 46(2), W02516.

Bronstert, A. (1999), Capabilities and limitations of detailed hillslope hydrological modelling, Hydrological Processes, 13(1), 21-48.

Buckingham, E. (1907), Studies in the movement of soil moisture, Bulletin 38, U.S. Department of Agriculture Bureau of Soils, Washington D.C.

Büttner, G., R. Pamer, and B. Wagner (2003), Hydrogeologische Raumgliederung von Bayern, Bayerisches Geologisches Landesamt, München.

Butts, M. B., J. T. Payne, M. Kristensen, and H. Madsen (2004), An evaluation of the impact of model structure on hydrological modelling uncertainty for streamflow simulation, Journal of Hydrology, 298(1-4), 242-266.

Campbell Scientific Inc. (2008), TDR100: Manual, Campbell Sci. Inc., Logan, USA.

Campbell Scientific Inc. (2009), CR1000 Measurement and Control System: Manual, Campbell Sci. Inc., Logan, USA.

Chapman, D. S., E. Sahm, and P. Gettings (2008), Monitoring aquifer recharge using repeated high-precision gravity measurements: A pilot study in South Weber, Utah, Geophysics, 73(6), WA83

Cho, M., Y. Choi, K. Ha, W. Kee, P. Lachassagne, and R. Wyns (2003), Relationship between the permeability of hard rock aquifers and their weathering, from geological and hydrogeological observations in South Korea, paper presented at International Association of Hydrogeologists IAH Conference on "Groundwater in fractured rocks", Prague.

Chow, L., Z. Xing, H. Rees, F. Meng, J. Monteith, and L. Stevens (2009), Field Performance of Nine Soil Water Content Sensors on a Sandy Loam Soil in New Brunswick, Maritime Region, Canada, Sensors, 9(11), 9398-9413.

Cooper, H. H., and C. E. Jacob (1946), A generalized graphical method for evaluating formation constants and summarizing well field history, American Geophysical Union Transactions, Volume 27(4), 526-534.

Corwin, D. L., J. Hopmans, and G. H. de Rooij (2006), From field- to landscape-scale vadose zone processes: scale isssues, modeling, and monitoring, Vadose Zone Journal, 5(1), 129-139.

Creutzfeldt, B., A. Güntner, T. Klügel, and H. Wziontek (2008), Simulating the influence of water storage changes on the superconducting gravimeter of the Geodetic Observatory Wettzell, Germany, Geophysics, 73(6), WA95.

Creutzfeldt, B., A. Güntner, H. Thoss, B. Merz, and H. Wziontek (2010a), Measuring the effect of local water storage changes on in-situ gravity observations: Case study of the Geodetic Observatory Wettzell, Germany, Water Resources Research, 46, W08531.

Creutzfeldt, B., A. Güntner, S. Vorogushyn, and B. Merz (2010b), The benefits of gravimeter observations for modelling water storage changes at the field scale, Hydrology and Earth System Science , 14, 1715-1730.

Creutzfeldt, B., A. Güntner, H. Wziontek, and B. Merz (2010c), Reducing local hydrology from high precision gravity measurements: a lysimeter-based approach, Geophysical Journal International, 183(1), 178-187.

Crossley, D., S. Xu, and T. v. Dam (1998), Comprehensive analysis of 2 years of SG data from Table Mountain, Colorado, in 13th International Symposium on Earth Tides, edited, Observatoire Royal de Belgique, Brussels.

Crossley, D., J. Hinderer, G. Casula, O. Francis, H.-T. Hsu, Y. Imanishi, G. Jentzsch, J. Kääriänen, J. Merriam, B. Meurers, J. Neumeyer, B. Richter, K. Shibuya, T. Sato, and T. v. Dam (1999), Network of superconducting gravimeters benefits a number of disciplines, EOS Transactions American Geophysical Union, 80(11), 121-126.

Crossley, D., J. Hinderer, M. Llubes, and N. Florsch (2003), The potential of ground gravity measurements to validate GRACE data, Advances in Geosciences, 1, 65-71.

Crossley, D., J. Hinderer, and J. P. Boy (2004), Regional gravity variations in Europe from superconducting gravimeters, Journal of Geodynamics, 38(3-5), 325-342.

Crossley, D., and J. Hinderer (2009), A review of the GGP network and scientific challenges, Journal of Geodynamics, 48(3-5), 299-304.

Crossley, D. J., and S. Xu (1998), Analysis of superconducting gravimeter data from Table Mountain, Colorado, Geophysical J. International, 135(3), 835-844.

Damiata, B. N., and T.-C. Lee (2006), Simulated gravitational response to hydraulic testing of unconfined aquifers, Journal of Hydrology, 318(1-4), 348-359.

de Jong, B., and G. Ros (2004), The effect of water storage changes on gravity near Westerbork, University of Wageningen, Wageningen.

De Lannoy, G. J. M., P. R. Houser, N. E. C. Verhoest, V. R. N. Pauwels, and T. J. Gish (2007), Upscaling of point soil moisture measurements to field averages at the OPE3 test site, Journal of Hydrology, 343(1-2), 1-11.

Delin, G. N., R. W. Healy, D. L. Lorenz, and J. R. Nimmo (2007), Comparison of local- to regional-scale estimates of ground-water recharge in Minnesota, USA, Journal of Hydrology, 334(1-2), 231-249.

DIN (1998), Pedologic site assessment - Designation, classification and deduction of soil parameters (normative and nominal scaling), Deutsches Institut für Normung, Berlin.

Döll, P., F. Kaspar, and B. Lehner (2003), A global hydrological model for deriving water availability indicators: model tuning and validation, Journal of Hydrology, 270(1-2), 105-134.

Dyck, S., and G. Peschke (1983), Grundlagen der Hydrologie, Ernst, Berlin [u.a.].

Ehrismann, W. (1973), Ein allgemeines Verfahren zur digitalen Berechnung der Schwerewirkung von Modellkörpern, Zeitschrift für Geophysik, 39, 131-166.

Entin, J. K., A. Robock, K. Y. Vinnikov, S. E. Hollinger, S. Liu, and A. Namkhai (2000), Temporal and spatial scales of observed soil moisture variations in the extratropics, Journal of Geophysical Research, 105(D9), 11865-11877.

Evett, S. R., R. C. Schwartz, J. A. Tolk, and T. A. Howell (2009), Soil profile water content determination: spatiotemporal variability of electromagnetic and neutron probe sensors in access tubes, Vadose Zone Journal, 8(4), 926-941.

Famiglietti, J. S., J. A. Devereaux, C. A. Laymon, T. Tsegaye, P. R. Houser, T. J. Jackson, S. T. Graham, M. Rodell, and P. J. van Oevelen (1999), Ground-based investigation of soil moisture variability within remote sensing footprints during the Southern Great Plains 1997 (SGP97) hydrology experiment, Water Resources Research, 35(6), 1839-1851.

Famiglietti, J. S., D. Ryu, A. A. Berg, M. Rodell, and T. J. Jackson (2008), Field observations of soil moisture variability across scales, Water Resourc. Res., 44, W01423.

Farrel, W. E. (1972), Deformation of the Earth by Surface Loads, Reviews of Geophysics, 10(3), 761-797.

Ferré, T. P. A., L. Bentley, A. Binley, N. Linde, A. Kemna, K. Singha, K. Holliger, J. A. Huisman, and B. Minsley (2009), Critical steps for the continuing advancement of hydrogeophysics, EOS Transactions American Geophysical Union, 90(23).

Forsberg, R. (1984), A study of terrain reductions, density anomalies and geophysical inversion methods in gravity field modelling, Department of Geodetic Science and Surveying, the Ohio State University, Ohio.

French, H. K., C. Hardbattle, A. Binley, P. Winship, and L. Jakobsen (2002), Monitoring snowmelt induced unsaturated flow and transport using electrical resistivity tomography, Journal of Hydrology, 267(3-4), 273-284.

Gehman, C. L., D. L. Harry, W. E. Sanford, J. D. Stedick, and N. A. Beckman (2008), Estimating specific yield and storage change in an unconfined aquifer using temporal gravity surveys, Water Resources Research, 45, W00D21.

Gettings, P., D. S. Chapman, and R. Allis (2008), Techniques, analysis, and noise in a Salt Lake Valley 4D gravity experiment, Geophysics, 73(6), WA71.

Goodkind, J. M. (1999), The superconducting gravimeter, Review of Scientific Instruments, 70(11), 4131-4152.

Götze, H.-J. (1976), Ein numerisches Verfahren zur Berechnung der gravimetrischen und magnetischen Feldgrößen für dreidimensionale Modellkörper, TU Clausthal.

Graeff, T., E. Zehe, S. Schlaeger, M. Morgner, A. Bauer, R. Becker, B. Creutzfeldt, and A. Bronstert (2010), A quality assessment of spatial TDR soil moisture measurements in homogenous and heterogeneous media with laboratory experiments, Hydrology and Earth System Sciences Discussion, 7(1), 269-311.

Grayson, R. B., and A. W. Western (1998), Towards areal estimation of soil water content from point measurements: time and space stability of mean response, Journal of Hydrology, 207(1-2), 68-82.

Güntner, A., J. Stuck, S. Werth, P. Döll, K. Verzano, and B. Merz (2007), A global analysis of temporal and spatial variations in continental water storage, Water Resources Research, 43(5).

Güntner, A. (2008), Improvement of global hydrological models using GRACE data, Surveys in Geophysics, 29(4), 375-397.

GWR (2009), iGravTM SG: Simplified superconducting gravimeter for portable operation, GWR Instruments, Inc., San Diego, USA.

Haarhoff, T. (1989), The effect of acid rain and forest die-back on groundwater - case studies in Bavaria, Germany (FRG), paper presented at Atmospheric Deposition. Proceedings of a Symposium held during the Third Scientific Assembly of the International Association of Hydrological Sciences, IAHS, Baltimore, Maryland.

Harnisch, G., and M. Harnisch (2006), Hydrological influences in long gravimetric data series, Journal of Geodynamics, 41(1-3), 276-287.

Harnisch, G., M. Harnisch, and R. Falk (2006), Hydrological influences on the gravity variations recorded at Bad Homburg, Bulletin d'Information des Marées Terrestres, 142, 11331-11342.

Harnisch, M., and G. Harnisch (2002), Seasonal variations of hydrological influences on gravity measurements at Wettzell, Bulletin d'Information des Marées Terrestres, 137, 10849-10861.

Harter, T., and D. Zhang (1999), Water flow and solute spreading in heterogeneous soils with spatially variable water content, Water Resources Research, 35(2), 415–426.

Hartmann, T., and H. G. Wenzel (1995), Catalogue HW95 of the tide generating potential, Bulletin d'Information des Marées Terrestres, 123, 9278-9301.

Hasan, S., P. A. Troch, J. Boll, and C. Kroner (2006), Modeling the hydrological effect in local gravity at Moxa, Germany, Journal of Hydrometeorology, 7(3), 346-354.

Hasan, S., P. A. Troch, P. W. Bogaart, and C. Kroner (2008), Evaluating catchment-scale hydrological modeling by means of terrestrial gravity observations, Water Resources Research, 44(8), W08416.

Haude, W. (1955), Zur Bestimmung der Verdunstung auf möglichst einfache Weise, Deutscher Wetterdienst, Bad Kissingen, Germany.

He, X. (2007), Using hydrological models to simulate time-lapse gravity changes at Danish permanent gravity stations, Technical University of Denmark.

Healy, R., and P. Cook (2002), Using groundwater levels to estimate recharge, Hydrogeology Journal, 10(1), 91-109.

Heck, B., and K. Seitz (2007), A comparison of the tesseroid, prism and point-mass approaches for mass reductions in gravity field modelling, Journal of Geodesy, 81(2), 121-136.

Heppner, C. S., and J. R. Nimmo (2005), A computer program for predicting recharge with a Master Recession Curve, U.S. Geological Survey, Washington, USA.

Hinderer, J., C. de Linage, and J. P. Boy (2006), How to validate satellite-derived gravity observations with gravimeters at the ground?, Bulletin d'Information des Marées Terrestres, 142, 11433-11442.

Hinderer, J., D. Crossley, and R. J. Warburton (2007), Gravimetric methods – superconducting gravity meters, Treatise on Geophysics, 3, 65-122.

Hohmann, M. (1997), Soil freezing - the concept of soil water potential. State of the art, Cold Regions Science and Technology, 25(2), 101-110.

Hokkanen, T., K. Korhonen, and H. Virtanen (2006), Hydrogeological effects on superconducting gravimeter measurements at Metsähovi in Finland, Journal of Environmental & Engineering Geophysics, 11(4), 261-267.

Hokkanen, T., K. Korhonen, H. Virtanen, and E. L. Laine (2007), Effects of the fracture water of bedrock on superconducting gravimeter data, Near Surface Geophysics, 5(2), 133-139.

Howell, T. A. (2004), Lysimetry, in Encyclopedia of soils in the environment, edited by D. Hillel, pp. 379-386, Elsevier Press, Oxford, UK.

Hubbell, J. M., M. J. Nicholl, J. B. Sisson, and D. L. McElroy (2004), Application of a Darcian approach to estimate liquid flux in a deep vadose zone, Vadose Zone Journal, 3(2), 560-569.

Huisman, J. A., J. J. J. C. Snepvangers, W. Bouten, and G. B. M. Heuvelink (2002), Mapping spatial variation in surface soil water content: Comparison of ground-penetrating radar and time domain reflectometry, Journal of Hydrology, 269(3-4), 194-207

Huisman, J. A., S. Hubbard, J. D. Redman, and A. P. Annan (2003), Measuring soil water content with ground penetrating radar: A review, Vadose Zone Journal, 2(4), 476-491.

Hupet, F., and M. Vanclooster (2002), Intraseasonal dynamics of soil moisture variability within a small agricultural maize cropped field, Journal of Hydrology, 261(1-4), 86-101.

Imanishi, Y., T. Sato, T. Higashi, W. Sun, and S. Okubo (2004), A network of superconducting gravimeters detects submicrogal coseismic gravity changes, Science, 306(5695), 476-478.

Imanishi, Y., K. Kokubo, and H. Tatehata (2006), Effect of underground water on gravity observation at Matsushiro, Japan, Journal of Geodynamics, 41(1-3), 221-226.

Jacob, C. E. (1944), Notes on determining permeability by pumping tests under watertable conditions, U.S. Geological Survey, Washington, USA.

Jacob, T., R. Bayer, J. Chery, H. Jourde, N. L. Moigne, J.-P. Boy, J. Hinderer, B. Luck, and P. Brunet (2008), Absolute gravity monitoring of water storage variation in a karst aquifer on the larzac plateau (Southern France), Journal of Hydrology, 359(1-2), 105-117.

Jacob, T., J. Chery, R. Bayer, N. L. Moigne, J.-P. Boy, P. Vernant, and F. Boudin (2009), Time-lapse surface to depth gravity measurements on a karst system reveal the dominant role of the epikarst as a water storage entity, Geophysical Journal International, 17(2), 347-360.

Juston, J., J. Seibert, and P.-O. Johansson (2009), Temporal sampling strategies and uncertainty in calibrating a conceptual hydrological model for a small boreal catchment, Hydrological Processes, 23(21), 3093-3109.

Kachanoski, R. G., and E. de Jong (1988), Scale dependence and the temporal persistence of spatial patterns of soil water storage, Water Resources Research, 24(1), 85-91.

Katsura, S. y., K. i. Kosugi, N. Yamamoto, and T. Mizuyama (2005), Saturated and Unsaturated Hydraulic Conductivities and Water Retention Characteristics of Weathered Granitic Bedrock, Vadose Zone Journal, 5(1), 35-47.

Kazama, T., and S. Okubo (2009), Hydrological modeling of groundwater disturbances to observed gravity: Theory and application to Asama Volcano, Central Japan, Journal of Geophysical Research, 114, B08402.

Kim, S. (2009), Multivariate analysis of soil moisture history for a hillslope, Journal of Hydrology, 374(3-4), 318-328.

Kirchner, J. W. (2006), Getting the right answers for the right reasons: Linking measurements, analyses, and models to advance the science of hydrology, Water Resources Research, 42(3), W03S04.

Kirchner, J. W. (2009), Catchments as simple dynamical systems: Catchment characterization, rainfall-runoff modeling, and doing hydrology backward, Water Resources Research, 45, W02429.

Klemes, V. (1986a), Dilettantism in hydrology: transition or destiny?, Water Resources Research, 22(9S), 177S-188S.

Klemes, V. (1986b), Operational testing of hydrological simulation models, Hydrological Sciences Journal, 31(1), 13–24.

Klügel, T., and H. Wziontek (2007), Atmosphärische Schwereeffekte: Modell-Zeitreihen aus 3-dimensionalen Wettermodellen, in Jahrestagung der DGG, edited, Aachen.

Klügel, T., and H. Wziontek (2009), Correcting gravimeters and tiltmeters for atmospheric mass attraction using operational weather models, Journal of Geodynamics, 48(3-5), 204-210.

Kolbenheyer, T. (1967), Die Schwerewirkungen eines geraden Prismas mit rechtwinkligem Querschnitt, Studia geophysica & geodætica, 11, 262-270.

Krásný, J., and J. M. Sharp (2007), Hydrogeology of fractured rocks from particular fractures to regional approaches: State-of-the-art and future challenges, in Groundwater in fractured rocks, edited by J. Krásný and J. M. Sharp, Routledge, Prague.

Krause, P., M. Naujoks, M. Fink, and C. Kroner (2009), The impact of soil moisture changes on gravity residuals obtained with a superconducting gravimeter, Journal of Hydrology, 373(1-2), 151-163.

Kroner, C., and T. Jahr (2006), Hydrological experiments around the superconducting gravimeter at Moxa Observatory, Journal of Geodynamics, 41, 268-275.

Kroner, C., T. Jahr, M. Naujoks, and A. Weise (2007), Hydrological signals in gravity - foe or friend?, in Dynamic Planet - Monitoring and Understanding a Dynamic Planet with Geodetic and Oceanographic Tools, edited by C. Rizos, Springer, Berlin.

Kruseman, G. P., and N. A. de Ridder (1990), Analysis and Evaluation of Pumping Test Data, 2nd (completely revised) ed., International Institute for Land Reclamation and Improvement, Wageningen.

LaCoste (2010a), FG5 gravity meter, Micro-g LaCoste - A Division of LRS, Lafayette, USA.

LaCoste (2010b), A10 portable absolute gravity meter, Micro-g LaCoste - A Division of LRS, Lafayette, USA.

Lambert, A., and C. Beaumont (1977), Nano variations in gravity due to seasonal groundwater movements; implications for the gravitational detection of tectonic movements, Journal of Geophysical Research, 82(2), 297-306.

Lambert, A., N. Courtier, and T. S. James (2006), Long-term monitoring by absolute gravimetry: Tides to postglacial rebound, Journal of Geodynamics, 41(1-3), 307-317.

Lampitelli, C., and O. Francis (2010), Hydrological effects on gravity and correlations between gravitational variations and level of the Alzette River at the station of Walferdange, Luxembourg, Journal of Geodynamics, 49(1), 31-38

Langguth, H.-R., and R. Voigt (1980), Hydrogeologische Methoden, 2. überarbeitete und erweiterte Auflage ed., Springer-Verlag, Berlin.

Leirião, S. (2007), Hydrological model calibration using ground based and spaceborne time-lapse gravity surveys, Technical University of Denmark.

Leirião, S., X. He, L. Christiansen, O. B. Andersen, and P. Bauer-Gottwein (2009), Calculation of the temporal gravity variation from spatially variable water storage change in soils and aquifers, Journal of Hydrology, 365(3-4), 302-309.

LfL (2009), Agrarmeteorologisches Messnetz Bayern: Wetterstation Nr.127, Allmannsdorf, Bayerische Landesanstalt für Landwirtschaft (Bavarian State Research Center for Agriculture) (LfL), Freising-Weihenstephan, Germany.

Llubes, M., N. Florsch, J. Hinderer, L. Longuevergne, and M. Amalvict (2004), Local hydrology, the Global Geodynamics Project and CHAMP/GRACE perspective: some case studies, J. of Geodynamics, 38(3-5), 355-374.

Lo, M.-H., J. S. Famiglietti, P. J.-F. Yeh, and T. H. Syed (2010), Improving parameter estimation and water table depth simulation in a land surface model using GRACE water storage and estimated baseflow data, Water Resources Research, in press.

Longuevergne, L., J. P. Boy, N. Florsch, D. Viville, G. Ferhat, P. Ulrich, B. Luck, and J. Hinderer (2009), Local and global hydrological contributions to gravity variations observed in Strasbourg, Journal of Geodynamics, 48(3-5), 189-194.

LVG (2007), DGM 5 aus Höhenlinien, edited, Landesamt für Vermessung und Geoinformation Bayern, München.

MacMillan, W. D. (1958), Theoretical mechanics: The theory of the potential, Dover Publications, Inc., New York.

Mader, K. (1951), Das Newtonsche Raumpotential prismatischer Körper und seine Ableitungen bis zur dritten Ordnung, Österreichische Zeitschrift für Vermessungswesen, Sonderheft 11.

Mäkinen, J., and S. Tattari (1988), Soil moisture and groundwater: Two sources of gravity variations, Bulletin d'Information des Marées Terrestres, 64, 103-110.

Mantovan, P., and E. Todini (2006), Hydrological forecasting uncertainty assessment: Incoherence of the GLUE methodology, Journal of Hydrology, 330(1-2), 368-381.

Maréchal, J. C., B. Dewandel, and K. Subrahmanyam (2004), Use of hydraulic tests at different scales to characterize fracture network properties in the weathered-fractured layer of a hard rock aquifer, Water Resources Research, 40, W11508.

Mazahrih, N. T., N. Katbeh-Bader, S. R. Evett, J. E. Ayars, and T. J. Trout (2008), Field calibration accuracy and utility of four down-hole water content sensors, Vadose Zone Journal, 7(3), 992-1000.

Meissner, R., J. Seeger, H. Rupp, M. Seyfarth, and H. Borg (2007), Measurement of dew, fog, and rime with a high-precision gravitation lysimeter, Journal of Plant Nutrition and Soil Science, 170(3), 335-344.

Merz, B., and E. J. Plate (1997), An analysis of the effects of spatial variability of soil and soil moisture on runoff, Water Resources Research, 33(12), 2909-2922.

Merz, B., and A. Bárdossy (1998), Effects of spatial variability on the rainfall runoff process in a small loess catchment, Journal of Hydrology, 212-213, 304-317.

Merz, R., J. Parajka, and G. Blöschl (2009), Scale effects in conceptual hydrological modeling, Water Resources Research, 45, W09405.

Meurers, B., M. V. Camp, and T. Petermans (2006), Correcting superconducting gravity time-series using rainfall modelling at the Vienna and Membach stations and application to Earth tide analysis, Journal of Geodesy, 81(11), 703-712.

Mohanty, B. P., T. H. Skaggs, and J. S. Famiglietti (2000), Analysis and mapping of field-scale soil moisture variability using high-resolution, ground-based data during the Southern Great Plains 1997 (SGP97) Hydrology Experiment, Water Resources Research, 36(4), 1023-1031.

Mroczkowski, M., P. G. Raper, and G. Kuczera (1997), The quest for more powerful validation of conceptual catchment models, Water Resources Research, 33(10), 2325–2335.

Mualem, Y. (1976), A new model for predicting the hydraulic conductivity of unsaturated porous media, Water Resources Research, 12(3), 513–522.

Mufti, I. R. (1973), Rapid Determination of Cube's Gravity Field, Geophysical Prospecting, 21, 724-735.

Nagy, D. (1966), The gravitational attraction of a right rectangular prism, Geophysics 31, 362-371.

Nash, J. E., and J. V. Sutcliffe (1970), River flow forecasting through conceptual models part I - A discussion of principles, Journal of Hydrology, 10(3), 282-290.

Naujoks, M., C. Kroner, T. Jahr, P. Krause, and A. Weise (2007), Gravimetric 3D modelling and observation of

time-dependent gravity variations to improve small-scale hydrological modelling, in IUGG XXIV General Assembly, edited, Perugia, Italy.

Naujoks, M., A. Weise, C. Kroner, and T. Jahr (2008), Detection of small hydrological variations in gravity by repeated observations with relative gravimeters, Journal of Geodesy, 82(9), 543-553.

Naujoks, M., C. Kroner, A. Weise, T. Jahr, P. Krause, and S. Eisner (2009), Evaluating small-scale hydrological modelling by time-dependent gravity observations and a gravimetric 3D model, Geophysical Journal International, submitted.

Nawa, K., N. Suda, I. Yamada, R. Miyajima, and S. Okubo (2009), Coseismic change and precipitation effect in temporal gravity variation at Inuyama, Japan: A case of the 2004 off the Kii peninsula earthquakes observed with a superconducting gravimeter, Journal of Geodynamics, 48(1), 1-5.

Neumeyer, J., J. Hagedoorn, J. Leitloff, and T. Schmidt (2004), Gravity reduction with three-dimensional atmospheric pressure data for precise ground gravity measurements, Journal of Geodynamics, 38(3-5), 437-450.

Neumeyer, J., F. Barthelmes, C. Kroner, S. Petrovic, R. Schmidt, H. Virtanen, and H. Wilmes (2008), Analysis of gravity field variations derived from superconducting gravimeter recordings, the GRACE satellite and hydrological models at selected European sites, Earth Planets Space, 60(5), 505-518.

Newton, I. (1687), Philosophiae naturalis principia mathematica.

Nimmo, J. R., D. A. Stonestrom, and K. C. Akstin (1994), The feasibility of recharge rate determinations using the steady-state centrifuge method, Soil Science Society of America Journal, 58(1), 49-56.

Pachepsky, Y. A., A. K. Guber, and D. Jacques (2005), Temporal persistence in vertical distribution of soil moisture contents, Soil Science Society of America Journal, 69(2), 347-352.

Peter, G., F. Klopping, and K. A. Berstis (1995), Observing and modeling gravity changes caused by soil moisture and groundwater table variations with superconducting gravimeters in Richmond, Florida, USA, in Cahiers du Centre Européen de Géodynamique et de Séismologie, edited by C. Poitevin, pp. 147–159, Walferdange.

Peters, A., K. Y. Chung, and S. Chu (2001), High-precision gravity measurements using atom interferometry, Metrologia, 38(1), 25-61.

Petrahn, G. (2000), Grundlagen der Vermessungstechnik, Cornelsen, Berlin.

Petrović, S. (1996), Determination of the potential of homogeneous polyhedral bodies using line integrals, Journal of Geodesy, 71(1), 44-52.

Petrović, S., and P. Skiba (2001), Polyhedra in the gravity field modeling, paper presented at Proceedings of the International Workshop on Perspectives of Geodesy in South-East Europe, Mitteilungen der geodätischen Institute der Technischen Univerasität Graz, Dubrovnik.

Pohanka, V. (1988), Optimum expression for computation of the gravity field of a homogeneous polyhedral body, Geophysical Prospecting, 36, 733-751.

Pool, D. R., and J. H. Eychaner (1995), Measurements of aquifer-storage change and specific yield using gravity surveys, Ground Water, 33(3), 425-432.

Pool, D. R. (2008), The utility of gravity and water-level monitoring at alluvial aquifer wells in southern Arizona, Geophysics, 73(6), WA49.

Prutkin, I., and R. Klees (2007), Environmental effects in time-series of gravity measurements at the Astrometric-Geodetic Observatorium Westerbork (The Netherlands), in Dynamic Planet - Monitoring and Understanding a Dynamic Planet with Geodetic and Oceanographic Tools, edited by C. Rizos, Springer, Berlin.

Ramillien, G., J. Famiglietti, and J. Wahr (2008), Detection of continental hydrology and glaciology signals from GRACE: a review, Surveys in Geophysics, 29(4), 361-374.

Raum, K. D. (2002), Markierungstechnische bruchtektonisch-gefügekundliche und fotogeologische Untersuchungen zur Ermittlung der Grundwasserfließ-verhältnisse in der Verwitterungszone kristalliner Gesteine in Quellgebieten des Oberpfälzer/Bayerischen Waldes (Ost-Bayern/Deutschland), 1-242 pp, Friedrich-Alexander-Universität, Erlangen-Nürnberg.

Rausenberger, O. (1888), Lehrbuch der analytischen Mechanik I., B.G. Teubner, Leipzig.

Reager, J. T., and J. S. Famiglietti (2009), Global terrestrial water storage capacity and flood potential using GRACE, Geophysical Research Letters, 36(23), L23402.

Refsgaard, J. C., and J. Knudsen (1996), Operational validation and intercomparison of different types of hydrological models, Water Resources Research, 32(7), 2189–2202.

Reynolds, J. M. (1997), An introduction to applied and environmental geophysics, Kohn Wiley & Sons ltd, West Sussex, England.

Richter, D. (1995), Ergebnisse methodischer Untersuchungen zur Korrektur des systematischen Meßfehlers des Hellmann-Niederschlagsmessers, Deutscher Wetterdienst, Offenbach am Main, Germany.

Risser, D., W. Gburek, and G. Folmar (2009), Comparison of recharge estimates at a small watershed in east-central Pennsylvania, USA, Hydrogeology J., 17(2), 287-298.

Robinson, D. A., S. B. Jones, J. M. Wraith, D. Or, and S. P. Friedman (2003), A review of advances in dielectric and electrical conductivity measurement in soils using time domain reflectometry, Vadose Zone Journal, 2(4), 444-475.

Rodell, M. (2004), The Global Land Data Assimilation System, Bull. Amer. Meteorol. Soc., 85, 381-394.

Rodell, M., I. Velicogna, and J. S. Famiglietti (2009), Satellite-based estimates of groundwater depletion in India, Nature, 460(7258), 999-1002.

Roth, C., M. Malicki, and R. Plagge (1992), Empirical evaluation of the relationship between soil dielectric constant and volumetric water content as the basis for calibrating soil moisture measurements by TDR, Journal of Soil Science, 43(1), 1-13.

Rubbert, T. K. (2008), Hydrogeologische Modellbildung eines kombinierten porös-geklüfteten Grundwasserleitersystems des Bayerischen Waldes, Ruhr-Universität, Bochum.

Saito, T., H. Fujimaki, H. Yasuda, and M. Inoue (2009), Empirical temperature calibration of capacitance probes to measure soil water, Soil Science Society of America Journal, 73(6), 1931-1937.

Sato, T., J. P. Boy, Y. Tamura, K. Matsumoto, K. Asari, H.-P. Plag, and O. Francis (2006), Gravity tide and seasonal gravity variation at Ny-Alesund, Svalbard in Arctic, Journal of Geodynamics, 41(1-3), 234-241.

Schlüter, W., N. Brandl, R. Dassing, H. Hase, T. Klügel, R. Kilger, P. Lauber, A. Neidhardt, C. Plötz, S. Riepl, and U. Schreiber (2007), Fundamentalstation Wettzell - ein geodätisches Observatorium, Zeitschrift für Vermessungswesen, 132(3), 158-167.

Schmerge, D., and O. Francis (2006), Set standard deviation, repeatability and offset of absolute gravimeter A10-008, Metrologia, 43(5), 414-418.

Schulz, J. (2002), Die Ökozonen der Erde, Eugen Ulmer, Stuttgart.

SEBA (2008), Data Logger MDS Dipper-TEC: Water Level, Temperature, Electrical Conductivity, SEBA Hydrometrie GmbH, Kaufbeuren, Germany.

Seibert, J. (1996), Estimation of parameter uncertainty in the HBV model, paper presented at Nordic Hydrological Conference, Nordisk Assn Hydrology, Akureyri, Iceland.

Seibert, J. (2003), Reliability of model predictions outside calibration conditions, Nordic hydrology, 34, 477-492.

Seibert, J., K. Bishop, A. Rodhe, and J. J. McDonnell (2003a), Groundwater dynamics along a hillslope: A test of the steady state hypothesis, Water Resources Research, 39(1), 1014.

Seibert, J., A. Rodhe, and K. Bishop (2003b), Simulating interactions between saturated and unsaturated storage in a conceptual runoff model, Hydrological Processes, 17(2), 379-390.

Seibert, J. (2005), HBV light version 2, user's manual, Uppsala University, Uppsala.

Shiomi, S. (2008), Proposal for a geophysical search for dilatonic waves, Physical Review D (Particles, Fields, Gravitation, and Cosmology), 78(4), 042001-042006.

Šimůnek, J., M. Šejna, H. Saito, M. Sakai, and M. T. van Genuchten (2008), The HYDRUS-1D software package for simulating the movement of water, heat, and multiple solutes in variably saturated media, version 4.0, HYDRUS software series 3 , Department of Environmental Sciences, University of California, Riverside, California.

Sommer (2007), Snow pillow 3 x 3 m, Sommer GmbH & Co KG, Koblach, Austria.

Sommer (2008), USH-8: Ultrasonic Snow Depth Sensor, Sommer GmbH & Co KG, Koblach, Austria.

Sophocleous, M. A. (1991), Combining the soilwater balance and water-level fluctuation methods to estimate natural groundwater recharge: Practical aspects, Journal of Hydrology, 124(3-4), 229-241.

Spence, C. (2007), On the relation between dynamic storage and runoff: A discussion on thresholds, efficiency, and function, Water Resources Research, 43(12), W12416.

Spence, C., X. J. Guan, R. Phillips, N. Hedstrom, R. Granger, and B. Reid (2009), Storage dynamics and streamflow in a catchment with a variable contributing area, Hydrological Processes, in press.

Stähli, M., P.-E. Jansson, and L.-C. Lundin (1996), Preferential water flow in a frozen soil - a two-domain model approach, Hydrological Processes, 10(10), 1305-1316.

Stähli, M., D. Bayard, H. Wydler, and H. Flühler (2004), Snowmelt infiltration into alpine soils visualized by dye tracer technique, Arctic, Antarctic, and Alpine Research, 36(1), 128-135.

Steffen, H., O. Gitlein, H. Denker, J. Müller, and L. Timmen (2009), Present rate of uplift in Fennoscandia from GRACE and absolute gravimetry, Tectonophysics, 474(1-2), 69-77.

Sugihara, M., and T. Ishido (2008), Geothermal reservoir monitoring with a combination of absolute and relative gravimetry, Geophysics, 73(6), WA37-WA47.

Takemoto, S., Y. Fukuda, T. Higashi, M. Abe, S. Ogasawara, S. Dwipa, D. S. Kusuma, and A. Andan (2002), Effect of groundwater changes on SG observations in Kyoto and Bandung, Bulletin d'Information des Marées Terrestres, 134, 10839-10848.

Tamura, Y. (1987), A harmonic development of the tide-generating potential, Bulletin d'Information des Marées Terrestres, 99, 6813-6855.

Tapley, B. D., S. Bettadpur, J. C. Ries, P. F. Thompson, and M. M. Watkins (2004), GRACE measurements of mass variability in the Earth system, Science, 305, 503-505.

Taylor, K. E. (2001), Summarizing multiple aspects of model performance in a single diagram, Journal of Geophysical Research, 106(D7), 7183–7192.

Teuling, A. J., and P. A. Troch (2005), Improved understanding of soil moisture variability dynamics, Geophysical Research Letters, 32, L05404.

TGL (1974), 23864/02-10 Hydrogeologie, Amt für Standardisierung, Messwesen und Warenprüfung der DDR (ASMW), Berlin, Germany.

Theis, C. V. (1935), The relation between the lowering of the piezometric surface and the rate and duration of discharge of a well using groundwater storage, American Geophysical Union Transactions, 16, 519-524.

Tolk, J. A., and S. R. Evett (2009), Lysimetry versus neutron moisture meter for evapotranspiration determination in four soils, Soil Science Society of America Journal, 73(5), 1693-1698.

Topp, G. C., J. L. Davis, and A. P. Annan (1980), Electromagnetic determination of soil water content: measurements in coaxial transmission lines, Water Resources Research, 16(3), 574–582.

Tsoulis, D., H. Wziontek, and S. Petrovic (2003), The use of bilinear surfaces in the computation of gravitational effects due to topographic masses given on a regular grid, paper presented at Cahiers du Centre Européen de Géodynamique et de Séismologie, Walferdange.

UN (1992), Agenda 21 - Chapter 18, United Nation, Rio de Janeiro.

Vachaud, G., A. Passerat De Silans, P. Balabanis, and M. Vauclin (1985), Temporal stability of spatially measured soil water probability density function, Soil Science Society of America Journal, 49(4), 822-828.

Van Camp, M., S. D. P. Williams, and O. Francis (2005), Uncertainty of absolute gravity measurements, Journal of Geophysical Research, 110, B05406.

Van Camp, M., M. Vanclooster, O. Crommen, T. Petermans, K. Verbeeck, B. Meurers, T. v. Dam, and A. Dassargues (2006), Hydrogeological investigations at the Membach station, Belgium, and application to correct long periodic gravity variations, Journal of Geophysical Research, 111, B10403.

van Genuchten, M. T. (1980), A closed-form equation for predicting the hydraulic conductivity of unsaturated soils, Soil Science Society of America Journal, 44(5), 892-898.

Vereecken, H., T. Kamai, T. Harter, R. Kasteel, J. Hopmans, and J. Vanderborght (2007), Explaining soil moisture variability as a function of mean soil moisture: A stochastic unsaturated flow perspective, Geophysical Research Letters, 34, L22402.

Virtanen, H. (1999), On the Observed Hydrological Environmental Effects on Gravity at the Metsähovi Station, Finland, in Cahiers du Centre Européen de Géodynamique et de Séismologie, edited by B. Ducarme and J. Barthélemy, Luxembourg.

Virtanen, H. (2001), Hydrological studies at the Gravity Station Metasahovi in Finland, Journal of the Geodetic Society of Japan, 47(1), 328-333.

Völkel, J. (1995), Periglaziale Deckschichten und Böden im Bayerischen Wald und seinen Randgebieten als geogene Grundlagen landschaftsökologischer Forschung im Bereich naturnaher Waldstandorte, Zeitschrift für Geomorphologie, 96.

von Unold, G., and J. Fank (2008), Modular design of field lysimeters for specific application needs, Water, Air, & Soil Pollution: Focus, 8(2), 233-242.

Vrugt, J. A., H. V. Gupta, L. A. Bastidas, W. Bouten, and S. Sorooshian (2003), Effective and efficient algorithm for multiobjective optimization of hydrologic models, Water Resources Research, 39(8), 1214.

Wahr, J. M. (1985), Deformation induced by polar motion, Journal of Geophysical Research, 90(B11), 9363–9368.

Weihermuller, L., J. A. Huisman, S. Lambot, M. Herbst, and H. Vereecken (2007), Mapping the spatial variation of soil water content at the field scale with different ground penetrating radar techniques, Journal of Hydrology, 340(3-4), 205-216.

Weise, A., C. Kroner, M. Abe, J. Ihde, G. Jentzsch, M. Naujoks, H. Wilmes, and H. Wziontek (2009), Terrestrial gravity observations with superconducting gravimeters for validation of satellite-derived (GRACE) gravity variations, Journal of Geodynamics, 48(3-5), 325-330.

Werth, S., A. Güntner, S. Petrovic, and R. Schmidt (2009a), Integration of GRACE mass variations into a global hydrological model, Earth and Planetary Science Letters, 277(1-2), 166-173.

Werth, S., A. Güntner, R. Schmidt, and J. Kusche (2009b), Evaluation of GRACE filter tools from a hydrological perspective, Geophysical Journal International, 179(3), 1499-1515.

Western, A. W., R. B. Grayson, and G. Blöschl (2002), Scaling of soil moisture: a hydrologic perspective, Annual Review of Earth and Planetary Sciences, 30(1), 149-180.

Western, A. W., S. L. Zhou, R. B. Grayson, T. A. McMahon, G. Blöschl, and D. J. Wilson (2004), Spatial correlation of soil moisture in small catchments and its relationship to dominant spatial hydrological processes, Journal of Hydrology, 286(1), 113-134.

Wilson, C. R., H. Wu, B. Scanlon, and J. M. Sharp (2007), Taking the superconducting gravimeter to the field - A new tool for hydrologic and other investigations.

Wittenberg, H. (1999), Baseflow recession and recharge as nonlinear storage processes, Hydrological Processes, 13(5), 715-726.

WMO (2008), Guide to meteorological instruments and methods of observation., World Meteorological Organization (WMO), Geneva, Switzerland.

Wziontek, H., R. Falk, H. Wilmes, and P. Wolf (2009a), Precise gravity time series and instrumental properties from combination of superconducting and absolute gravity measurements, in Observing our Changing Earth, edited by M. G. Sideris, pp. 301-306.

Wziontek, H., H. Wilmes, B. Creutzfeldt, and A. Güntner (2009b), High precision gravimetric time series in comparison with global and local hydrology models, in 2009 AGU Fall Meeting, edited, American Geophysical Union, San Francisco, USA.

Wziontek, H., H. Wilmes, P. Wolf, S. Werth, and A. Güntner (2009c), Time series of superconducting gravimeters and water storage variations from the global hydrology model WGHM, Journal of Geodynamics, 48(3-5), 166-171.

Yang, J., B. Li, and L. Shiping (2000), A large weighing lysimeter for evapotranspiration and soil-water-groundwater exchange studies, Hydrological Processes, 14(10), 1887-1897.

Zaitchik, B. F., M. Rodell, and R. H. Reichle (2008), Assimilation of GRACE terrestrial water storage data into a land surface model: results for the mississippi river basin, Journal of Hydrometeorology, 9(3), 535-548.

Zehe, E., T. Graeff, M. Morgner, A. Bauer, and A. Bronstert (2009), Plot and field scale soil moisture dynamics and subsurface wetness control on runoff generation in a headwater in the Ore Mountains, Hydrol. Earth Syst. Sci. Discuss., 6(6), 7503-7537.

Zreda, M., D. Desilets, T. P. A. Ferré, and R. L. Scott (2008), Measuring soil moisture content non-invasively at intermediate spatial scale using cosmic-ray neutrons, Geophysical Research Letters, 35, L21402.

Author's declaration

I prepared this dissertation without illegal assistance. The work is original except where indicated by special reference in the text and no part of the dissertation has been submitted for any other degree. This dissertation has not been presented to any other University for examination, neither in Germany nor in another country.

Noah Angelo Benjamin Creutzfeldt
Berlin, April 2010